

SKB R-25-08

ISSN 1402-3091

ID 2072854

June 2025

Evaluation and analysis of Cu samples exposed at elevated temperature to various bentonites

Alice Moya Núñez, Helen Pahverk, Salil Sainis, Claes Taxén,
Xuying Wang, Dan Persson, Illia Dobryden

RISE Research Institutes of Sweden AB

This report concerns a study which was conducted for Svensk Kärnbränslehantering AB (SKB). The conclusions and viewpoints presented in the report are those of the authors. SKB may draw modified conclusions, based on additional literature sources and/or expert opinions.

This report is published on www.skb.se

© 2025 Svensk Kärnbränslehantering AB

Content

1	Introduction	2
1.1	Background and objectives	2
1.1.1	Sample preparation in Kista	2
1.1.2	Exposure in bentonite by SKB	2
2	Materials and methods	3
2.1	Sample reception	3
2.2	Sample preparation	3
2.3	Scanning electron microscopy and energy dispersive spectroscopy	3
2.4	X-ray diffraction	4
2.5	Thickness measurement (LayerProbe)	4
2.6	Mass loss analysis	4
2.7	Surface roughness characterization (Alicona)	4
2.8	Infrared spectroscopy	5
2.9	Raman spectroscopy	5
3	Results	6
3.1	Appearance of received exposed samples	6
3.2	LayerProbe	7
3.2.1	Before exposure	7
3.2.2	After exposure (6 months)	8
3.3	Results from SEM/EDS analysis	9
3.4	Results from XRD	15
3.5	Results from the gravimetric analysis	17
3.6	Results from surface analysis (Alicona)	18
3.7	Infrared Spectroscopy Results	20
3.8	Raman Spectroscopy Results	22
4	Discussion	24
5	Conclusions	26
6	References	27
7	Appendix	28
7.1	As-received photographs	28
7.2	Mass loss plots (gravimetry)	38
7.3	Alicona characterization results	50
7.4	SEM/EDS Surface analysis	82
7.4.1	Sample C1-3	82
7.4.2	Sample C2-3	87
7.4.3	Sample C3-4	92
7.4.4	Sample C4-2	98
7.4.5	Sample C5-3	103
7.4.6	Sample C6-3	109
7.4.7	Sample C7-3	113
7.4.8	Sample C8-3	119
7.5	Cross section analysis (SEM/EDS)	123
7.6	Complementary Raman Results	125

1 Introduction

1.1 Background and objectives

In this report, copper specimens in contact with bentonite exposed inside a hydrothermal reactor were characterized regarding the extent and type of formed corrosion products.

1.1.1 Sample preparation in Kista

Pieces of pure copper were delivered to Kista to manufacture cylinders of 26 mm diameter and 7 mm thickness.

The copper cylinders were then cut using electrical discharge machining (wire cutting) into four equal pieces and ground up to P2500 grit SiC paper. Each quarter was labelled on its side using an engraving pen, which also identifies the top and bottom surfaces of the samples. The samples were later polished using diamond paste up to $\frac{1}{4}$ μm and degreased in an ethanol/acetone bath for 15 minutes and weighed in a 5 decimal scale (brand Mettler Toledo). Upper and bottom surfaces had a mirror-like finish. Each quarter was ground and polished individually and manually using a standard metallographic clamp. The side surfaces were not prepared in any way and did not form part of the intended analyses before or after exposure.

The samples were packed in cotton wool and then aluminium foil to prevent damage to the polished surfaces prior to exposure. It is likely that some mechanical damage such as scratches occurred prior to exposure. Selected samples were characterized using an infinite focus microscope (brand Alicona) and postprocessed using the software Mountains Map. Defects from polishing were recorded and roughness measurements were performed on both surfaces.

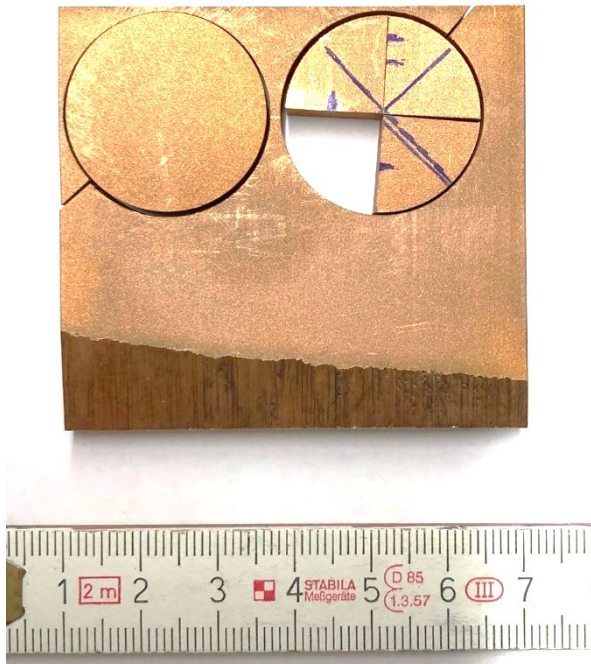


Figure 1-1. Electrical discharge machined cylinders from the material supplied by SKB.

1.1.2 Exposure in bentonite by SKB

Polished samples were sent for exposure at SKB facilities with the intention of determining potential interactions between the copper samples and different types of bentonite. The samples were exposed inside a hydrothermal reactor for 6 (C1, C2, C3, C4) or 12 months (C5, C6, C7, C8). The details of the exposures were not formally disclosed to RISE AB.

2 Materials and methods

2.1 Sample reception

The samples were delivered to RISE AB inside a cardboard box, each one of them vacuum sealed in a plastic bag inside another aluminium foil bag.

The samples were unpackaged from their containers inside a glovebox containing nitrogen gas. The objective was to avoid exposure of the samples to air (oxygen) as much as possible. Photographs were taken while the samples were inside the glove box. Care was taken to not scratch the samples. After photographing the samples, these images were sent to SKB to agree upon areas to examine using SEM/XRD techniques.

Visually, the samples generally had small amounts of surface deposits/bentonite adhered to their surface, with some exceptions (C4 and C8 samples). No washing of any kind was performed to remove the possible adhered bentonite. The specimens were taken as they were received to be analysed in the SEM/XRD instruments.

Samples C5 in contact with MX80 bentonite showed a blackened rim on the outer sections. These blackened edges did not appear for the C1 samples. The SEM/XRD characterization was focused therefore on these areas, instead of the upper surface that was previously polished.

The samples were numbered as shown in the following table.

Table 2-1. Sample numbering.

Purpose	Cylinder number	Samples
Bentonite MX80 exposure	C1	C1-1, C1-2, C1-3, C1-4
Bentonite Moroccan exposure	C2	C2-1, C2-2, C2-3, C2-4
Bentonite Calcigel exposure	C3	C3-1, C3-2, C3-3, C3-4
Bentonite Asha 505 exposure	C4	C4-1, C4-2, C4-3, C4-4
Bentonite MX80 exposure	C5	C5-1, C5-2, C5-3, C5-4
Bentonite Moroccan exposure	C6	C6-1, C6-2, C6-3, C6-4
Bentonite Calcigel exposure	C7	C7-1, C7-2, C7-3, C7-4
Bentonite Asha 505 exposure	C8	C8-1, C8-2, C8-3, C8-4
Reference	C9	C9-1, C9-2, C9-3, C9-4

2.2 Sample preparation

The specimens were not prepared for surface analysis in any way after exposure.

2.3 Scanning electron microscopy and energy dispersive spectroscopy

The samples were characterized using a scanning electron microscope (SEM) Zeiss Sigma 3000VP instrument, equipped with energy dispersive spectroscopy (EDS) detector X-max^N (Oxford Instruments). The electron beam voltage was 15 keV and the current about 1-2 nA. A Secondary Electron (SE) detector was used to image the surface of the specimens. The SEM and EDS were operated using the software SmartSEM and AZtec, respectively. Carbon was deconvoluted from the spectra as it is assumed to be completely or partially a contaminant from the sample or the chamber. The analyses in EDS are semi-quantitative.

2.4 X-ray diffraction

The X-ray diffraction (XRD) analyses were done using a Bruker D8 Discover instrument. The data were collected between 4 and 110° (2 θ) with a copper K α beam of 1.5418 Å, for about 35 min. A Ni filter was used to reduce the intensity of the Cu K β X-rays. A universal beam collimator of approximately 0.5 mm spot size was used for this analysis. The Crystallographic Open Database (COD) was used for peak identification.

The analysis areas were chosen in agreement with SKB, after preliminary presentation and consideration of SEM-EDS results.

2.5 Thickness measurement (LayerProbe)

Layerprobe (LP) measurements were done on the prepared surface of one sample, before and after exposure. The objective was to measure the thickness of the pre-exposure oxide layer and determine its evolution after exposure.

Layerprobe (LP) is a software tool provided by Oxford Instruments and is a module in AZtec. It complements the elemental and phase information provided from EDS by also calculating the composition and thickness of the individual layers beneath the surface. The maximum total thickness is the X-ray excitation depth (~2–10 μm using 30 keV depending on the material). The measured layer should preferably consist of one unique element, if more elements are present the results might be less accurate. The thickness measurements were carried out on one sample before exposure and one sample after exposure. Both results are reported.

2.6 Mass loss analysis

Gravimetric analysis or mass loss analysis was used to quantify the extent of the corrosion on the analysed specimens. The specimens were pickled in order to remove corrosion products and bentonite remains. Several rounds of pickling are usually needed to remove all corrosion products from the surface of the specimens. The specimens are weighed after each pickling round and the procedure is repeated until the mass loss between two consecutive treatments is very small, and comparable to the mass loss of an unexposed reference copper specimen. A 5 decimal scale (brand Mettler Toledo) was used to weigh the samples. Ideally, the pickling process does not affect the underlying base metal surface and only removes the corrosion products. A reference specimen was used to verify this.

Given the experience of past reports (Johansson et al. 2020), sulfamic acid (5 wt%) was selected to be used during the pickling procedure. Intervals of 30 seconds to 1 minute of pickling at room temperature followed by manual cleaning of 1 minute using a soft-bristled brush were applied to the specimens. The specimens exposed to Asha 505 (C4 and C8) took more than 20 rounds of pickling and cleaning until they were deemed appropriate for surface characterization (Alicona). The gravimetry analysis is based on ISO 8407:2021 using a linear regression.

2.7 Surface roughness characterization (Alicona)

The surface profile or topography was characterized using an Alicona InfiniteFocusSL 3D optical microscope based on focus-variation. A 10x magnification objective lens was used to scan the entire surface of the Cu samples with vertical and lateral resolution of 0.7 μm and 6 μm , respectively. The 3D topography data was further processed using Mountains Map 9 image processing software. Minimal post-measurement processing was performed and included image cropping and form correction. Two types of roughness are reported here – one based on roughness of a random line profile (length 9 mm) drawn on the surface data and the other based on surface roughness of the entire sample surface (surface area ~113 mm²). For line roughness, ISO 4287 standard was applied, and ISO 25187 implemented for surface roughness estimation. The results from before exposure are also reported for comparison purposes.

2.8 Infrared spectroscopy

FTIR-spectroscopy was performed using a Bruker Vertex 70 spectrometer equipped with a Hyperion 3000 microscope (Bruker). The measurements were made with specular reflection measurements using the microscope in the region 400–4000 cm^{-1} . The area analysed was 200x200 μm^2 . Specular reflection measurements were also made using a multireflection accessory in the spectrometer in the region 50–4000 cm^{-1} , with an analysis area in the order of a few mm and finally using an ATR¹-accessory with a diamond internal reflection elements in the region 50–4000 cm^{-1} . The analysed area with the ATR-accessory is 1.8 mm in diameter. The measurements performed down to 50 cm^{-1} were made using a wide range beamsplitter. The measurements were performed using 8 cm^{-1} resolution.

Only sample C5-3 (blackened edge) was examined using this technique.

2.9 Raman spectroscopy

The measurements were carried out using a confocal Raman instrument A WITec Alpha 300 system equipped with a 532 nm excitation laser.

A 50x ZEISS LD EC Epiplan-Neofluar objective was used, and the power was optimized to about 3–5 mW to avoid surface burning. The sample was stored in an envelope with adsorbent material and the indicator did not show any increased humidity. The measurements were conducted using the 1800 gr/mm grating which can provide spatial resolution of up to 0.5 μm using a 100x objective and the spectral resolution of up to 0.5 rel.cm . The sample was mounted on a cover slide and then on the CRM sample stage.

Only sample C5-3 (blackened edge) was examined using this technique.

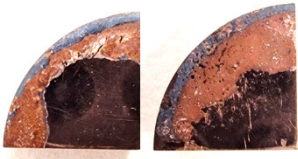
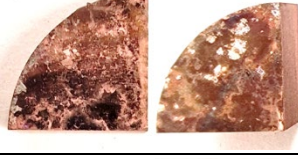
¹ Attenuated Total Reflectance (ATR) is a methodology for FTIR spectroscopy based on infrared light reflection at the crystal-specimen interface.

3 Results

3.1 Appearance of received exposed samples

All the photographs from the as-received specimens are reported in the Appendix. A short description of the specimen's visual appearance at reception is given in Table 3-1. In general, the visual appearance of as-received samples shows some edge effects. Edge effects are most pronounced at samples C1-3 in Figure 7-3, C1-4 in Figure 7-4, C5-2 in Figure 7-18. Causes for the appearance of edge effects may be related to the corrosion process or to the adhesion of corrosion products and bentonite.

Table 3-1. Visual appearance of received exposed samples.

Specimen	Selected photographs	Visual appearance
C1		C1: The specimens exposed to MX-80 bentonite visually exhibited mostly a shiny and clean surface. Some areas were covered with a thin deposits and borders generally exhibited a thicker deposit with a greenish hue, especially C1-3.
C2		C2: The surface of the specimens exposed to Moroccan bentonite visually exhibited a mostly shiny and clean surface, the deposit was not homogeneously covering the whole top or bottom surfaces. The affected areas were covered with a thin deposit. Specimen C2-4 exhibited an area with a deposit with an orange hue on one of its sides.
C3		C3: The surface of the specimens exposed to Calcigel bentonite visually exhibited a deposit covered most of the surface. White and orange deposits are observed as islands covering some areas of the surface.
C4		C4: The specimens exposed to Asha 505 bentonite visually exhibited a deposit covering most of the surface. Thick deposits of white and bright orange hue cover preferentially one of the sides of the specimens. The other side of the specimens exhibits a thinner deposit covering their surface.
C5		C5: The specimens exposed to MX-80 for one year visually exhibited a deposit covering almost all of the surface with the exception of one side of C5-2, which was almost completely shiny and clean. Generally lighter coloured deposits were observed on the borders.
C6		C6: The specimens exposed to Moroccan bentonite for one year visually exhibited a thin deposit covering most of the surfaces, although some areas remained shiny and clean. At least two different deposit colours and thickness are visible preferentially on one side of the specimens.
C7		C7: The specimens exposed to Calcigel bentonite for one year visually exhibited a thin deposit covering most of the surfaces. Some white-coloured deposits are found as separate islands. Specimen C7-2 (right picture) shows marks where deposit was removed during manipulation. The specimen C7-3 exhibited a bright orange area on one of its surfaces.
C8		C8: The specimens exposed to Asha 505 bentonite for one year exhibit a thick deposit preferentially covering one of the sides. These deposits had a white, orange, red or purple hue. The other sides exhibit a thinner deposit covering most of their surfaces.

3.2 LayerProbe

The thickness measurement using the software LayerProbe (Aztec) was performed on one sample before and after exposure (C1-3). “The sigma value corresponds to a standard deviation based on an estimation of composition measurement uncertainty, which can be interpreted as thickness uncertainty, estimated by the software (Aztec).”

3.2.1 Before exposure

Experimental conditions:

- Microscope: Zeiss Sigma 3000VP.
- 3.5 keV, low beam energy.
- Model assumes that the oxide is Cu₂O (density of 6 g/cm³) and the bulk material underneath is pure Cu.
- For calibration Cu₂O oxide and pure Si was used.
- The measurement was done in 19 spectra.

Table 3-2. Oxide layer thickness before exposure.

Spectrum	Layer 1 Thickness (nm)	Layer 1 Thickness Sigma (nm)
1	3.3	0.8
2	4.7	0.6
3	5.4	0.6
4	3.7	0.7
5	6.4	0.6
6	7.5	0.6
7	9.3	0.6
8	5.1	0.6
9	11.0	0.6
10	7.2	0.6
11	5.0	0.6
12	5.5	0.6
13	10.2	0.6
14	3.3	0.7
15	8.4	0.6
16	13.1	0.6
17	8.9	0.6
18	16.8	0.6
19	5.7	0.6
Average	7.4	0.6

3.2.2 After exposure (6 months)

Experimental conditions:

- Microscope: Zeiss Sigma 3000VP.
- 5 keV, 120 μm aperture, high current mode.
- Model assumes that the oxide is Cu_2O (density of 6 g/cm^3) and the bulk material underneath is pure Cu.
- For calibration Cu_2O oxide and pure Si was used.
- The measurement was done in two areas, with 15 spectra per area analysed.

Table 3-3. Oxide layer thickness after exposure (first area).

Spectrum	Layer 1 Thickness (nm)	Layer 1 Sigma (nm)
1	14.6	2.15
2	11.47	2.22
3	12.32	2.17
4	15.25	2.14
5	13.99	2.15
6	13.73	2.15
7	14.87	2.13
8	9.96	2.19
9	17.93	2.17
10	16.08	2.1
11	13.39	2.14
12	11.45	2.18
13	13.05	2.16
14	14.99	2.18
15	18.7	2.16
Average	14.12	2.16

Table 3-4. Oxide layer thickness after exposure (second area).

Spectrum	Layer 1 Thickness (nm)	Layer 1 Sigma (nm)
16	11.51	2.18
17	15.69	2.17
18	10.98	2.21
19	13.58	2.18
20	19.77	2.19
21	13.92	2.15
22	20.13	2.2
23	11.16	2.17
24	16.12	2.14
25	18.46	2.19
26	13.98	2.16
27	12.35	2.2
28	17.4	2.18
29	19.05	2.18
30	13.91	2.18
Average	15.20	2.18

3.3 Results from SEM/EDS analysis

This section will briefly describe the findings from the SEM/EDS surface analysis. The samples were not prepared after exposure and prior to the analysis. The zones to be examined were chosen by SKB. The complete surface analyses using SEM/EDS are compiled in the Appendix. The EDS results are reported in wt%.

Specimens in contact with MX-80 bentonite exhibited in some areas increased amounts of sulphur. The sulphur signals were found in coexistence with Cu, which might indicate the presence of copper sulphides, for example spectrum 2 in sample C1-3, Area 1, see Figure 7-91 and Table 7-1. Thicker deposit was found in some areas following the outer border of the specimens (grey-hue deposit), with the presence of iron, aluminium and silicon. Large areas in EDS maps show mostly copper and sulphur in coexistence (see Figure 7-90). The rim of the specimen exposed for 12 months (C5, see Figure 3-1) exhibited a dark colour which was not visible in other samples, including the ones exposed to the same type of bentonite for 6 months (C1). This rim was examined by SEM/EDS and XRD, showing mainly signals from Cu, O, Si, Ca, S and Al (see Figure 3-2).



Figure 3-1. Blackened edge observed on sample C5-3.

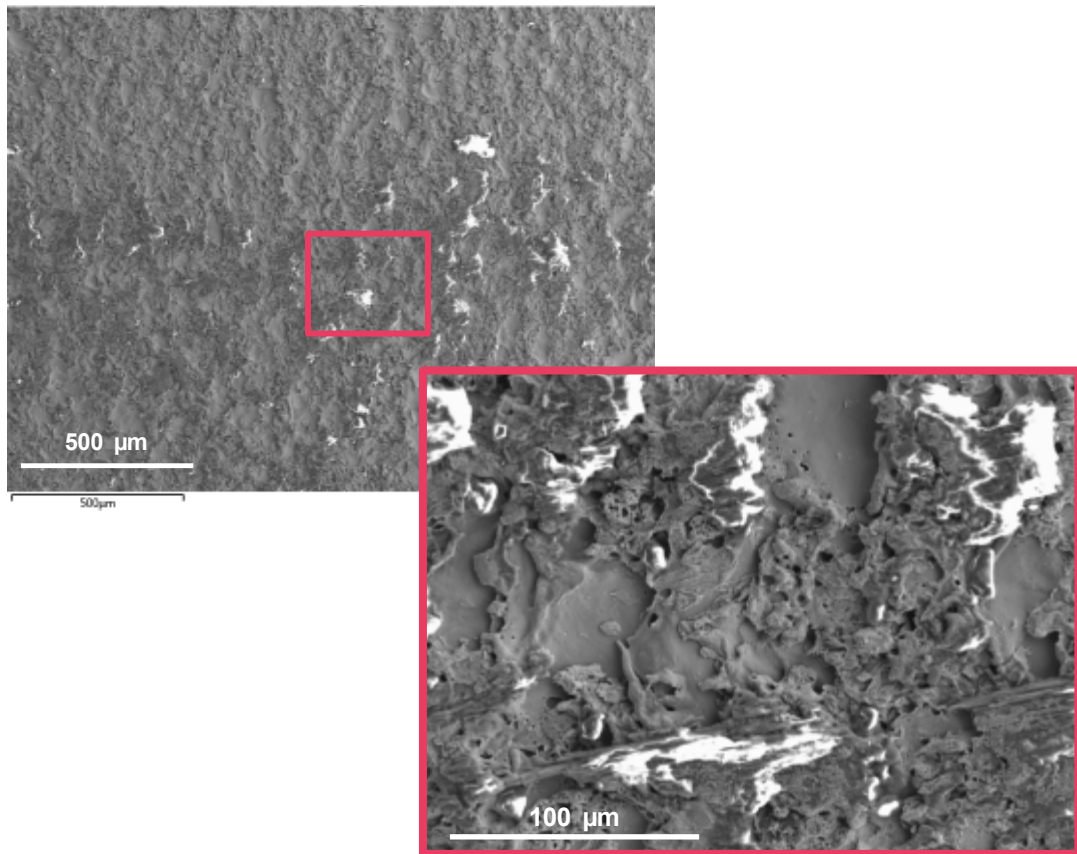


Figure 3-2. SEM image of specimen C5-3 (blackened edge shown in Figure 3-1, approximately inside the green square). The image to the right corresponds to a magnification (1000x) of the red square area.

Specimens in contact with Moroccan bentonite (C2 and C6) exhibited relatively thin deposits that were mostly attributed to the bentonite itself. Thicker deposits had low concentrations of copper, indicating a limited reaction with the substrate. Elevated levels of chlorine (for example Spectrum 9 and 16 of Table 7-8) were found in some areas.

Specimens in contact with Calcigel bentonite (C3 and C7) exhibited increased amounts of sulphur in some areas. However, these deposits do not seem to have interacted with the underlying copper substrate, which is indicated by the EDS maps showing distinctly separate areas containing either copper or sulphur. Thick deposits are observed on the surface of this specimen, with visible white deposits (see images in Table 3-1) containing mostly O-Ca-S (see EDS maps in Figure 7-110 and Figure 7-159), possibly calcium sulphate (gypsum).

Specimens in contact with Asha bentonite (C4 and C8) exhibited large areas of their surfaces covered with deposit. These deposits contained mostly O, Na, Mg, Al, Si, Ca and Cu. Areas without deposit were observed as well. It was observed in the specimen exposed for 12 months (C8-3) a structure resembling pits (see Figure 3-3), without visible corrosion products. Spots with higher amounts of iron were also observed in all examined areas, in connection with silicon.

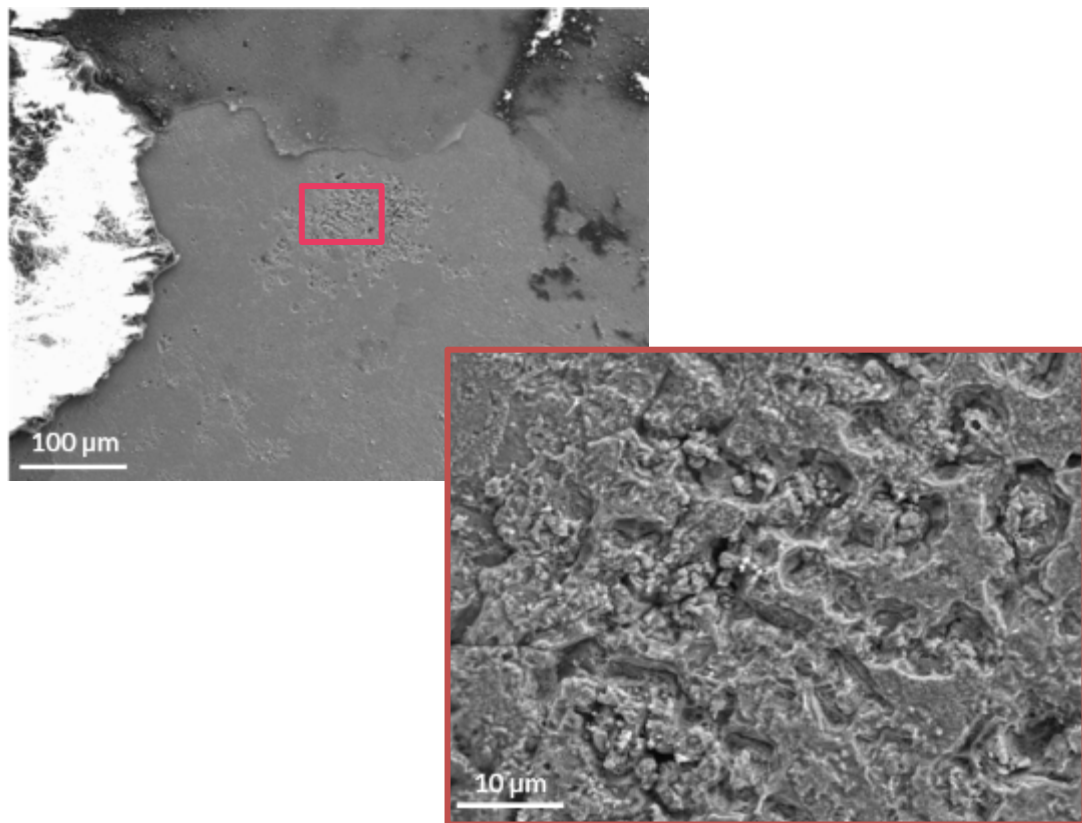


Figure 3-3. Examined surface of specimen C8-3 (Area 1). The image to the right corresponds to a higher magnification of the squared area (1000x). A structure resembling pits is observed in areas not covered by bentonite or deposits. The pits were analyzed using EDS and no visible corrosion products were identified.

The specimen C4-2 was examined once more after observing the pit-like damage in C8-3 (Figure 3-4 and Figure 3-5). Different types of damage were identified at the surface, including preferential grain dissolution, grain boundary attack, and formation of deep pit-like features.

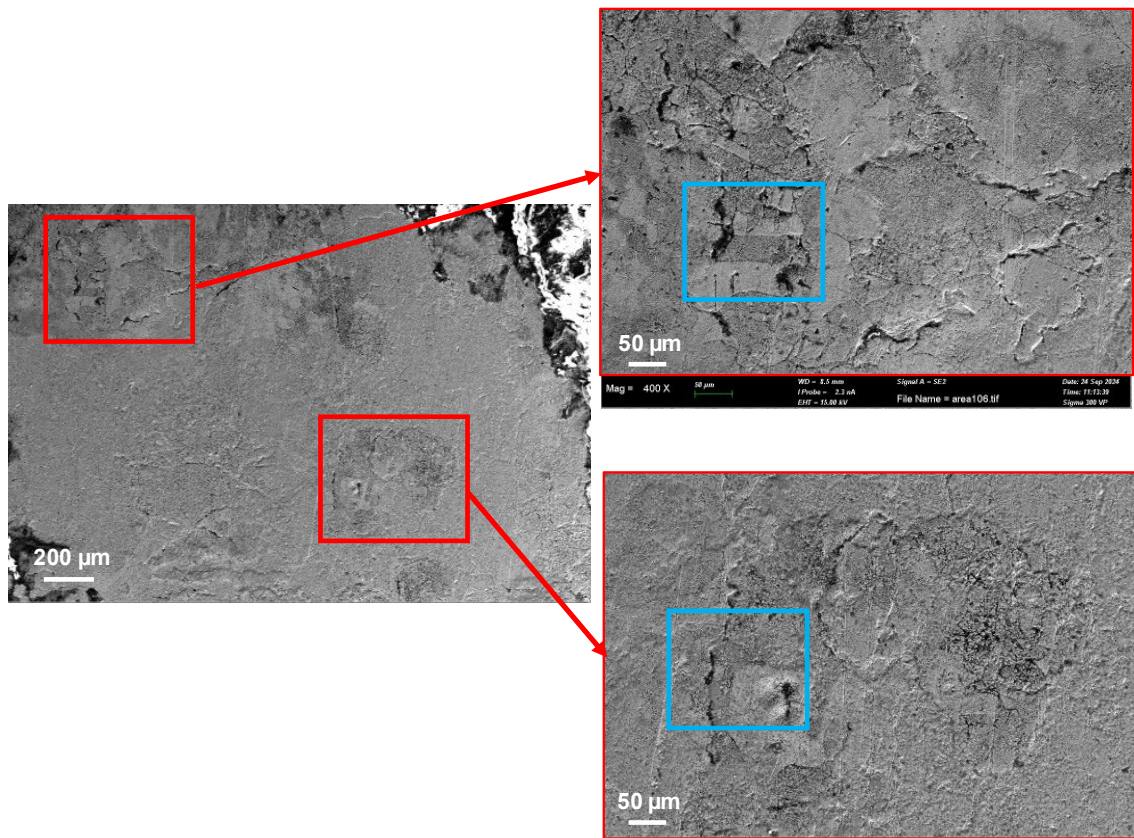


Figure 3-4. Examined surface of specimen C4-2. The image to the right corresponds to a higher magnification of the squared areas in red. The blue squares are shown magnified in Figure 3-5.

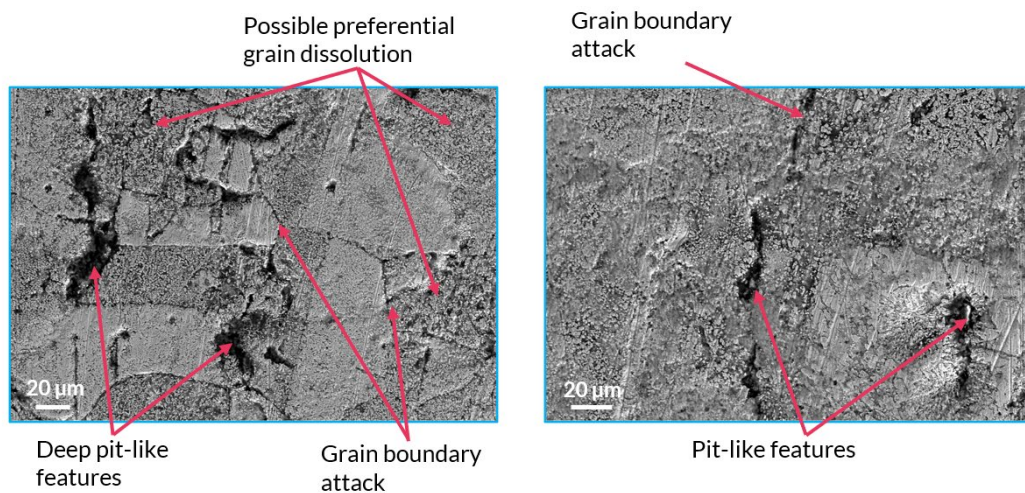


Figure 3-5. Magnified areas from Figure 3-4. Examples of preferential grain dissolution, grain boundary attack, and pit-like features are indicated. Note that not all affected areas have been marked.

The bentonite deposits were carefully removed from C4-2 with a soft plastic brush and the specimen was once more examined using SEM. Similar degradation patterns were observed underneath the bentonite deposit (see Figure 3-6 and Figure 3-7).

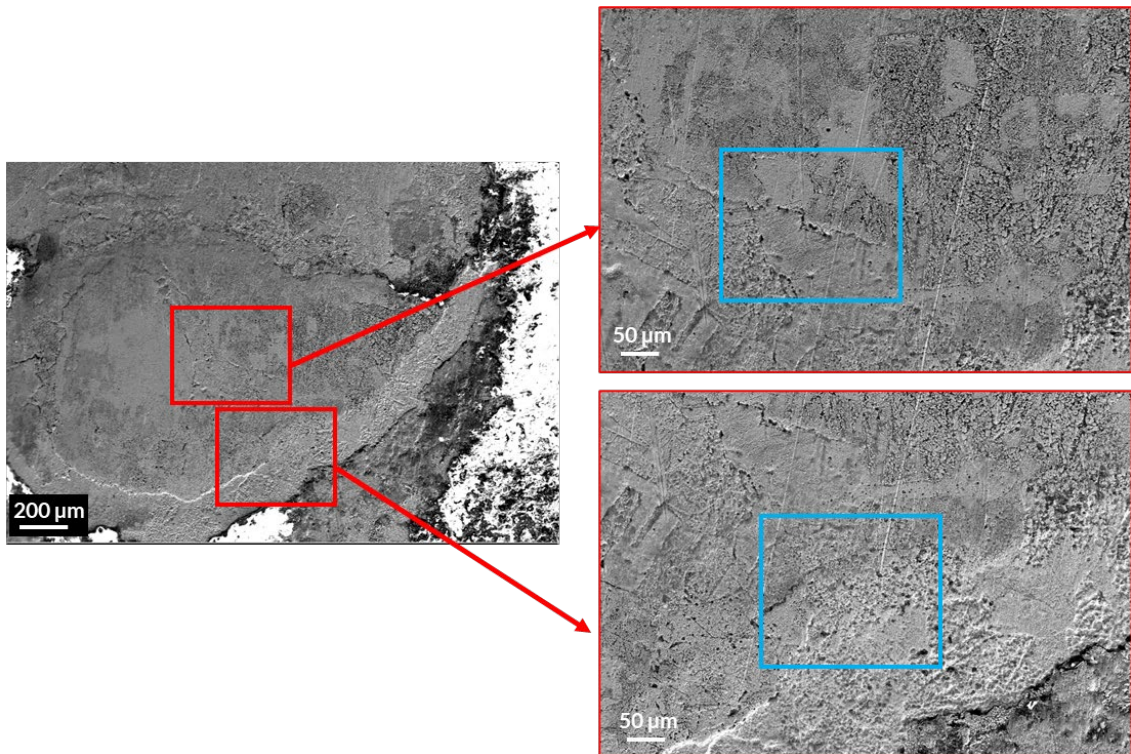


Figure 3-6. Examined surface of specimen C4-2, underneath bentonite deposit (mechanically removed). The image to the right corresponds to a higher magnification of the squared areas in red. The blue squares are shown magnified in Figure 3-7.

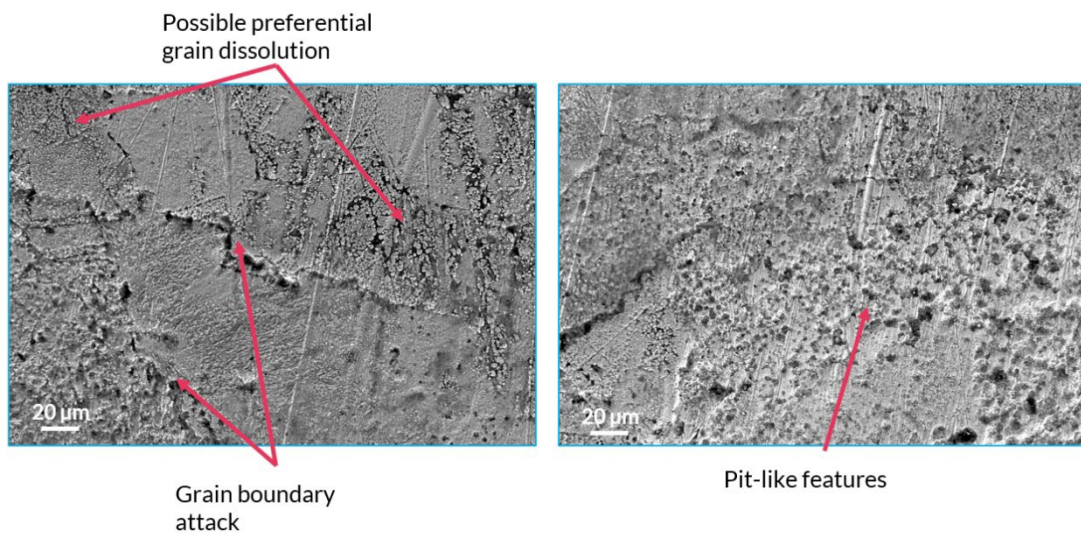


Figure 3-7. Magnified areas from Figure 3-6. Examples of preferential grain dissolution and pit-like features are indicated. Note that not all affected areas have been marked.

The specimen C4-2 was further examined by cross sectional analysis using SEM/EDS (see Figure 3-8), approximately from the areas previously examined by surface analysis. The specimen was cut at a low speed using a precision cutting machine and no cutting fluid. The bottom side's (as shown in Figure 3-8) cross section (see Figure 3-9) generally exhibited fewer pit-like features than the top side (heavily covered in bentonite deposits, see Figure 3-10). Complementary SEM images are shown in the Appendix of this report.

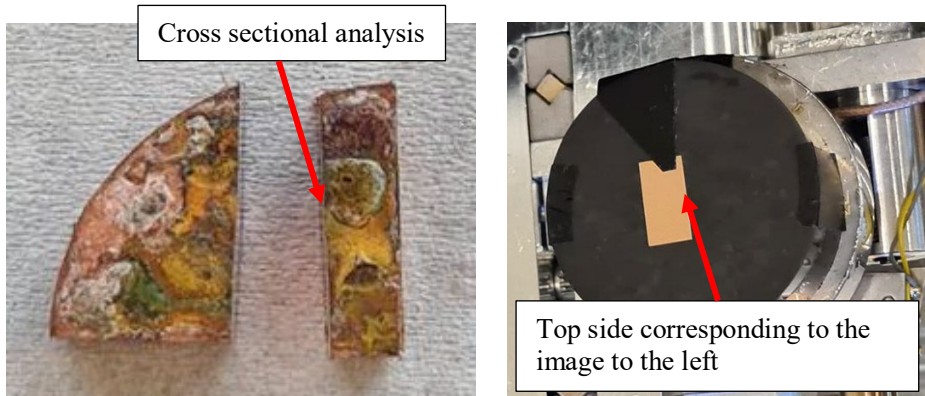


Figure 3-8. Left: Cross section of specimen C4-2. Right: Mounted sample in conductive medium.

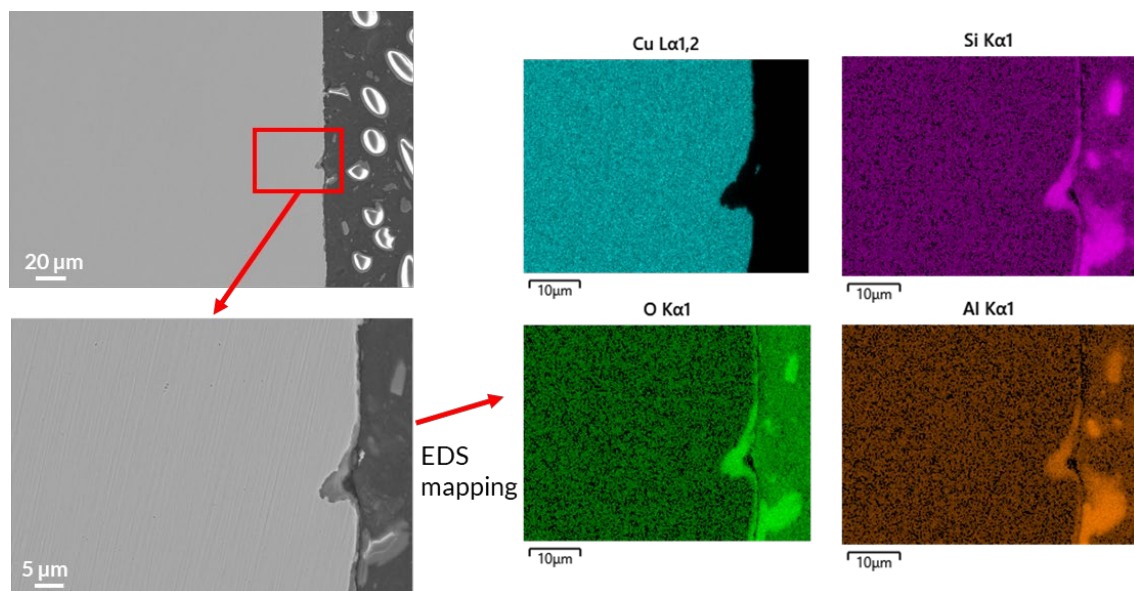


Figure 3-9. SEM/EDS analysis of cross section of specimen C4-2. Side corresponding to the bottom of the left image in Figure 3-8.

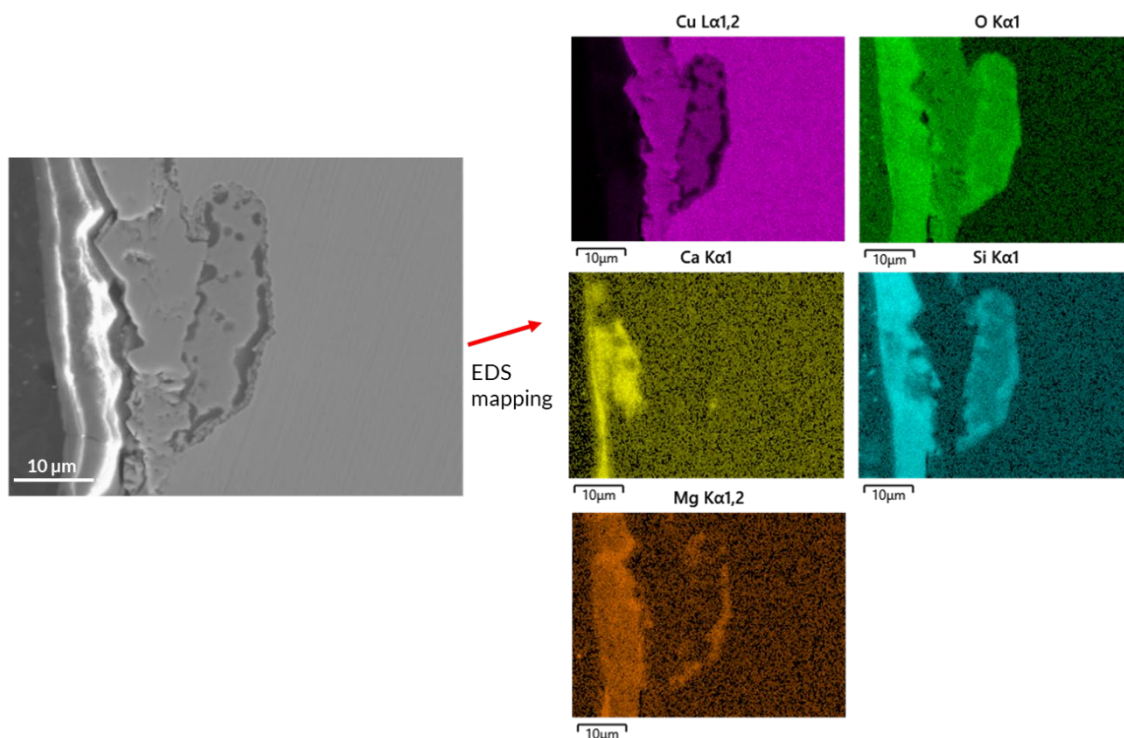


Figure 3-10. SEM/EDS analysis of cross section of specimen C4-2. Side corresponding to the top of the left image in Figure 3-8.

3.4 Results from XRD

The XRD analyses were performed on specimens C1-3, C2-3, C3-4, C4-2, C5-3, C6-3, C7-3, and C8-3 at areas approximately defined by the images in Appendix section 7.2 (equivalent areas were examined by SEM/EDS).

The XRD analysis (Figure 3-11) generally showed copper and copper oxide (cuprite Cu_2O) in most of the samples. The patterns are individually normalized to visualize the lower intensity peaks. The highest intensity peaks are in all specimens the ones corresponding to the base copper.

The specimen C3-4 Area 2 had one peak at approximately $2\theta = 25.4^\circ$ that matches with the double peak with highest intensity of the anhydrous form of gypsum. Minor peaks between $0-20^\circ$ were not indexed. Other phases specifically atacamite, paratacamite, or malachite were not identified in any sample. No copper sulphides were identified in any sample.

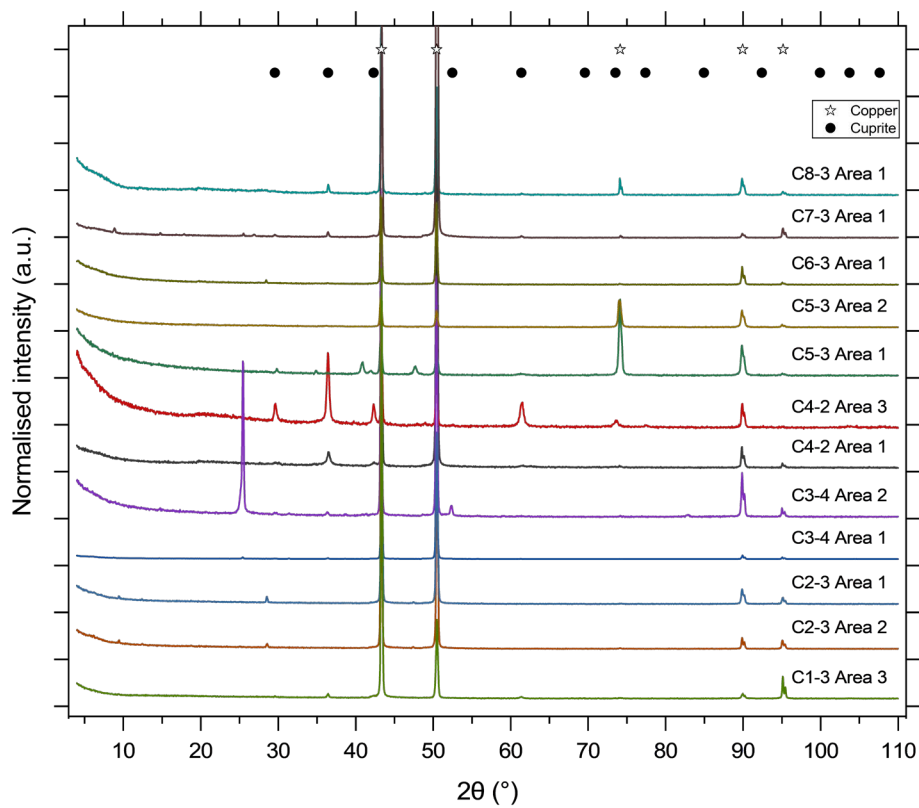


Figure 3-11. Normalised intensity of XRD patterns for the investigated specimens. One or two areas of each specimen were analysed and reported in the stacked plot. The designated "Areas" correspond to the images shown in the Appendix.

3.5 Results from the gravimetric analysis

The appearance of the pickled specimens was somewhat tarnished, nonetheless the pickling process indicates that the cleaning was complete. This means that further pickling does not seem to remove any corrosion products, i.e. the last stage in the stepwise pickling process gave approximately the same mass as the step before (see methodology section for details about the pickling procedure). Table 6 shows the results from the gravimetric analysis.

Table 3-5. Results from the gravimetric analysis. Three samples from each cylinder were chosen for mass loss analysis. See the accompanying Appendix for pickling curves.

Specimen	C1-1	C1-2	C1-3	C1-4	Average
Mass loss [g]	0.00045	0.00025	NA	0.00043	0.00038
Mass loss [g/m²]	1.10	0.62	NA	1.05	0.92
Specimen	C2-1	C2-2	C2-3	C2-4	Average
Mass loss [g]	0.00084	0.00051	NA	0.00095	0.00077
Mass loss [g/m²]	2.05	1.24	NA	2.31	1.87
Specimen	C3-1	C3-2	C3-3	C3-4	Average
Mass loss [g]	0.00034	0.00095	0.00030	NA	0.00053
Mass loss [g/m²]	0.83	2.31	0.73	NA	1.29
Specimen	C4-1	C4-2	C4-3	C4-4	Average
Mass loss [g]	0.00487	NA	0.00178	0.00291	0.00319
Mass loss [g/m²]	11.93	NA	4.36	7.12	7.80
Specimen	C5-1	C5-2	C5-3	C5-4	Average
Mass loss [g]	0.00054	0.00037	NA	0.00057	0.00049
Mass loss [g/m²]	1.31	0.91	NA	1.38	1.20
Specimen	C6-1	C6-2	C6-3	C6-4	Average
Mass loss [g]	0.00060	0.00046	NA	0.00035	0.00047
Mass loss [g/m²]	1.47	1.11	NA	0.85	1.14
Specimen	C7-1	C7-2	C7-3	C7-4	Average
Mass loss [g]	0.00021	0.00022	NA	0.00036	0.00026
Mass loss [g/m²]	0.51	0.53	NA	0.89	0.64
Specimen	C8-1	C8-2	C8-3	C8-4	Average
Mass loss [g]	0.00210	0.00134	NA	0.00135	0.00159
Mass loss [g/m²]	5.13	3.28	NA	3.29	3.90

3.6 Results from surface analysis (Alicona)

The surface was characterized using an infinite focus microscope (Alicona®) and data analyzed using the software Mountains Map® (Table 7). In this report, line roughness parameters are reported including Average roughness (Ra) along with Rz of a random line (average value of maximum peak to valley height of a line measurement) for all samples. An example of such an analysis is provided in Figure below, where the z-heights along the line profile can be seen. An ISO 4287 based methodology was followed for estimating the line roughness parameters. See Figure 3-13 for a schematic defining these values.

The difference in roughness before and after exposure and pickling was generally of one order of magnitude, with the exception of specimens C4-1 and C6-1.

The surface topography of the specimens is reported in the Appendix.

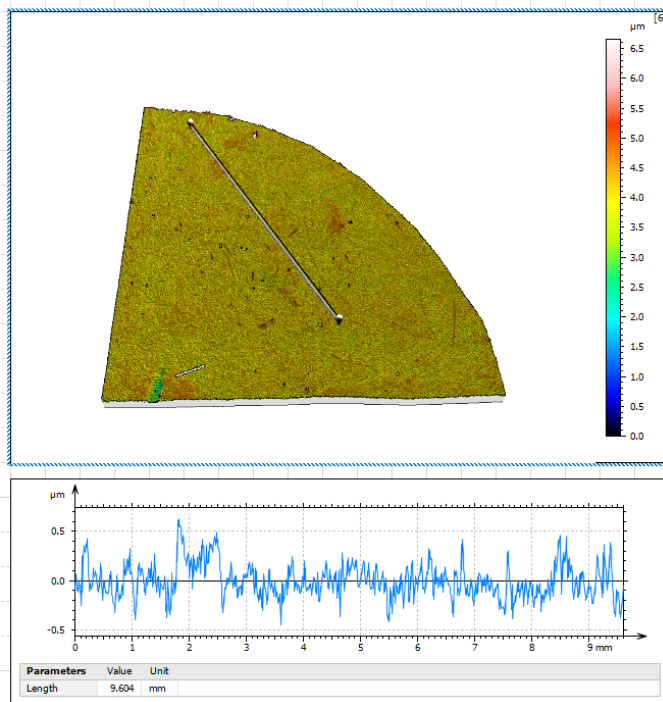


Figure 3-12. Example of a line profile drawn on the surface of exposed and pickled sample C5-1 (bottom side). Image from software MountainsMap.

Table 3-6. Roughness of specimens before and after exposure.

Sample ID	Before exposure		After exposure and pickling		Difference	
	Rz [μm]	Ra [μm]	Rz [μm]	Ra [μm]	Rz [μm]	Ra [μm]
C1-1 backside	0.06	0.01	0.35	0.07	0.29	0.06
C1-1 topside	0.06	0.01	0.73	0.1	0.67	0.09
C2-1 backside	0.09	0.02	1	0.18	0.91	0.16
C2-1 topside	0.08	0.02	0.37	0.08	0.29	0.06
C3-1 backside	0.10	0.02	0.79	0.13	0.69	0.11
C3-1 topside	0.10	0.02	0.5	0.09	0.40	0.07
C4-1 backside	0.07	0.02	1.73	0.29	1.66	0.27
C4-1 topside	0.07	0.01	11.23	1.2	11.16	1.19
C5-1 backside	0.11	0.02	0.71	0.11	0.60	0.09
C5-1 topside	0.11	0.03	0.47	0.09	0.36	0.06
C6-1 backside	0.09	0.02	2.37	0.4	2.28	0.38
C6-1 topside	0.08	0.02	0.57	0.11	0.49	0.09
C7-1 backside	0.08	0.02	0.81	0.12	0.73	0.10
C7-1 topside	0.08	0.02	0.75	0.12	0.67	0.10
C8-1 backside	0.14	0.03	0.94	0.15	0.80	0.12
C8-1 topside	0.10	0.02	0.7	0.11	0.60	0.09

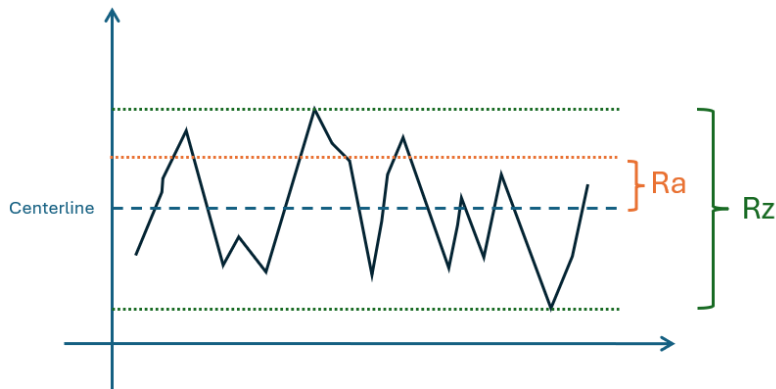


Figure 3-13. Schematic showing the definition of Ra and Rz. Ra corresponds to the average value of roughness from the software-defined centreline for the whole surface. Rz is the average value of maximum peak to valley heights within a number of sampling lengths of a line measurement.

3.7 Infrared Spectroscopy Results

Infrared spectroscopy measurements were performed within the marked area on the black top on sample C5-3, see Figure 3-14. The spectra obtained by ATR-measurements are shown in Figure 3-15. At higher wavenumbers, IR-bands due to stretching vibrations from hydroxyl groups for bentonite are seen at 3621 cm^{-1} and water at 3388 cm^{-1} . C-H vibrations from organic contamination are seen clearly. A OH-bending band for water is present at 1633 cm^{-1} . Bands due to carbonate and Si-O vibrations due to bentonite are seen in the region from $1500\text{--}500\text{ cm}^{-1}$, see Table 3-7 for band assignments. Metal-S vibrations in sulphides are often seen in the far-IR region $500\text{ to }100\text{ cm}^{-1}$ (Brusentsova et al. 2012). It could be possible that the band 438 and 208 cm^{-1} have contributions from Cu-S vibrations due to copper-sulphide compounds, although the assignment to sulphide is quite uncertain. It has been reported that the transmission IR-spectra for CuS and Cu_2S are largely featureless (Brusentsova et al. 2012, Kendix 2009). Here, we can see strong relatively distinct and broad bands in the far-IR region. It is also possible that bentonite have bands in the far-IR region, including lattice vibrations as seen in various silicates (Farmer 1974). Measurements of bentonite references should be performed as well as for copper sulphides.



Figure 3-14. Side of specimen C5-3. The blue rectangle indicates the area where infrared spectroscopy measurements were performed.

The reflection spectra obtained with the multireflection accessory have large problems with baseline bending and inverted bands at low wavenumbers which makes the interpretation and correction of data (such as baseline correction) difficult (see Figure 3-16). The spectra obtained with specular reflection measurements with the microscope do not cover wavenumbers below 400 cm^{-1} where vibrational bands due to sulphides can be found (see Figure 3-17).

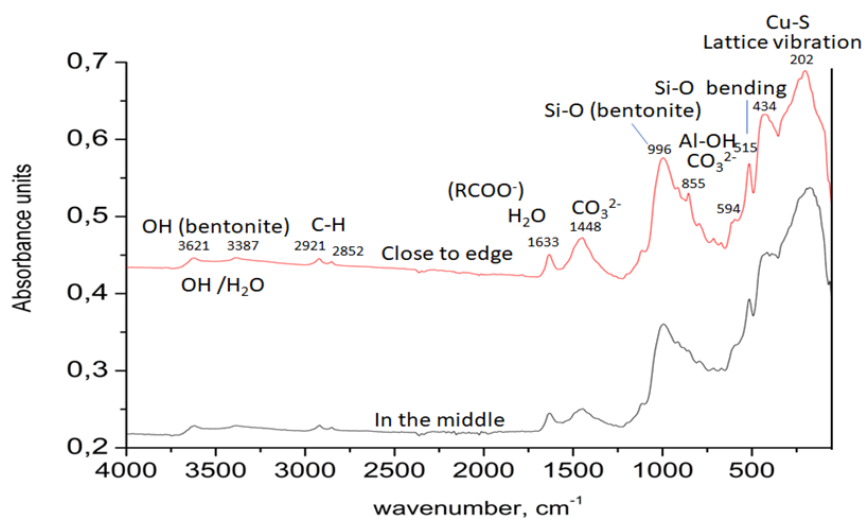


Figure 3-15. FTIR-ATR spectra of sample in the region $50\text{--}4000\text{ cm}^{-1}$. Red spectrum was measured close to samples edge and black spectrum on the middle of the studied area.

Table 3-7. Peak and band assignments of ATR-spectra of the sample.

Maxima, cm^{-1}	Assignments
3620	O-H stretching (hydroxyl bentonite)
3388	O-H stretching (water, hydroxyl)
2920, 2851	C-H stretching
1633	O-H bending (water) (carboxylate RCOO^-)
1448	CO_3^{2-} asymmetric stretch (CaCO_3)
1114	Si-O stretching (Bentonite), (S-O stretching (SO_4^{2-}))
996	Al-OH bending, Si-O stretching (Bentonite), (S-O stretching (SO_4^{2-}))
915	Al-OH bending, Si-O stretching (Bentonite)
864	CO_3^{2-} deformation
799	Si-O stretching (Bentonite)
714	CO_3^{2-} deformation
594	Si-O bending, Cu_2O
515	Si-O bending
438	Si-O bending, Cu-S ?
330 sh	Lattice vibrations, Cu-S ?
205	Lattice vibrations, Cu-S ?
107 sh	Lattice vibrations, Cu-S ?

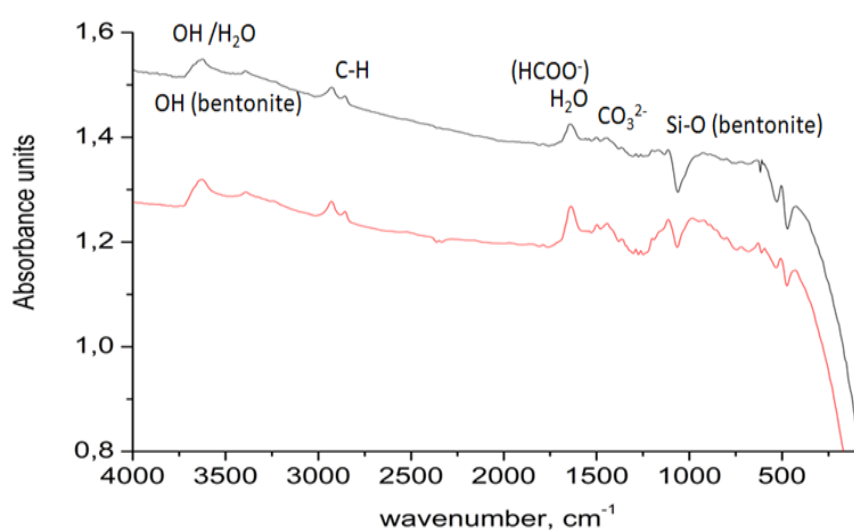


Figure 3-16. FTIR specular reflection spectra obtained in the region $50\text{--}4000\text{ cm}^{-1}$ measured with multireflection accessory. The black and red spectra correspond to two different areas measured within the marked area.

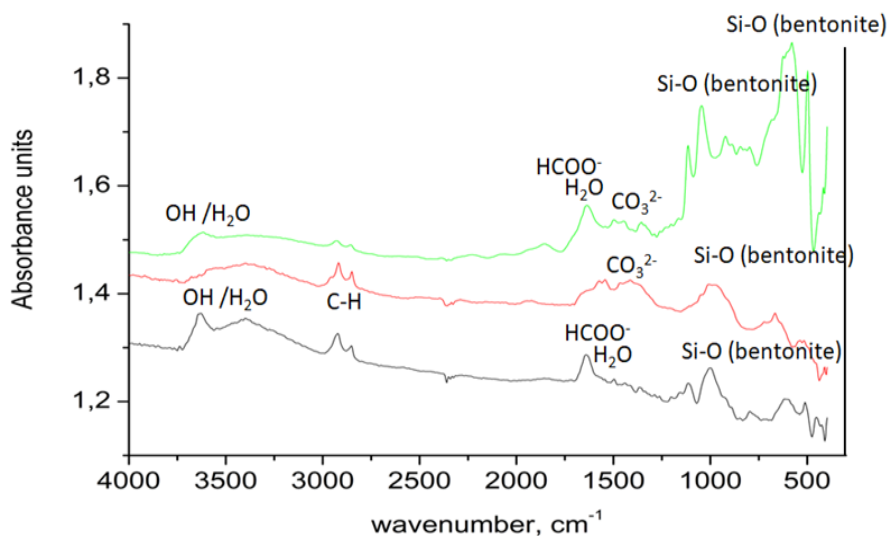


Figure 3-17. FTIR specular reflection spectra obtained in the region $400\text{--}4000\text{ cm}^{-1}$ measured with microscope. The green, red and black spectra correspond to three different areas measured within the marked area.

3.8 Raman Spectroscopy Results

Nine (9) various areas on the blackened edge of sample C5-3 were measured with Raman spectroscopy (see Figure 3-1, the total area is approximately the one indicated by the green square, all spectra is taken from inside this area). An example of the Raman spectrum taken from Area 9 is shown in Figure 3-18. The remaining spectra (Areas 1-8) are presented in the Appendix of the present report. Additionally, Raman mapping was carried out on area 10 (inside the green square in Figure 3-1). The Raman maps and characteristic spectra are shown in Figure 3-19. The identified Raman maps most likely correspond to a mix of two copper oxides, such as CuO (shown in red) and Cu₂O (shown in green).

The conducted Raman measurements indicate that most of the studied areas have characteristic Raman features for copper oxides Cu₂O (often, 8 out of 9 studied areas) and CuO (seldom, 1 out of 9 studied areas). There is also a possibility that hydrated copper chloride (CuCl₂·2H₂O) is formed on the surface, since some characteristic bands can overlap with the Cu₂O.

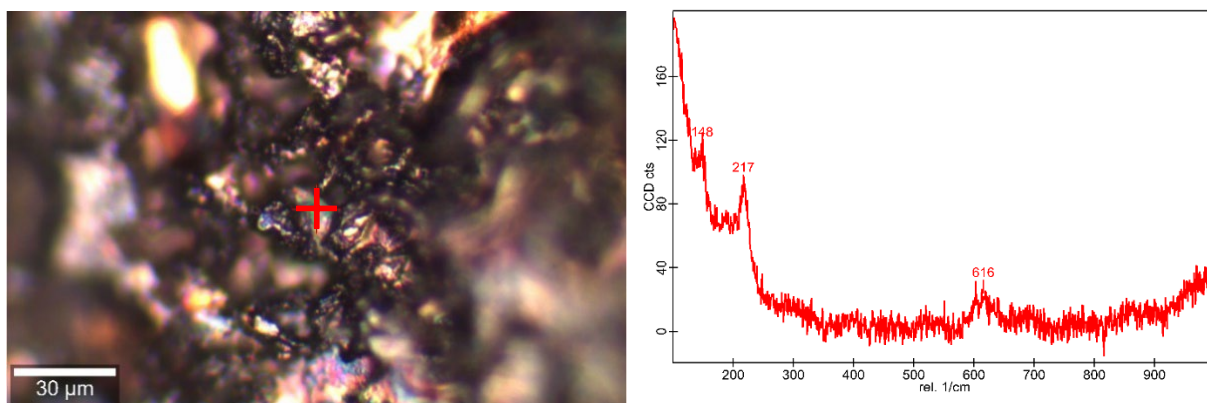


Figure 3-18. Area 9. Left: The studied area where the spectrum was measured is marked with a red cross (optical image). Right: Measured Raman spectrum.

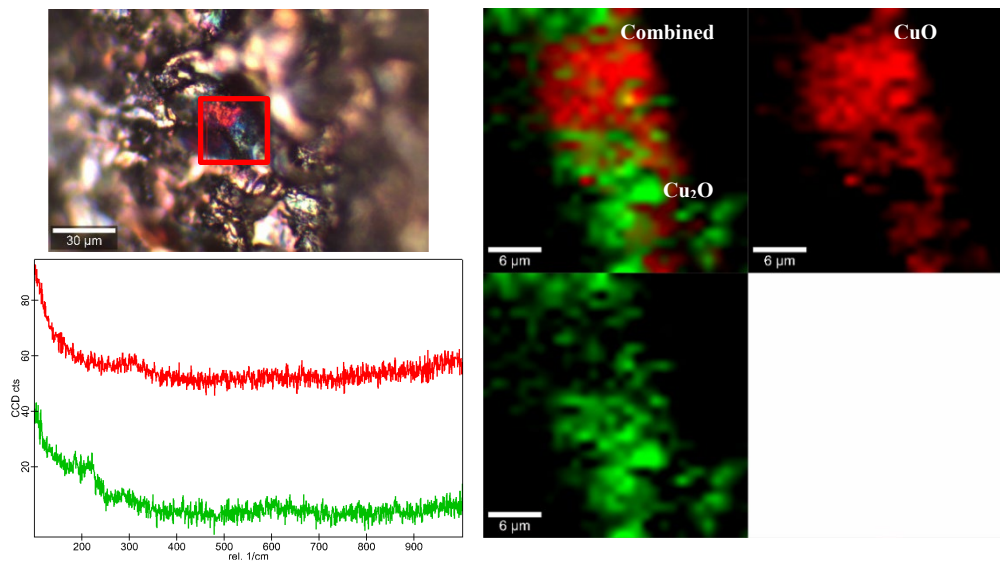


Figure 3-19. Top left: Optical image showing the studied area for the mapping (red square). The reconstructed Raman maps for combined and individual signal map (CuO shown in red and Cu₂O shown in green) are shown to the right. The measured typical spectra used to reconstruct the maps are also shown (CuO shown in red, Cu₂O shown in green).

4 Discussion

Oxygen free copper specimens were exposed for 6 and 12 months in compacted bentonite by SKB. The specimens were then examined by RISE AB by different techniques. This report corresponds to a “results report” that summarizes the findings and briefly discusses them in the following paragraphs.

With respect to mass loss, the gravimetry analysis showed no clear correlation between the exposure period and the mass loss. Additionally, the pickling and cleaning process had several complications (especially in the case of C4 and C8 specimens) due to the adhesion of bentonite to the specimens and difficulty in its removal. In general, the specimens appeared stained after pickling (see Alicona results in the Appendix), however no further cleaning cycle attempts were made to avoid excessive mass loss of metallic copper. Asha bentonite specimens (C4 and C8) exhibited the largest mass losses of all the specimens. These mass losses could have been affected by oxygen possibly having been present at the beginning of the exposures.

Specimen C4-2 (non-pickled) was examined a second time using SEM, with special attention to the surface underneath bentonite deposits. Pit-like features and possibly preferential dissolution of certain grains were observed, as well as intergranular attack. The cross section of C4-2 revealed heavier pitting-like features on the side with more bentonite deposits, suggesting a link between the type of bentonite and the observed degradation.

A structure resembling pitting corrosion was observed in specimen C8-3. The appearance of the pitting resembles the so-called “ant-nest” corrosion, which affects copper and its alloys in different industrial applications. It is however mostly associated with the presence of formic acid (Corbett and Elliott 2000). The observed pits could have been formed entirely during the exposure or possibly constitute slightly corroded cavities from pre-exposure defects in the material. However, existence of pre-exposure defects would not by itself explain the difference in observed pits, depth and frequency, between the various bentonite qualities. The EDS analysis of that area showed little to negligible amounts of corrosion products. The area was not covered in bentonite either, which suggests that a dissolution mechanism might have taken place. If bentonite was present at the pitted area, copper could conceivably have migrated into the bentonite by some kind of ion exchange. The corroded copper could be transported out of the cavity as dissolved ions or complexes. Copper in dissolved form from corrosion usually requires oxidizing conditions. Oxidizing conditions generates Cu(I) in the forms: Cu^+ , $\text{CuOH}(\text{aq})$, $\text{Cu}(\text{OH})^{-2}$, but mostly as chloride complexes. While Cu(II) in the forms: Cu^{2+} and in hydroxide, carbonate and sulphate complexes. Dissolved oxygen is usually the oxidant for these corrosion products. However, pit-like features can also form during reducing conditions when sulphide is present at a concentration in the order of 1mM, as HS^- (Taxén et al. 2023). In this case, the oxidant could be water. The oxidant can also be copper (e.g. solid copper oxide). Simultaneous presence of dissolved oxygen and dissolved sulphide does not seem likely. It is recommended to perform cross sections of the affected areas to study the phenomena further, whether the pits have penetrated into the bulk and if there are corrosion products present there. It is recommended as well to perform a compositional analysis on the Asha bentonite used for this exposure, to determine if there was any noticeable increase in Cu content. Laser Ablation Inductively Coupled Plasma Mass Spectrometry (LA-ICP-MS) or possibly GDOES on the bentonite surface could give a copper profile, perpendicular to the metal surface.

Samples exposed to bentonite MX-80 had sulphur signals in connection with calcium. The XRD analysis however does not clearly show the presence of calcium sulphate on these samples (COD 2300259), however there is an indication of the presence of the anhydrous form anhydrite (COD 5000040) at $2\theta = 25.4^\circ$. Further analysis using FTIR or Raman techniques is recommended to rule out the presence of sulphides at the darkened rim of sample C5-3. Additionally, zinc was observed on the outer surface of C5-3 but not on C1-3 using EDS analysis. There are however overlapping peaks between zinc and sodium (Zn $L\alpha = 1.012$ keV, Zn $L\beta = 1.034$ keV, Na $K\alpha = 1.041$ keV) that might be overestimating the contribution of zinc to the spectra. WDS (wavelength-dispersive spectrometry) analysis is recommended to distinguish both signals and result in a better quantification.

Higher levels of Cl were detected using EDS in samples exposed with Moroccan bentonite, especially in sample C2-3. EDS point analyses on top of structures that resemble crystals indicate the presence of only Cu and Cl, which suggests the formation of copper chlorides.

Specimens exposed to Calcigel exhibited thick deposits covering most of the surface of the specimen. The high levels of S were observed in connection with Ca, Al and Si, which indicates that there was limited reaction between S and Cu. This limited reaction may be reflected by the observation that S is present mostly as sulphate in Calcigel, e.g. as gypsum. No features such as pits were identified in these samples.

With respect to Layer Probe, the examination before exposure resulted in the detection of a very thin copper layer, which was challenging to identify. The operator lowered the current and voltage, as well as using an extra sensitive EDS detector for light elements. The results however should be interpreted critically, as the accuracy of the measurement could not be properly assessed. The oxide layer thickness before exposure was about 7.4 nm in average. After six months of exposure, the sample had a thicker oxide layer which could be identified with more ease using the software. The operator chose higher energy and voltage to determine the oxide layer thickness. After exposure the value was found to be about 14 nm. Assuming a density of 6 g/cm^3 for Cu_2O and ideal compactness, the 14 nm of Cu_2O corresponds to a copper mass loss of 0.075 g/m^2 which is about one order of magnitude lower than the gravimetry results for the average of C1-1, C1-2 and C1-4 (0.93 g/m^2). It is worth mentioning that gravimetry measurements have associated errors, however this technique is much more well established. Furthermore, we have followed the procedure stated by the ISO standard to minimize such errors. The Layer Probe technique is not well established yet and other techniques are recommended to be used to validate these results. To validate this technique in this range of thickness XPS, Auger or SIMS with ion sputtering can be used in a similar manner to GDOES.

The topography measurements can give a good idea of the roughness values before exposure. However, after exposure and pickling, the scans should focus on certain smaller areas, so the resolution allows for the characterization/measurement of pits or other features of interest, i.e. higher magnification could be used to allow for identification of smaller features.

FTIR measurements on one copper sample (C5-3) were made with ATR- and specular reflection measurements. The results obtained with ATR-measurements seems to provide more easily interpretable information compared to specular reflection measurements on this sample. The ATR-spectra show bands related to bentonite and carbonate, probably CaCO_3 . At wavenumbers below 500 cm^{-1} there are several broad bands which can have contributions from copper sulphide compounds. However, complementary measurements should be performed on references; bentonite(s), CuS , Cu_2S .

With respect to the Raman spectroscopy measurements, nine areas located on the blackened edge of sample C5-3 were measured with high lateral resolutions. Additionally, a Raman map was carried out. The sample's surface is inhomogeneous, demonstrating various colours. The Raman measurement results suggest that both copper oxides (CuO and Cu_2O) are present on the examined areas. There is also a possibility that hydrated copper chloride ($\text{CuCl}_2 \cdot 2\text{H}_2\text{O}$) has been formed on some locations. No copper sulphides, neither CuS nor Cu_2S , have been identified on the examined areas, as there was no clear 474 rel.cm^{-1} band which is a specific and clear band (Parker et al. 2008). As well as for the infrared spectroscopy, reference measurements are recommended to improve the possibility of identifying copper sulphides.

5 Conclusions

Generally it was found that the samples had not corroded during the exposure, as was observed by the appearance of the exposed samples (see Table 3-1) as well as the mass loss analyses (see Table 3-5). The chemical analyses indicated the presence of sulphur in C1 and C5 samples, although mostly in connection with calcium, however no indication of gypsum was identified in the XRD analysis of these samples. Raman spectroscopy of C5-3 specimen gave no indication of copper sulphides, however some bands from the spectra obtained by FTIR could be contributions from copper sulphides. It is recommended to perform complementary Raman and IR analysis on reference samples of Cu_2S and different types of bentonite. Specimens C2 and C6 exhibited high amounts of chlorine in the EDS analysis, with some areas showing signs of the formation of copper chlorides. C3 and C7 specimens contained sulphur in connection with calcium. The XRD analysis of these samples shows an indication of the anhydrous form of gypsum (see Figure 3-11).

Localized corrosion was mainly observed for specimens exposed in Asha bentonite. Both inter-crystalline, pitting corrosion and ant-nest corrosion was found. There are corrosion pits that are not filled by solids which is taken as evidence for aqueous corroded copper. Available analyses do not give any suggestions for the composition of the corrosion products from these local corrosion attacks, neither solid nor dissolved. Green corrosion products which could indicate Cu^{+2} was not found. Chloride or sulphide complexes with Cu^+ could explain the apparent aqueous transport of copper in the corrosion pits. Complexes with HS^- are well known but there may be other forms with sulphur in a higher oxidation state e.g. S^- as in pyrite. Knowledge of the composition of the solid corrosion products seems essential in order to recalculate local corrosion layer thickness to mass loss and local corrosion. A study of copper gradient in the bentonite would also be required. The observed local corrosion cannot be explained without understanding the form in which corroded copper diffuses or migrates out of corrosion pits. The determination of the possible corrosion mechanism is out of the scope of this work as the exposure conditions are not known to the authors.

6 References

SKB's (Svensk Kärnbränslehantering AB) publications can be found at www.skb.com/publications.

Brusentsova T, Peale R E, Maukonen D, Figueiredo P, Harlow G E, Ebel D S, Nissinboim A, Sherman K, Lisse C M, 2012. Laboratory far-infrared spectroscopy of terrestrial sulphides to support analysis of cosmic dust spectra, *Mon. Not. R. Astron. Soc.* 420, 2569–2579.
<https://doi.org/10.1111/j.1365-2966.2011.20228.x>

Corbett R A, Elliott P. 2000. Ant Nest Corrosion - Digging the Tunnels. Paper presented at the CORROSION 2000, Orlando, Florida, March 2000. Paper Number: NACE-00646 Published: March 26.
<http://dx.doi.org/10.5006/C2000-00646>

Deng Y, Handoko A D, Du Y, Xi S, Siang Yeo B, 2016. In Situ Raman Spectroscopy of Copper and Copper Oxide Surfaces during Electrochemical Oxygen Evolution Reaction: Identification of CuIII Oxides as Catalytically Active Species. *ACS Catalysis* 6 (4), 2473-2481.
<http://doi.org/10.1021/acscatal.6b00205>

Farmer V C, 1974. The Infrared Spectra of Minerals. Mineralogical Society.
<https://doi.org/10.1180/mono-4>

Johansson A J, Svensson D, Gordon A, Pahverk H, Karlsson O, Brask J, Lundholm M, Malmström D, Gustavsson F, 2020. Corrosion of copper after 20 years exposure in the bentonite field tests LOT S2 and A3. SKB TR-20-14, Svensk Kärnbränslehantering AB.

Kendix E, 2009. Transmission and Reflection (ATR) Far-Infrared Spectroscopy Applied in the Analysis of Cultural Heritage Materials, Thesis, University of Bologna.

Medeiros F E O, Araújo B S, Ayala A P, 2018. Raman spectroscopy investigation of the thermal stability of the multiferroic CuCl₂ and its hydrated form, *Vibrational Spectroscopy*, Volume 99, Pages 1-6, ISSN 0924-2031. <https://doi.org/10.1016/j.vibspec.2018.08.006>

Parker G K, Woods R, Hope G A, 2008. Raman investigation of chalcopyrite oxidation, *Colloids and Surfaces A: Physicochemical and Engineering Aspects*, Volume 318, Issues 1–3, Pages 160-168.
<https://doi.org/10.1016/j.colsurfa.2007.12.030>

Ravichandiran C, akthivelu A, Deva Arun Kumar K, Davidprabu R, Valanarasu S, Kathalingam A, Ganesh V, Mohd Shkir, Algarni H, AlFaify S, 2019. Influence of rare earth material (Sm³⁺) doping on the properties of electrodeposited Cu₂O films for optoelectronics. *J Mater Sci: Mater Electron* 30, 2530–2537. <https://doi.org/10.1007/s10854-018-0527-6>

Sriyutha Murthy P, Venugopalan V P, Arunya D D, Dhara S, Pandiyan R, Tyagi A K, 2011. Antibiofilm activity of nano sized CuO, *International Conference on Nanoscience, Engineering and Technology (ICONSET 2011)*, Chennai, India, pp. 580-583.
<https://doi.org/10.1109/ICONSET.2011.6168037>

Taxén C, Moya Núñez A, Lilja C. 2023. Stress corrosion of copper in sulfide solutions: Variations in pH-buffer, strain rate, and temperature. *Materials and Corrosion*, 74, 1632–1644.
<https://doi.org/10.1002/maco.202313759>

7 Appendix

7.1 As-received photographs

The following images show the appearance the samples as-received. The samples are 13 mm long on the straight edges and are not cropped to the same scale in the images below. The left image corresponds to the top side of the samples, while the image to the right is the top. Shiny surfaces are often seen where there was no visible deposition of bentonite or other products, and resemble the appearance of the polished surfaces before exposure.



Figure 7-1. C1-1



Figure 7-2. C1-2 (surfaces mostly shiny, glare from the camera lens is visible).



Figure 7-3. C1-3 (surfaces mostly shiny, glare from the camera lens is visible).



Figure 7-4. C1-4 (surfaces mostly shiny, glare from the camera lens is visible).

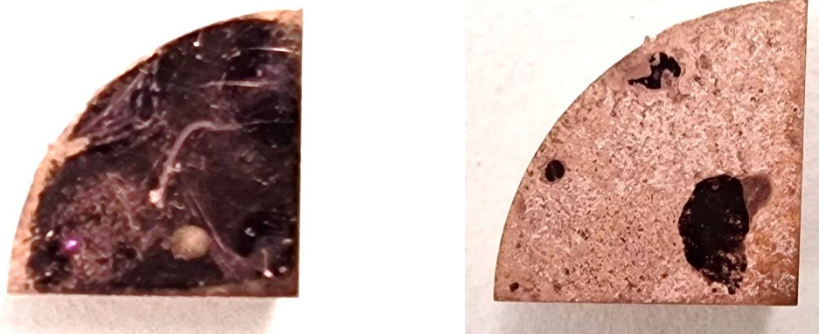


Figure 7-5. C2-1 (surfaces from left image are mostly shiny, glare from the camera lens visible).



Figure 7-6. C2-2 (shiny surfaces appear dark due to camera lens reflection).

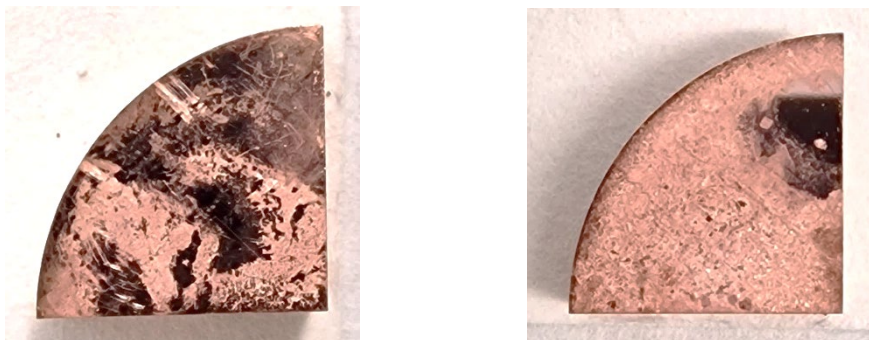


Figure 7-7. C2-3 (shiny surfaces appear dark due to camera lens reflection).

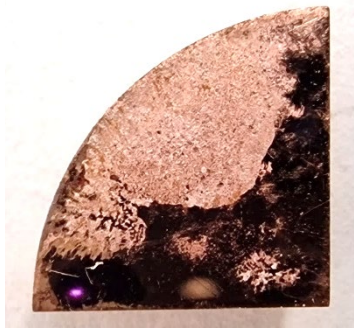


Figure 7-8. C2-4 (glare from camera lens visible).

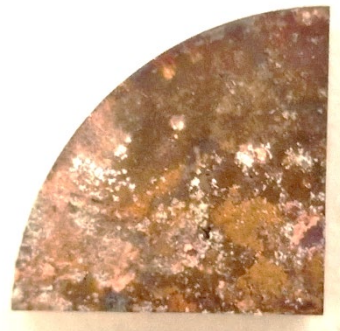


Figure 7-9. C3-1



Figure 7-10. C3-2



Figure 7-11. C3-3



Figure 7-12. C3-4



Figure 7-13. C4-1



Figure 7-14. C4-2





Figure 7-15. C4-3

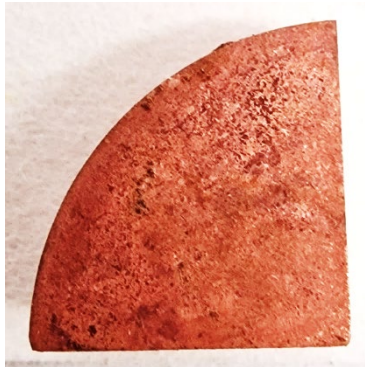


Figure 7-16. C4-4



Figure 7-17. C5-1





Figure 7-18. C5-2



Figure 7-19. C5-3

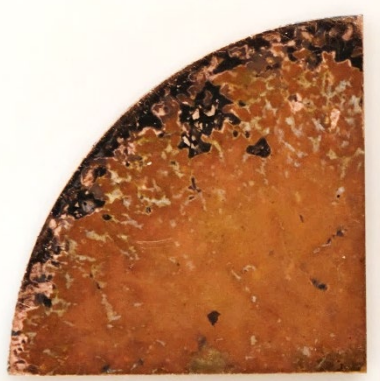


Figure 7-20. C5-4

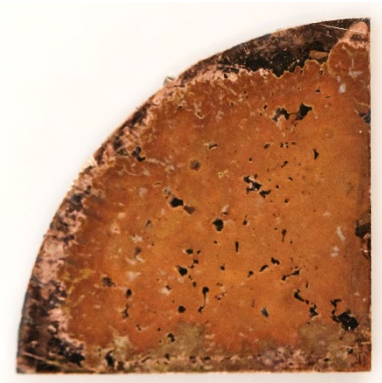




Figure 7-21. C6-1

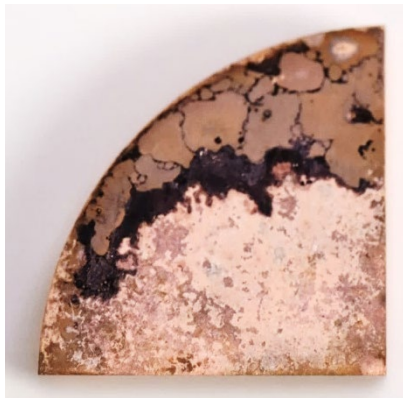


Figure 7-22. C6-2 (shiny areas look black due to camera lens reflection)



Figure 7-23. C6-3 (shiny areas look black due to camera lens reflection)

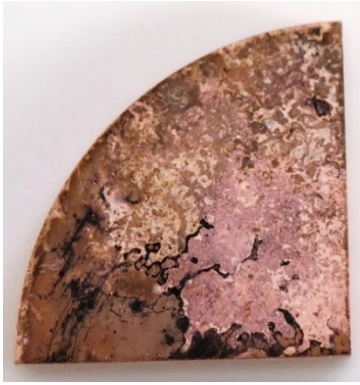


Figure 7-24. C6-4 (shiny areas look dark due to camera lens reflection)



Figure 7-25. C7-1



Figure 7-26. C7-2

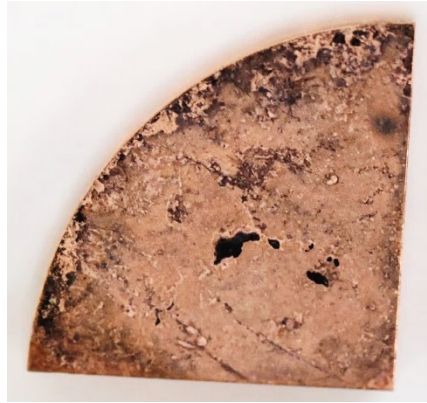


Figure 7-27. C7-3 (shiny areas look black due to camera lens reflection)



Figure 7-28. C7-4



Figure 7-29. C8-1



Figure 7-30. C8-2

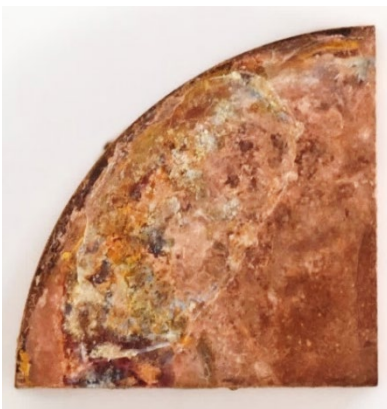


Figure 7-31. C8-3



Figure 7-32. C8-4



7.2 Mass loss plots (gravimetry)

The pickling curves for each specimen are shown below. A linear regression has been done to calculate the mass loss according to ISO 8407. The total pickling time is reported in minutes. Please note that the y-axes are not at the same scale for all plots.

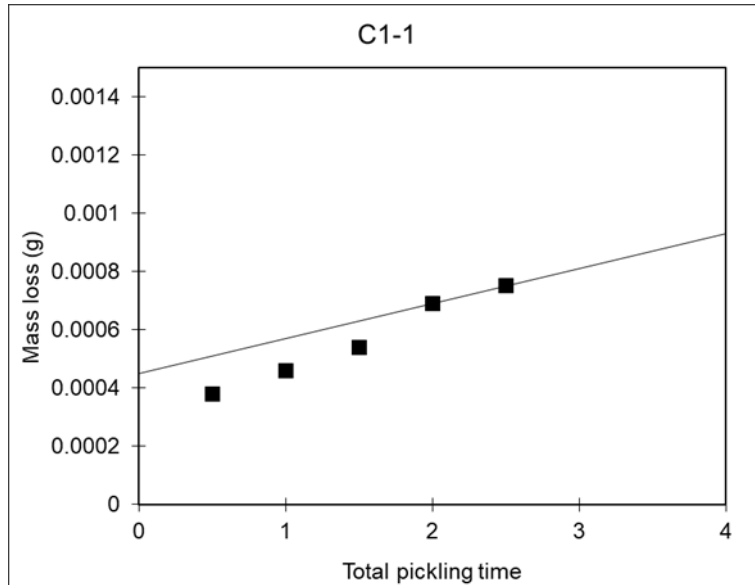


Figure 7-33. Pickling curve for specimen C1-1. Total pickling time in minutes.

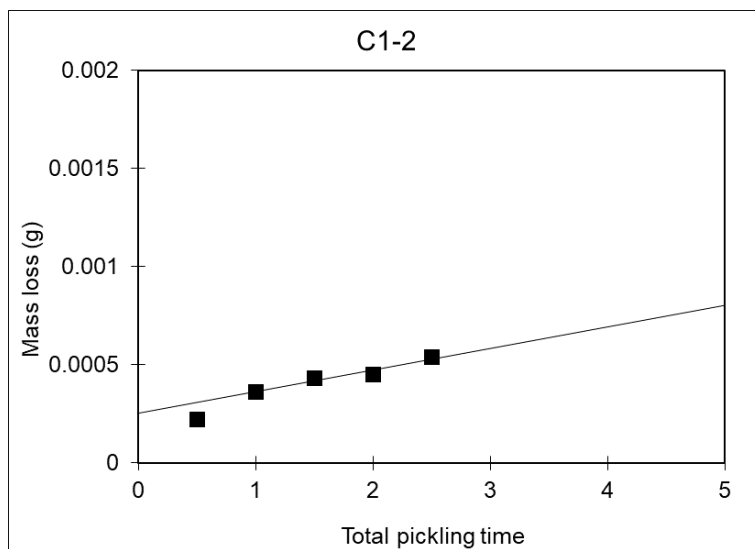


Figure 7-34. Pickling curve for specimen C1-2. Total pickling time in minutes.

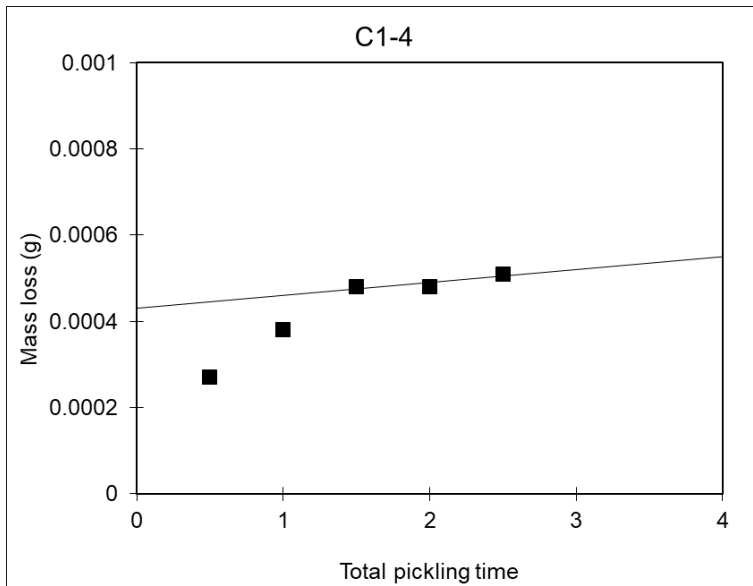


Figure 7-35. Pickling curve for specimen C1-4. Total pickling time in minutes.

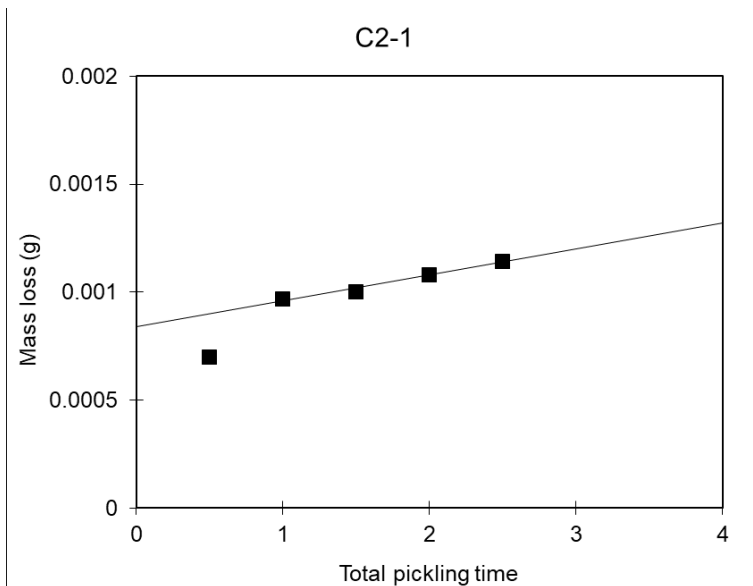


Figure 7-36. Pickling curve for specimen C2-1. Total pickling time in minutes.

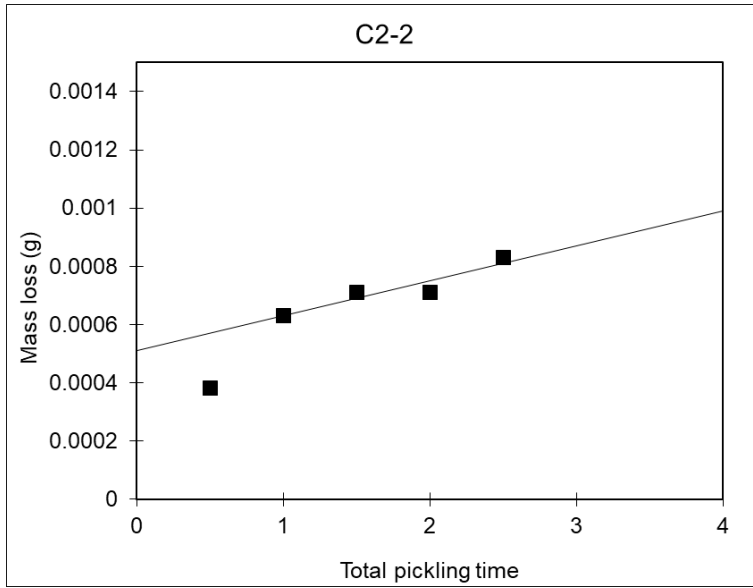


Figure 7-37. Pickling curve for specimen C2-2. Total pickling time in minutes.

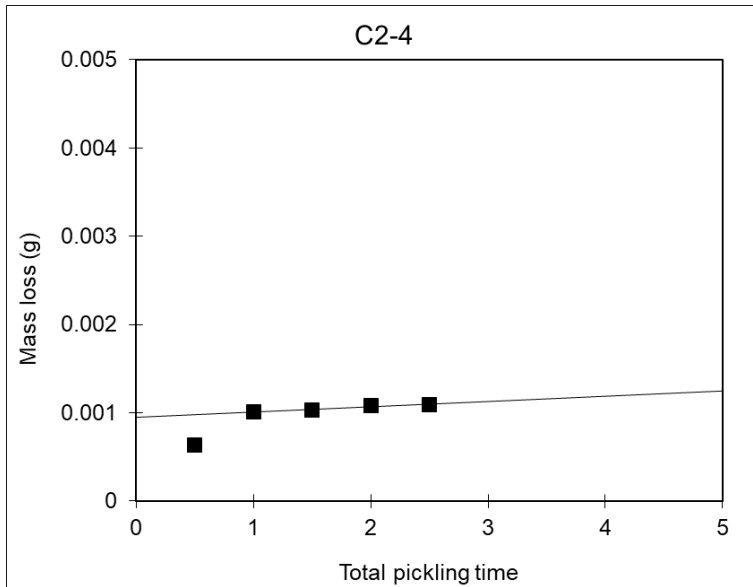


Figure 7-38. Pickling curve for specimen C2-4. Total pickling time in minutes.

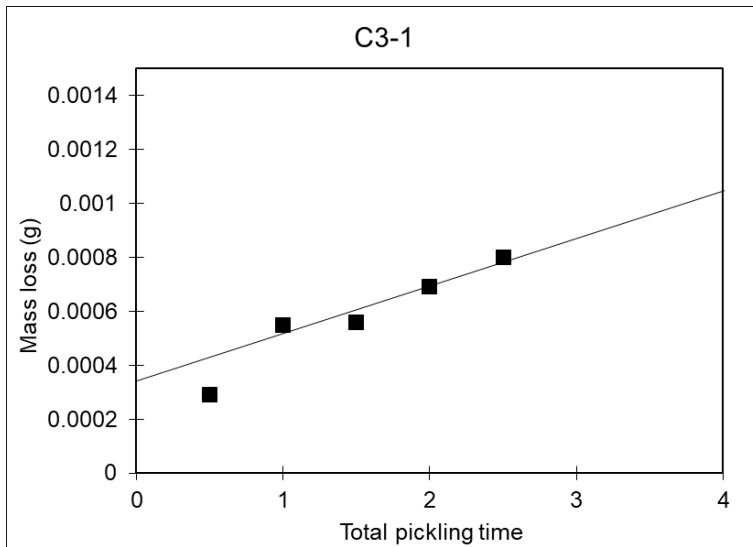


Figure 7-39. Pickling curve for specimen C3-1. Total pickling time in minutes.

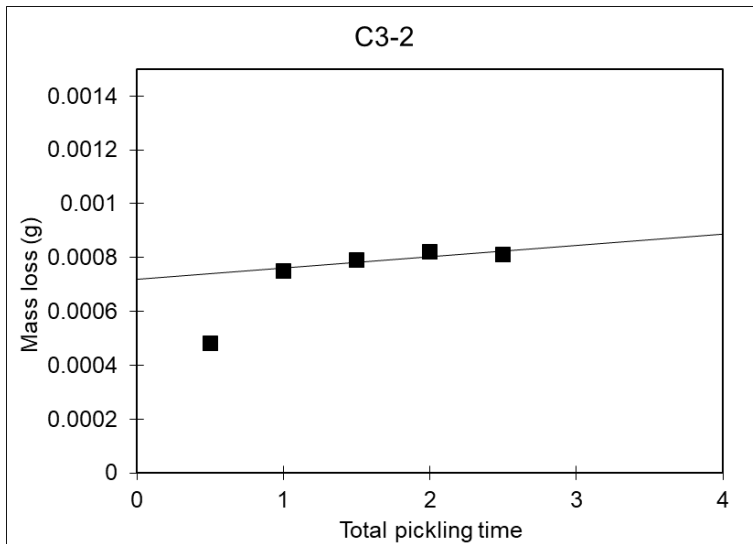


Figure 7-40. Pickling curve for specimen C3-2. Total pickling time in minutes.

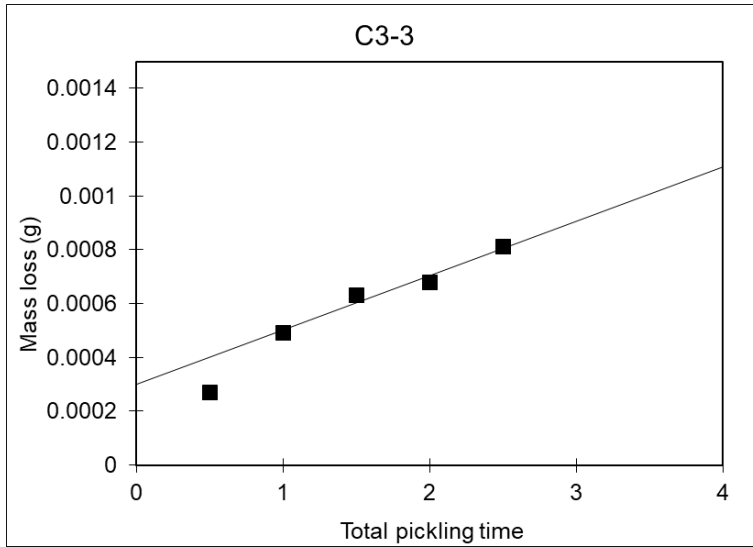


Figure 7-41. Pickling curve for specimen C3-3. Total pickling time in minutes.

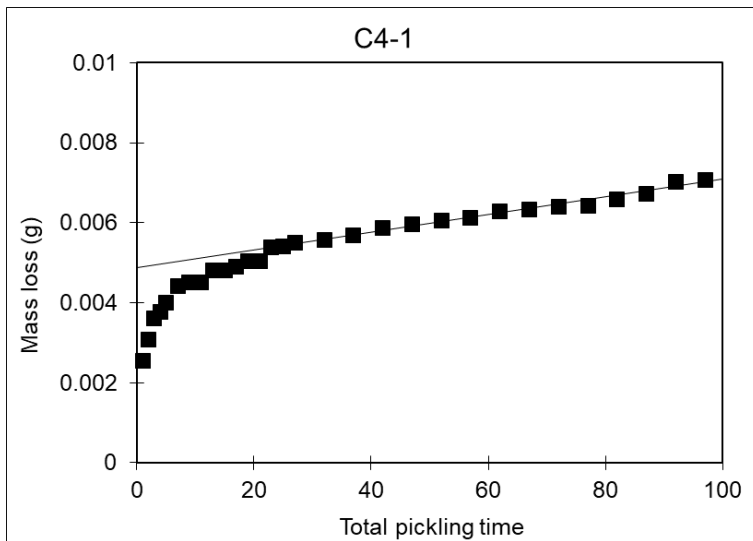


Figure 7-42. Pickling curve for specimen C4-1. Total pickling time in minutes.

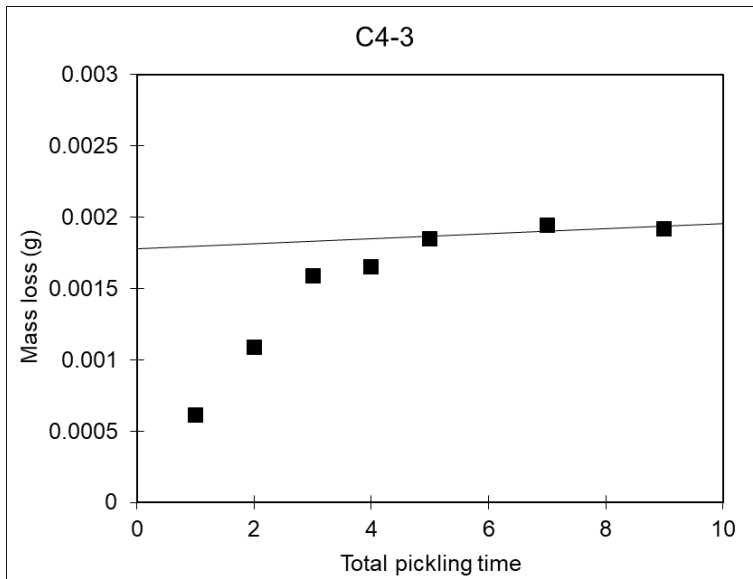


Figure 7-43. Pickling curve for specimen C4-3. Total pickling time in minutes.

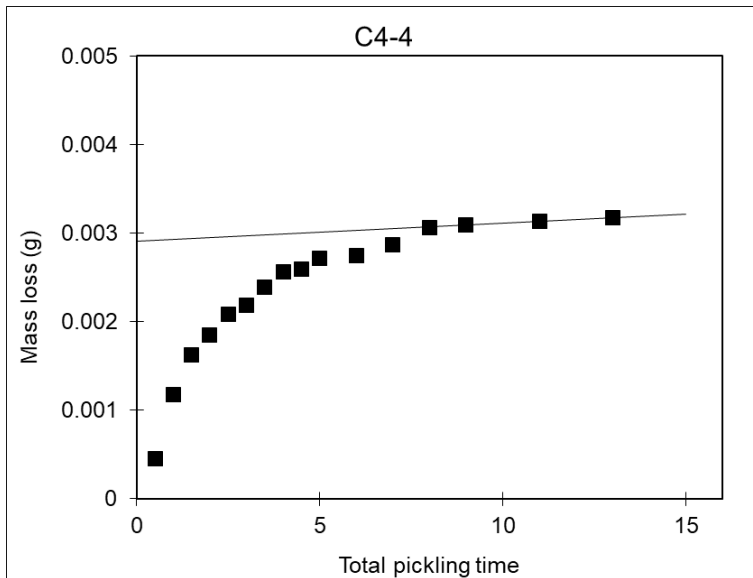


Figure 7-44. Pickling curve for specimen C4-4. Total pickling time in minutes.

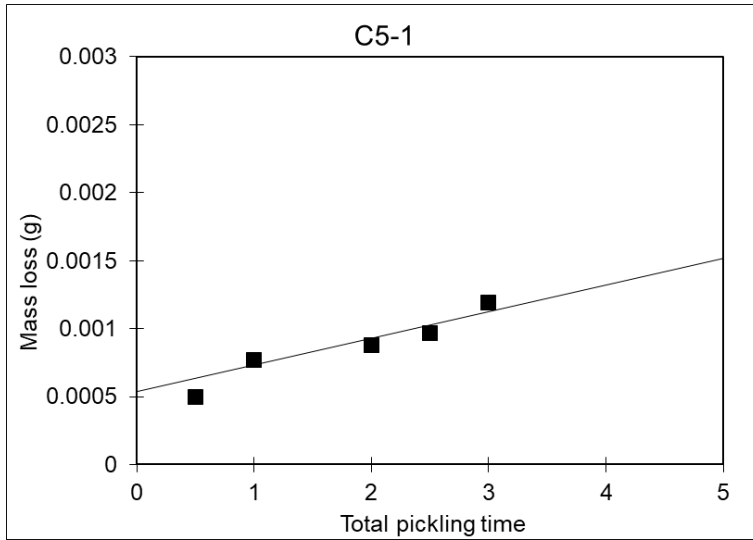


Figure 7-45. Pickling curve for specimen C5-1. Total pickling time in minutes.

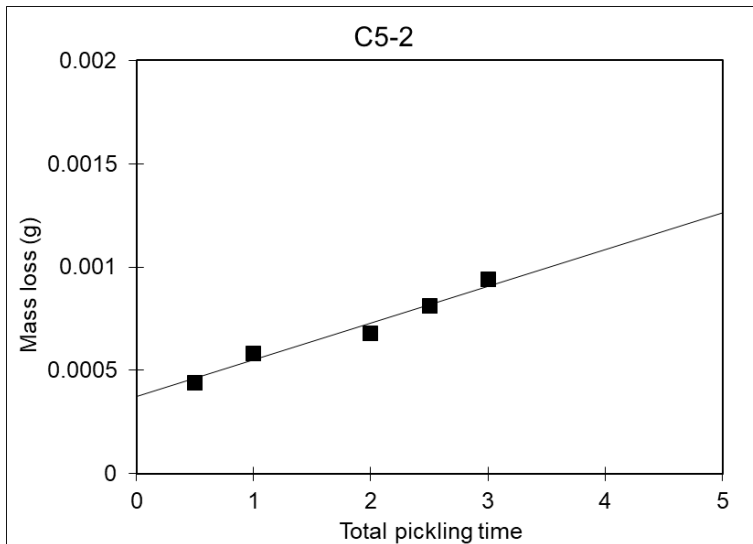


Figure 7-46. Pickling curve for specimen C5-2. Total pickling time in minutes.

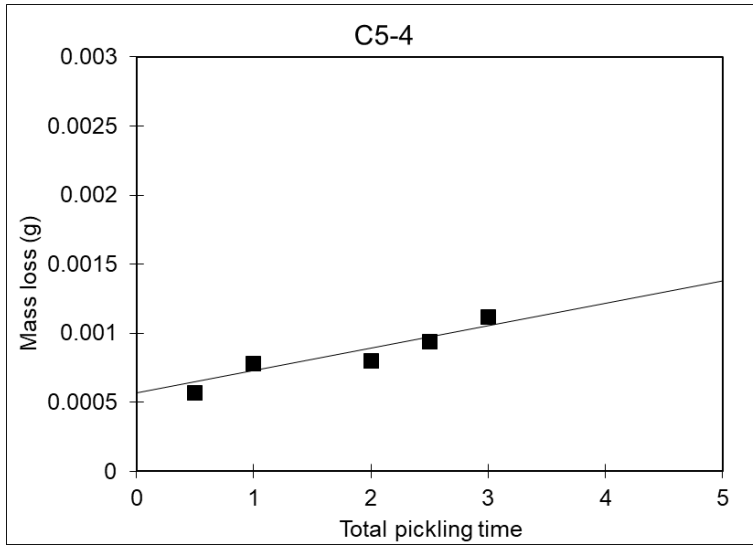


Figure 7-47. Pickling curve for specimen C5-4. Total pickling time in minutes.

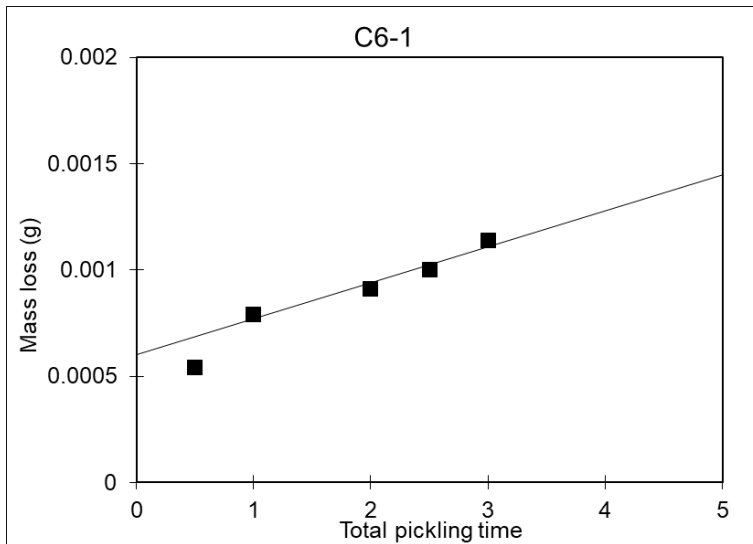


Figure 7-48. Pickling curve for specimen C6-1. Total pickling time in minutes.

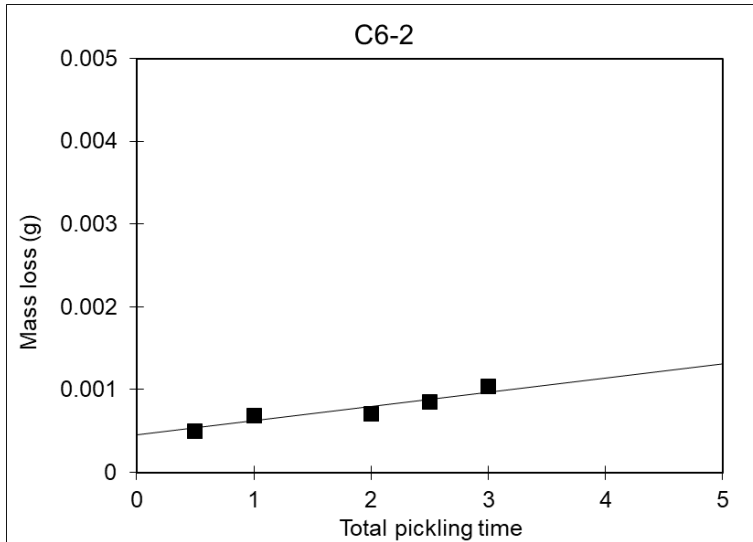


Figure 7-49. Pickling curve for specimen C6-2. Total pickling time in minutes.

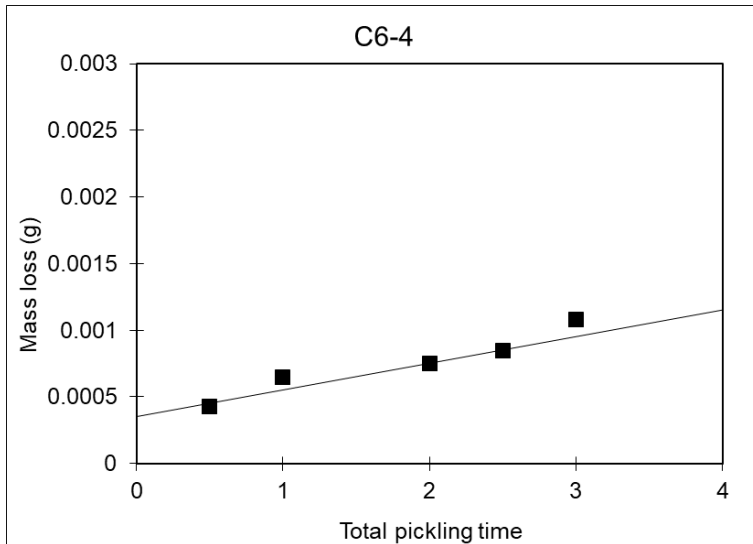


Figure 7-50. Pickling curve for specimen C6-4. Total pickling time in minutes.

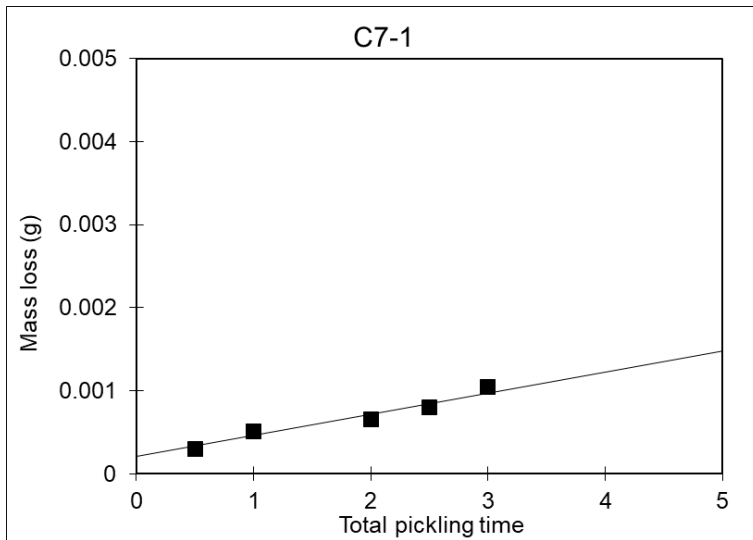


Figure 7-51. Pickling curve for specimen C7-1. Total pickling time in minutes.

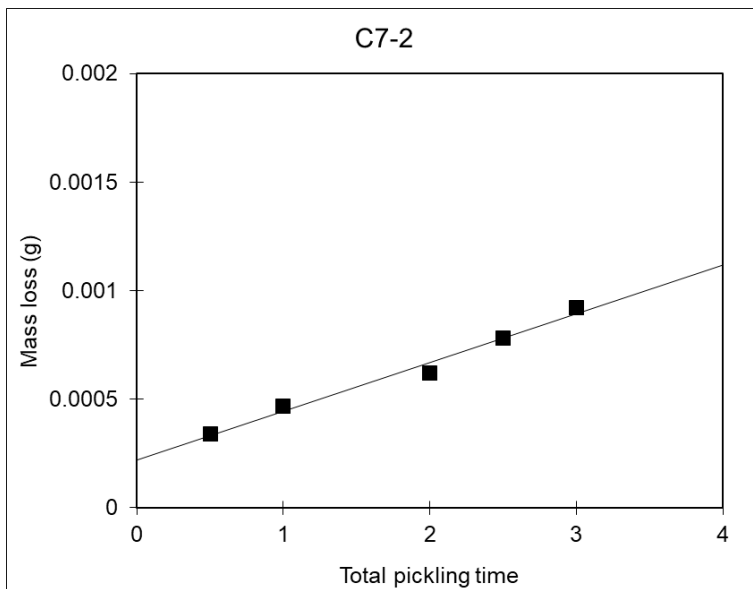


Figure 7-52. Pickling curve for specimen C7-2. Total pickling time in minutes.

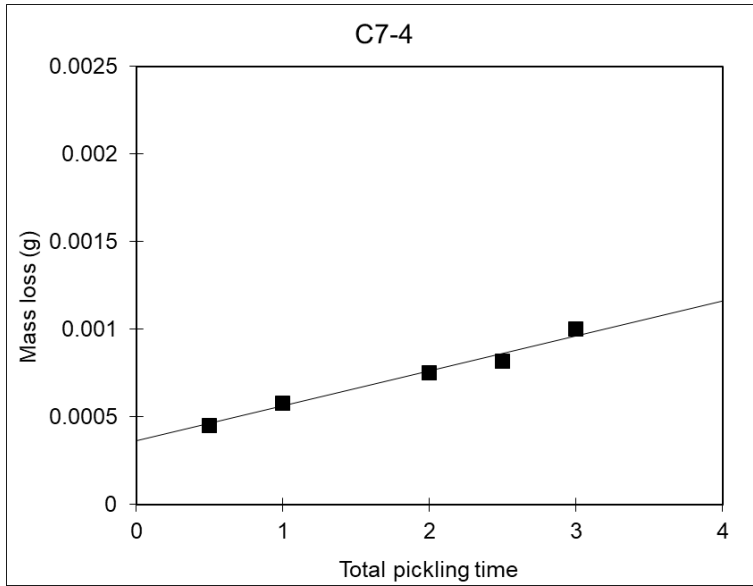


Figure 7-53. Pickling curve for specimen C7-4. Total pickling time in minutes.

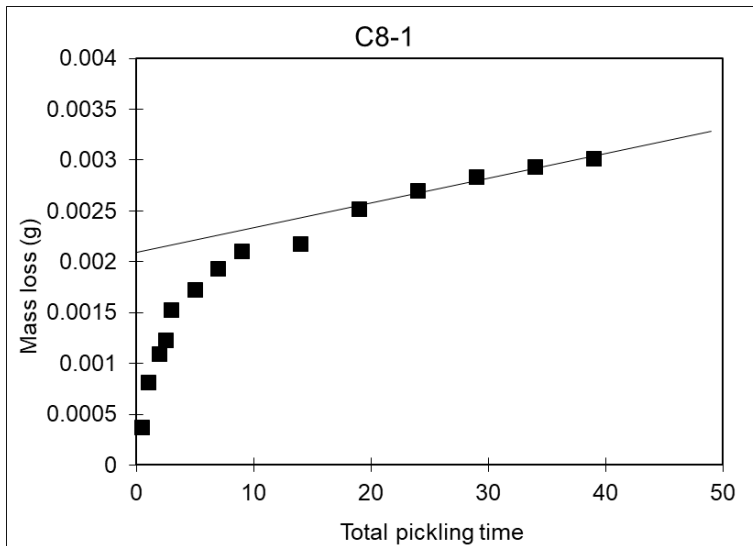


Figure 7-54. Pickling curve for specimen C8-1. Total pickling time in minutes.

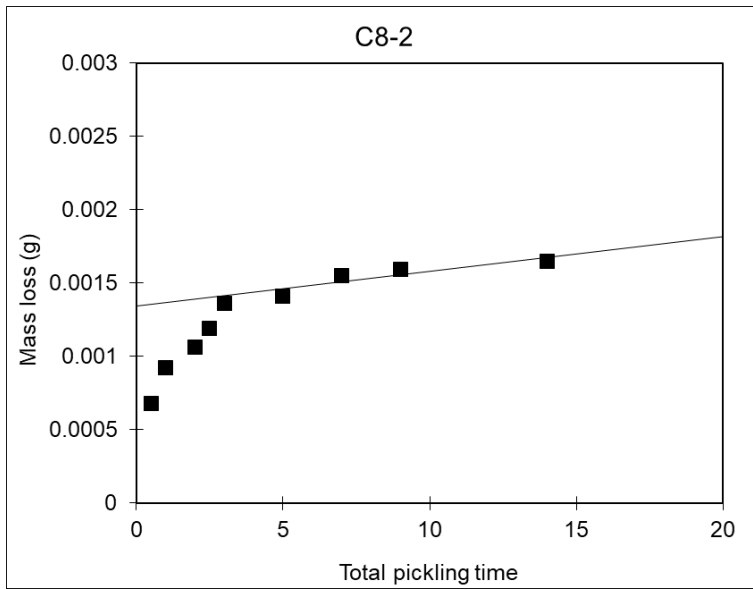


Figure 7-55. Pickling curve for specimen C8-2. Total pickling time in minutes.

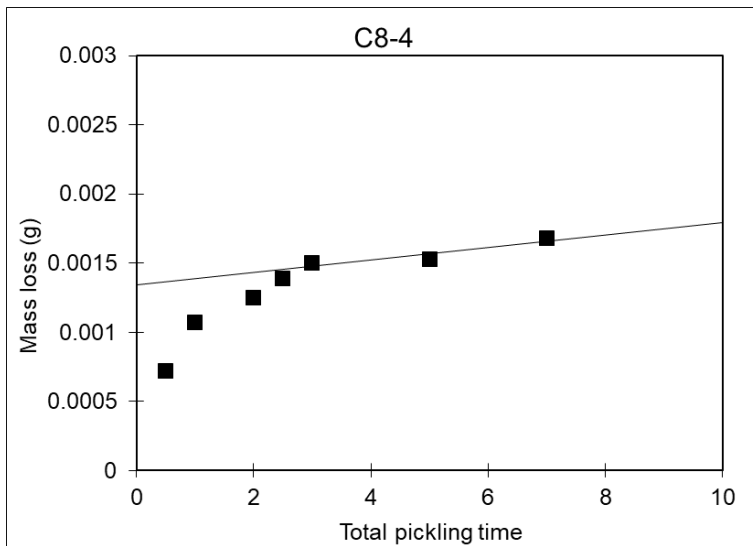


Figure 7-56. Pickling curve for specimen C8-4. Total pickling time in minutes.

7.3 Alicona characterization results

The samples marked CX-1 were examined before and after exposure. This Appendix contains all the results obtained by the surface characterization. The top and bottom of each flat surface was analyzed.

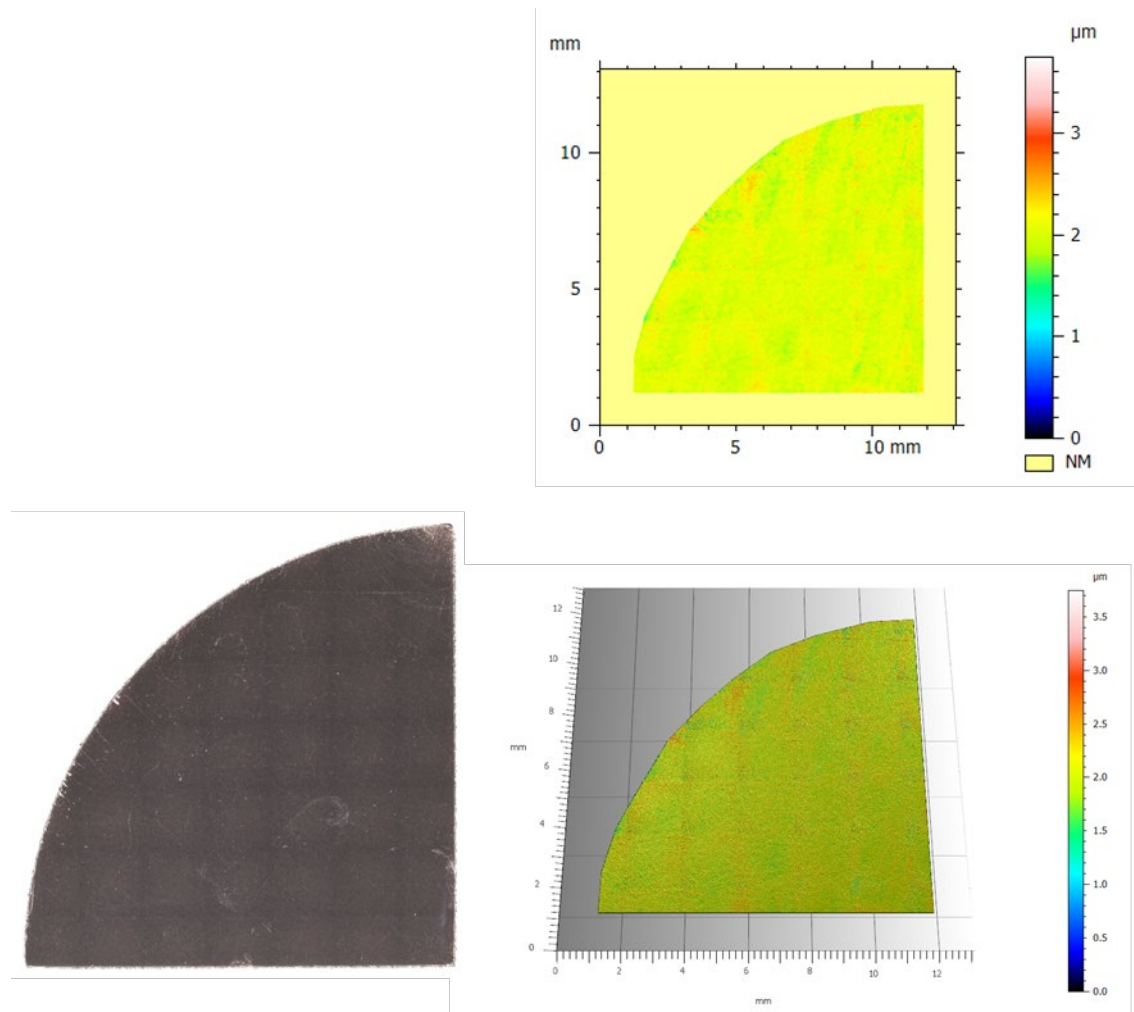


Figure 7-57. Surface characterization of non-exposed sample CI-1 (top side).

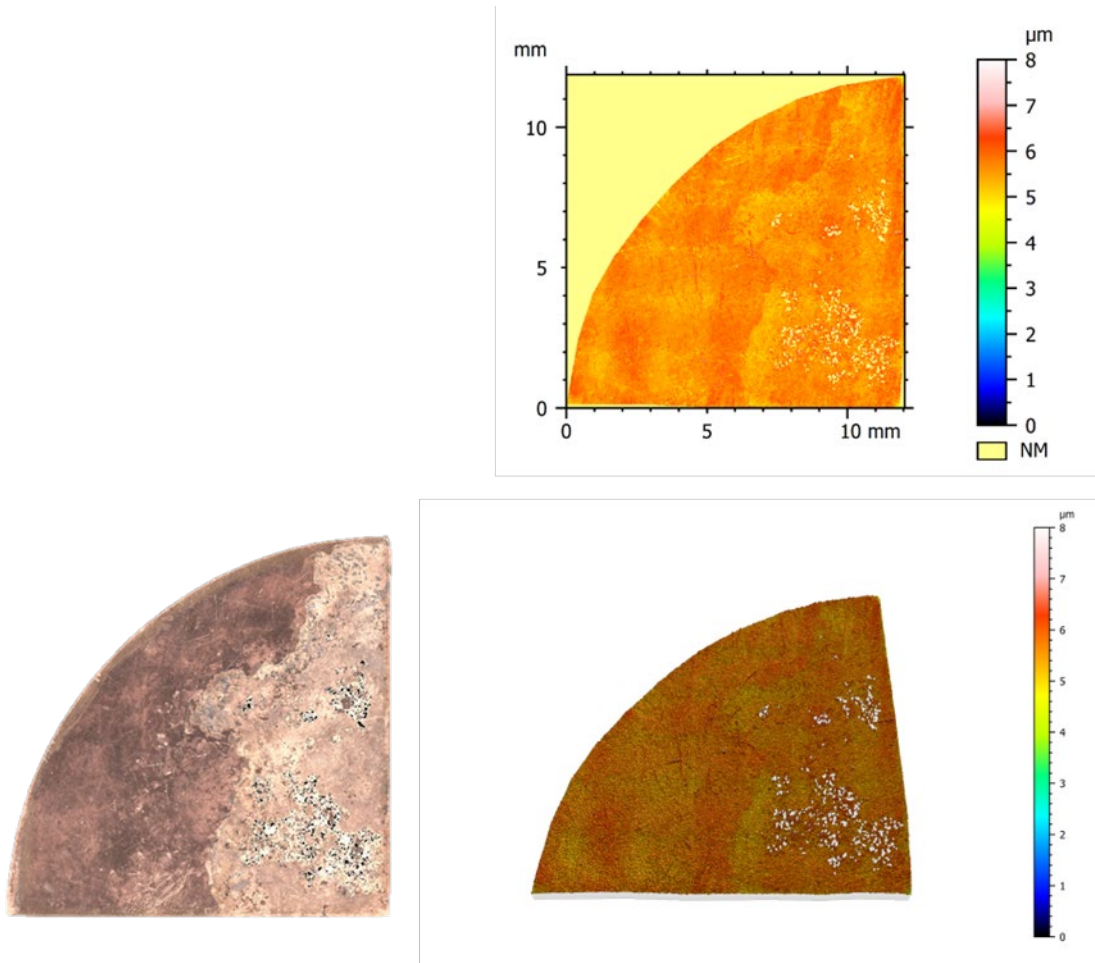


Figure 7-58. Surface characterization of exposed and pickled sample C1-1 (top side).

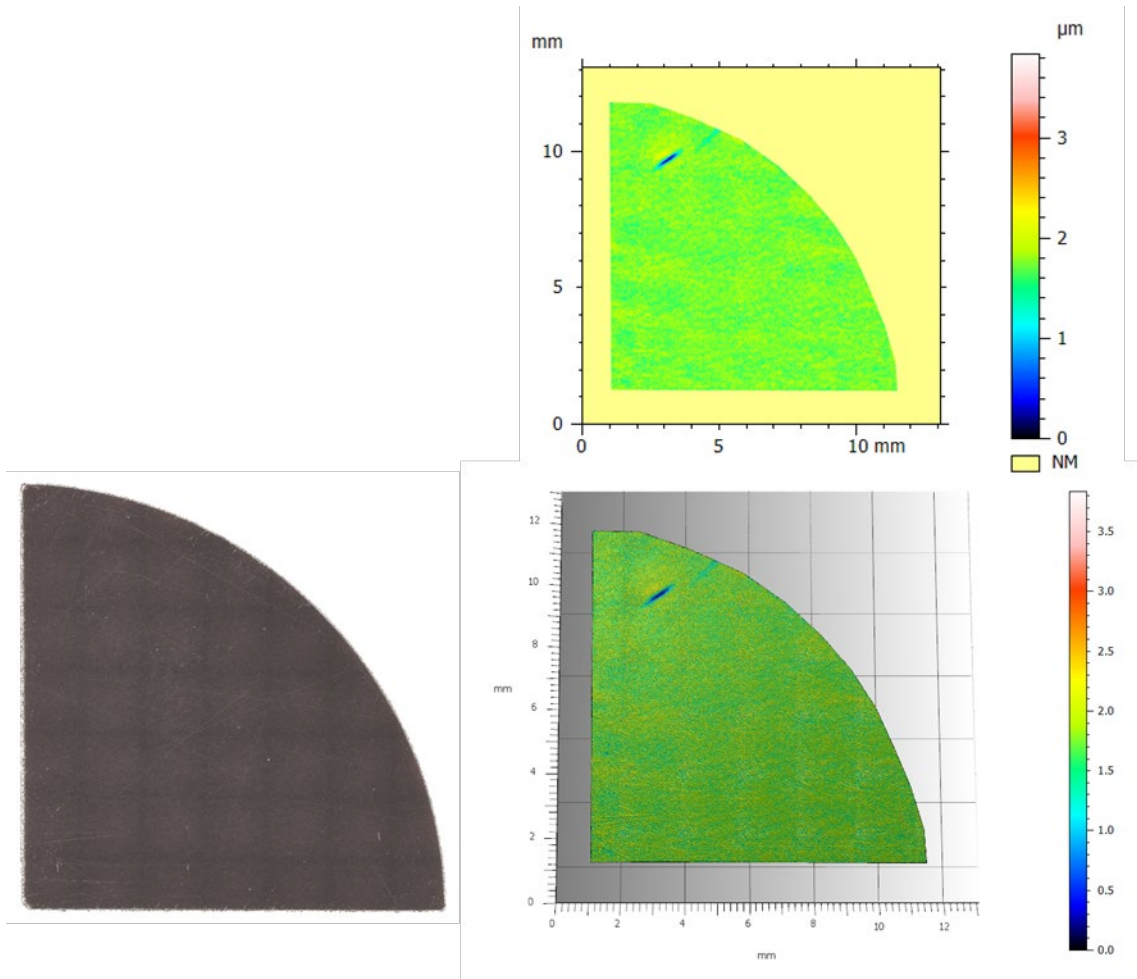


Figure 7-59. Surface characterization of non-exposed sample C1-1 (bottom side).

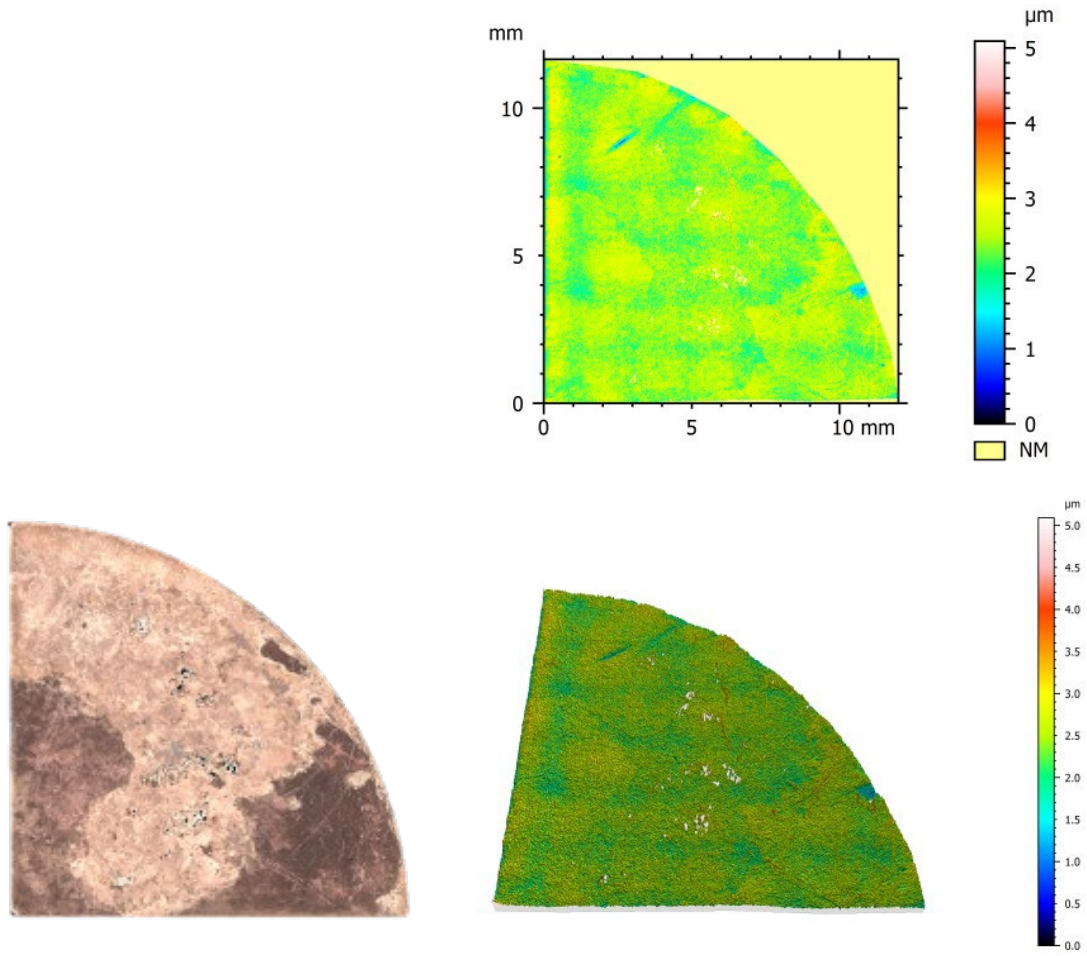


Figure 7-60. Surface characterization of exposed and pickled sample C1-1 (bottom side).

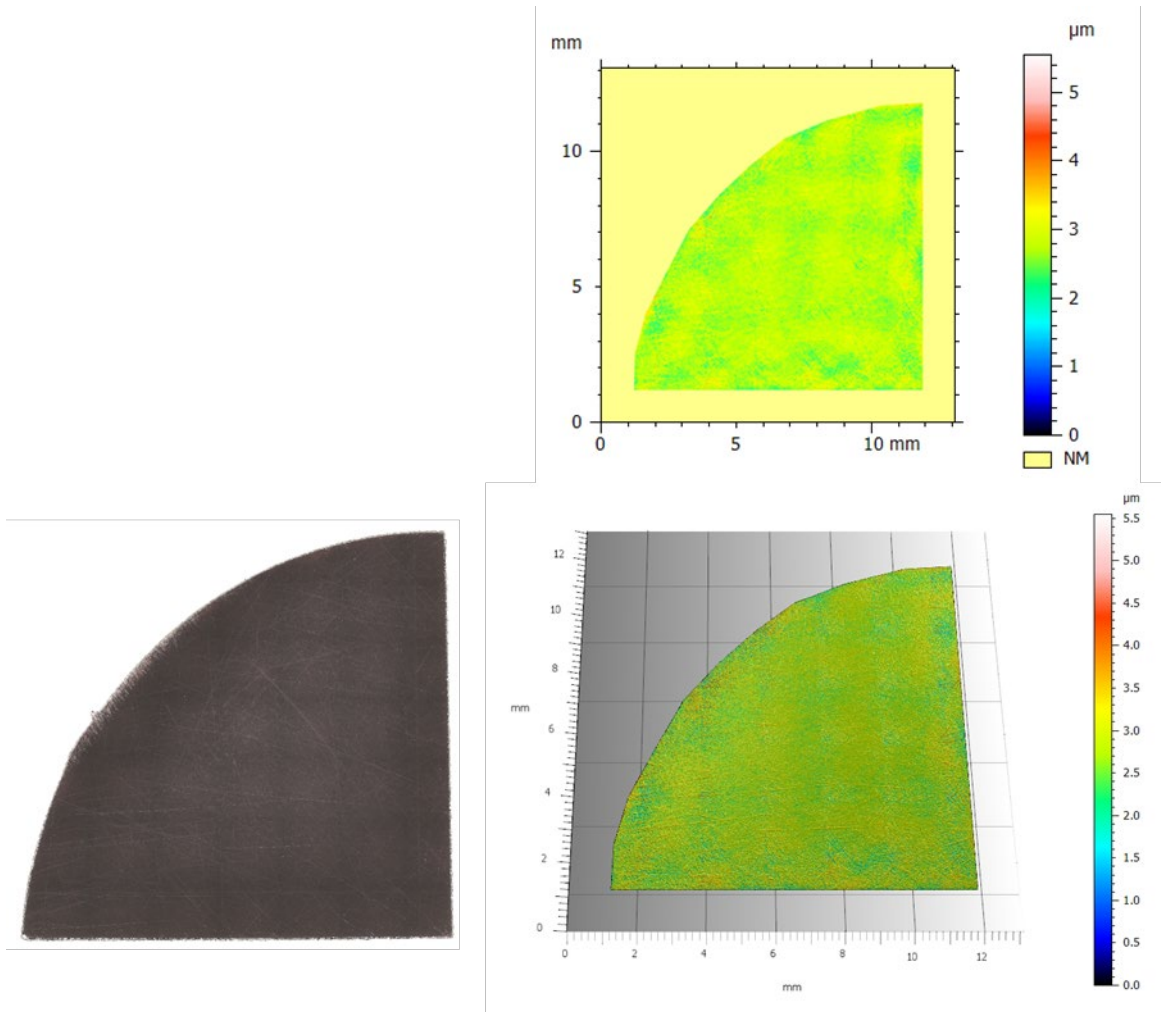


Figure 7-61. Surface characterization of non-exposed sample C2-1 (top side).

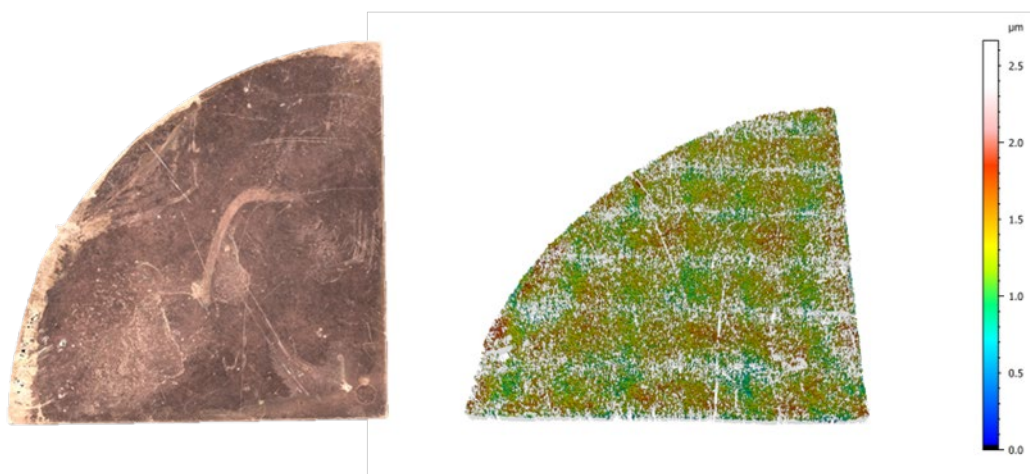
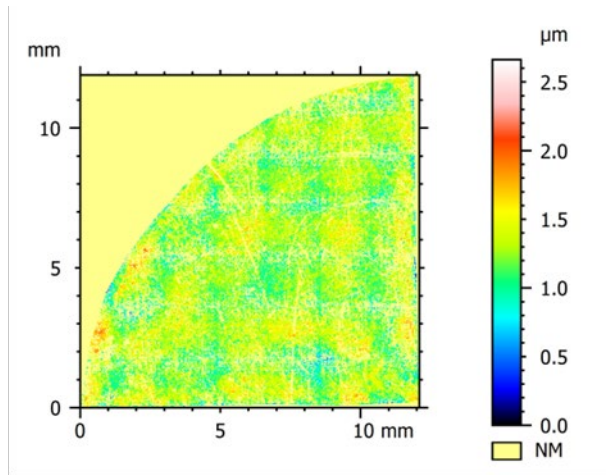


Figure 7-62. Surface characterization of exposed and pickled sample C2-1 (top side).

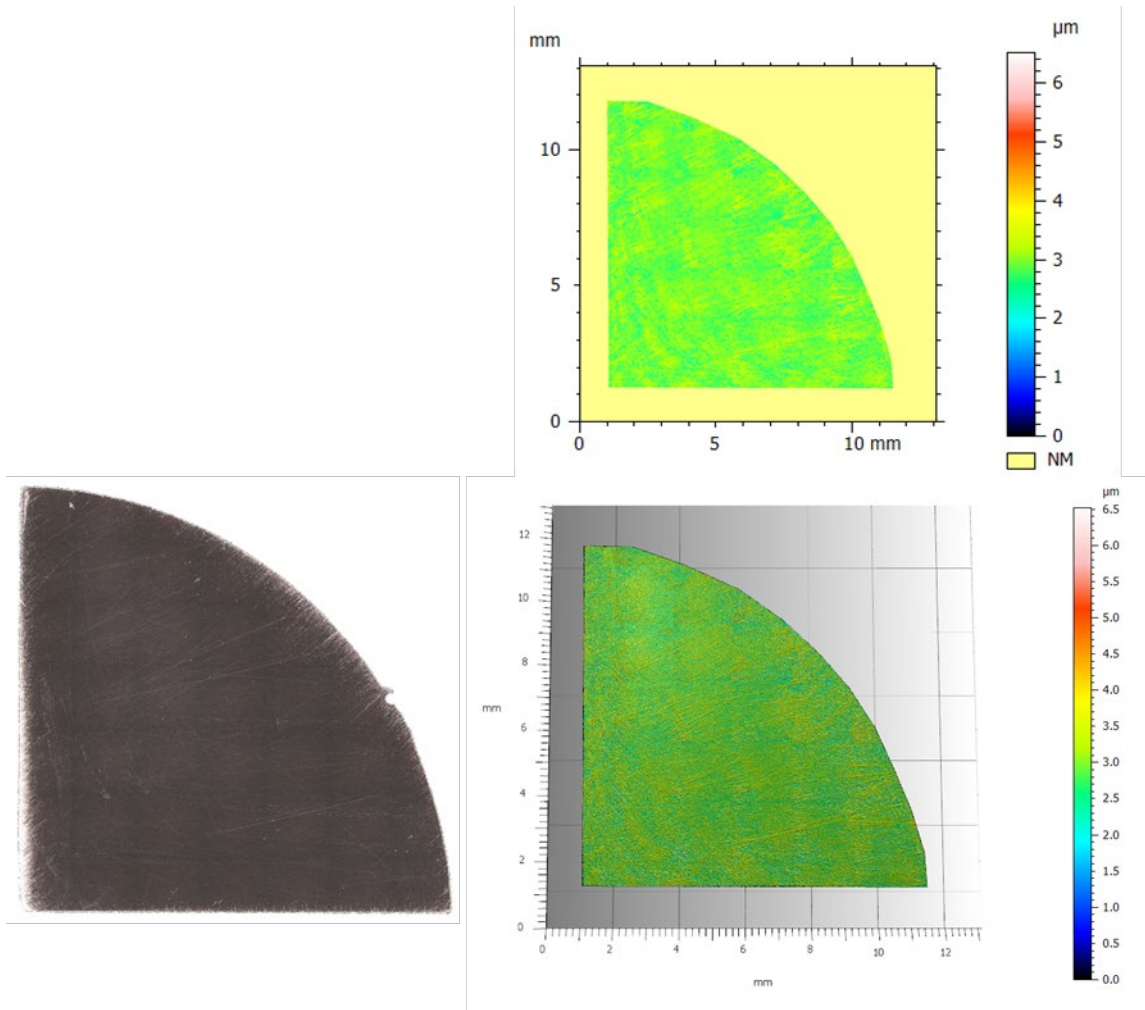


Figure 7-63. Surface characterization of non-exposed sample C2-1 (bottom side).

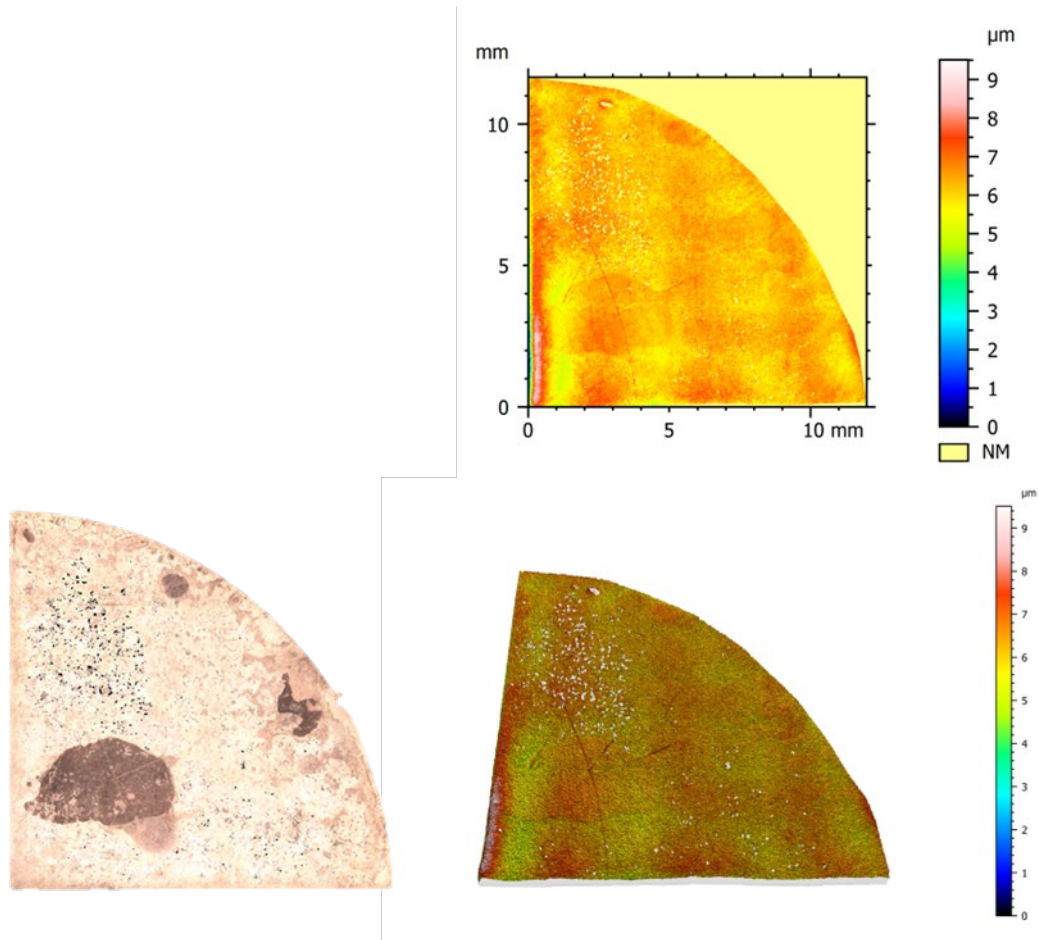


Figure 7-64. Surface characterization of exposed and pickled sample C2-1 (bottom side).

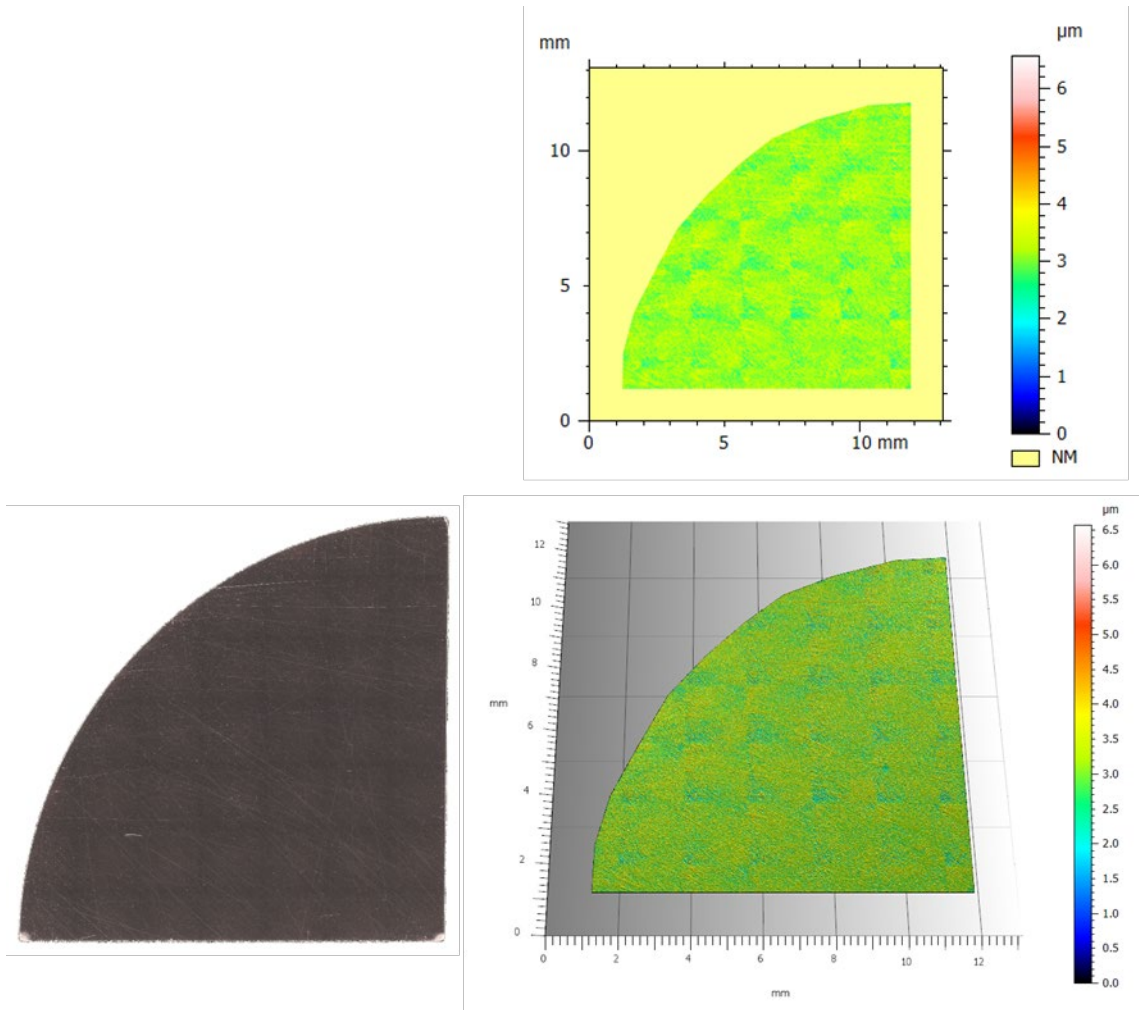


Figure 7-65. Surface characterization of non-exposed sample C3-1 (top side).

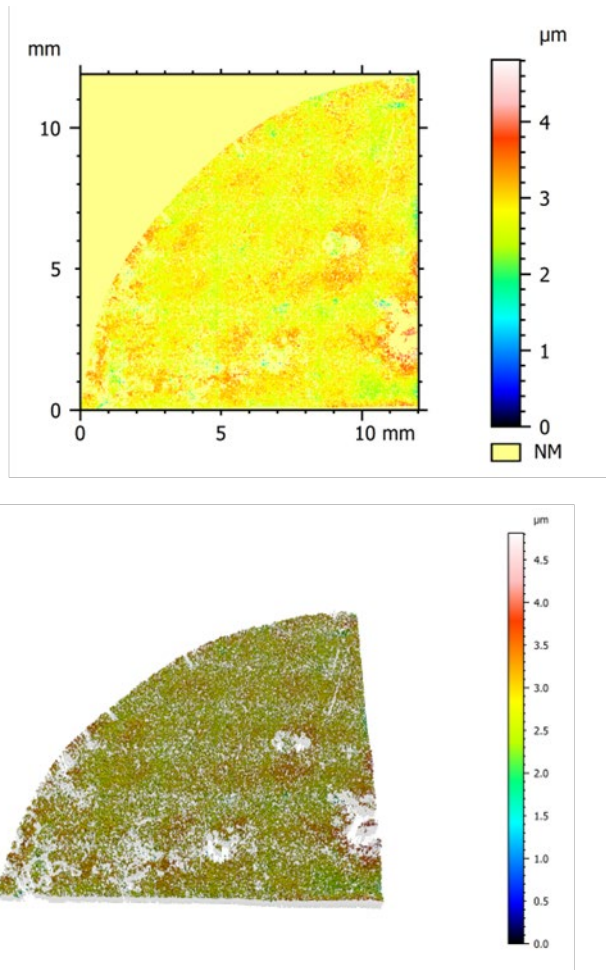


Figure 7-66. *Surface characterization of exposed and pickled sample C3-1 (top side).*

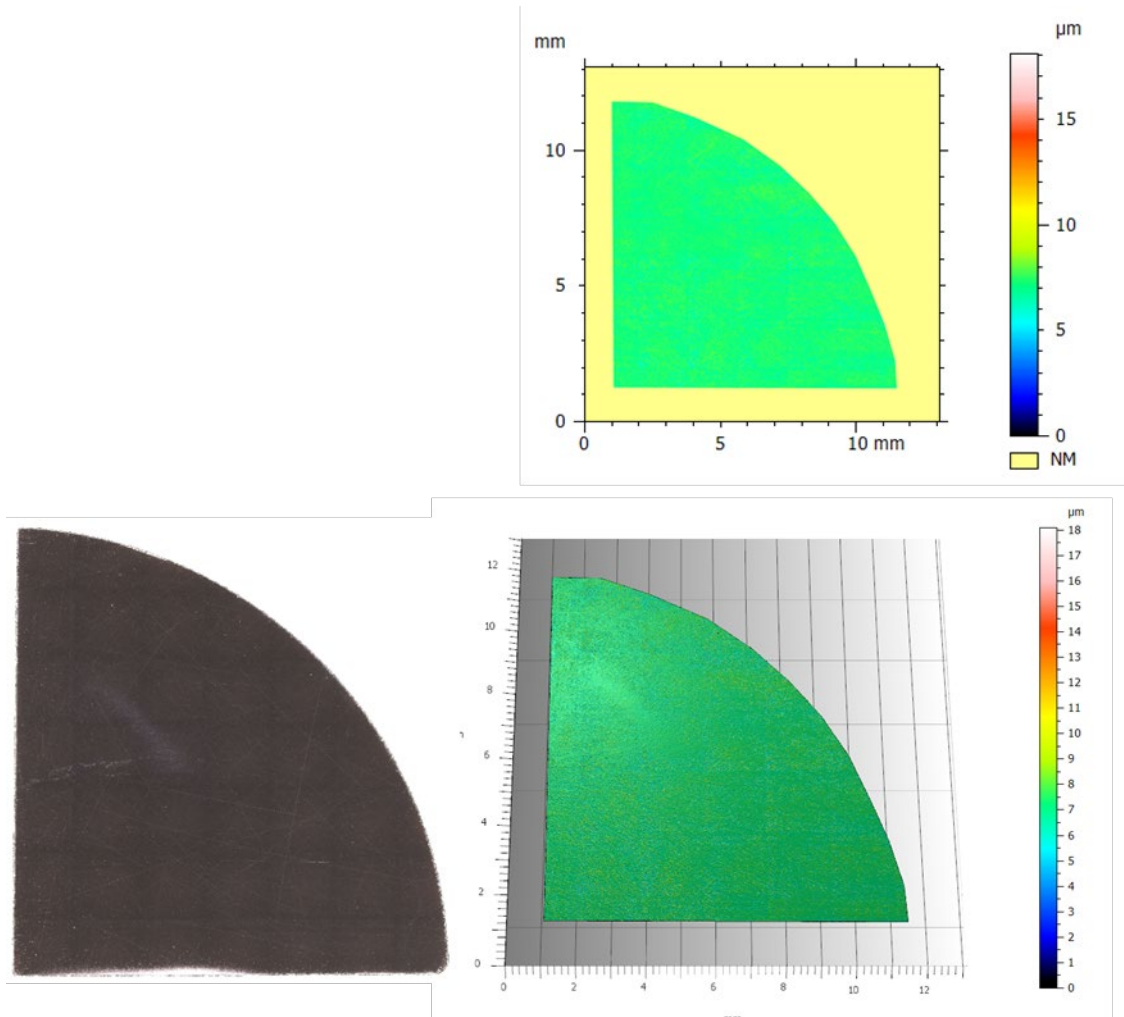


Figure 7-67. Surface characterization of non-exposed sample C3-1 (bottom side).

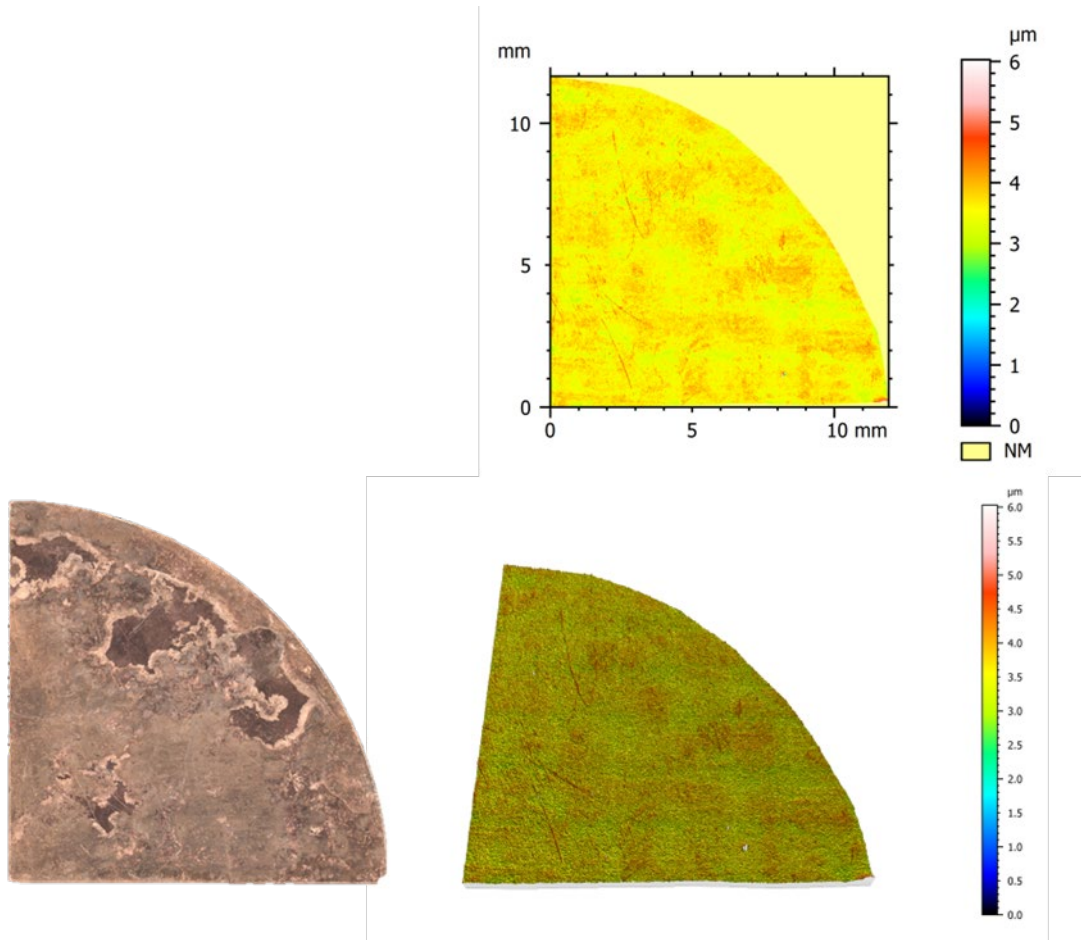


Figure 7-68. Surface characterization of exposed and pickled sample C3-1 (bottom side).

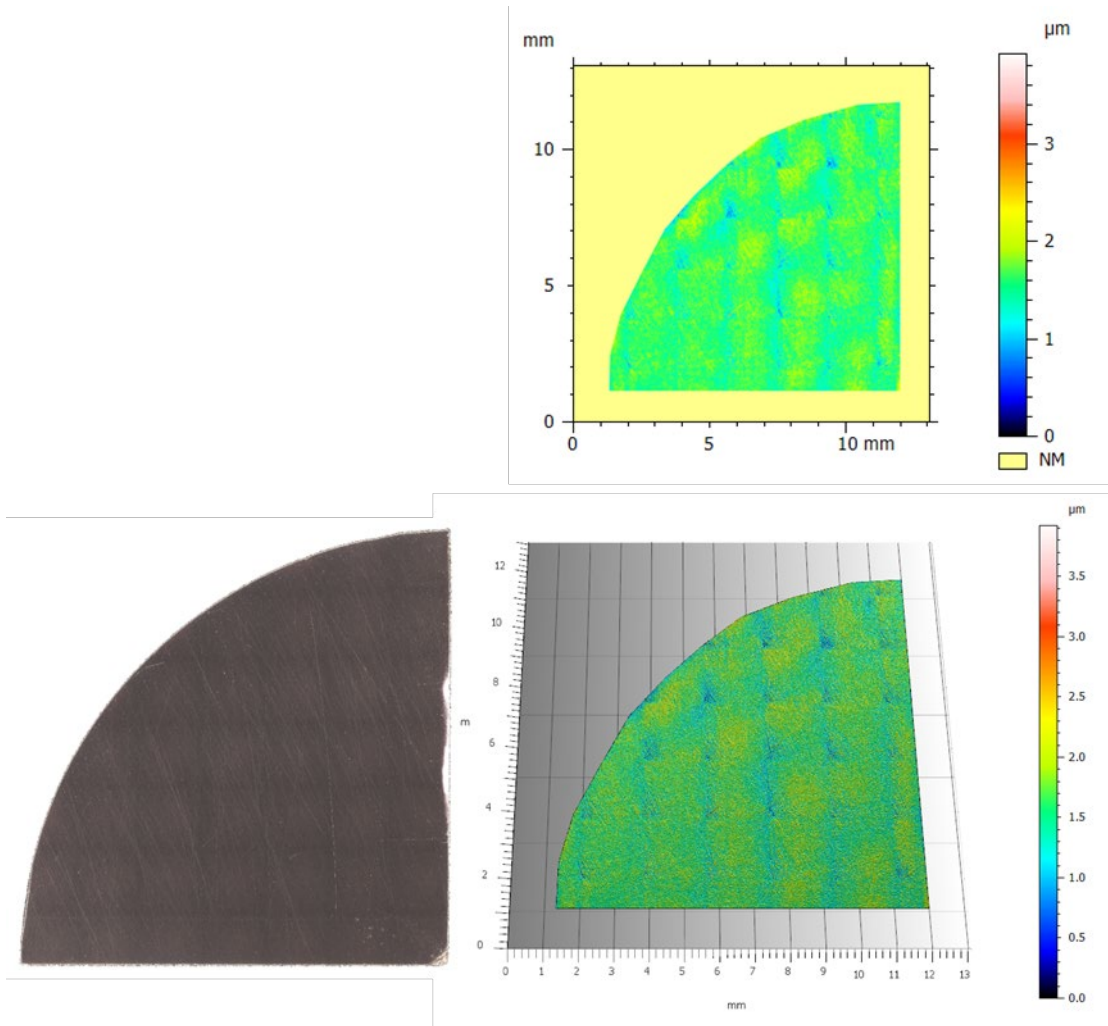


Figure 7-69. Surface characterization of non-exposed sample C4-1 (top side).

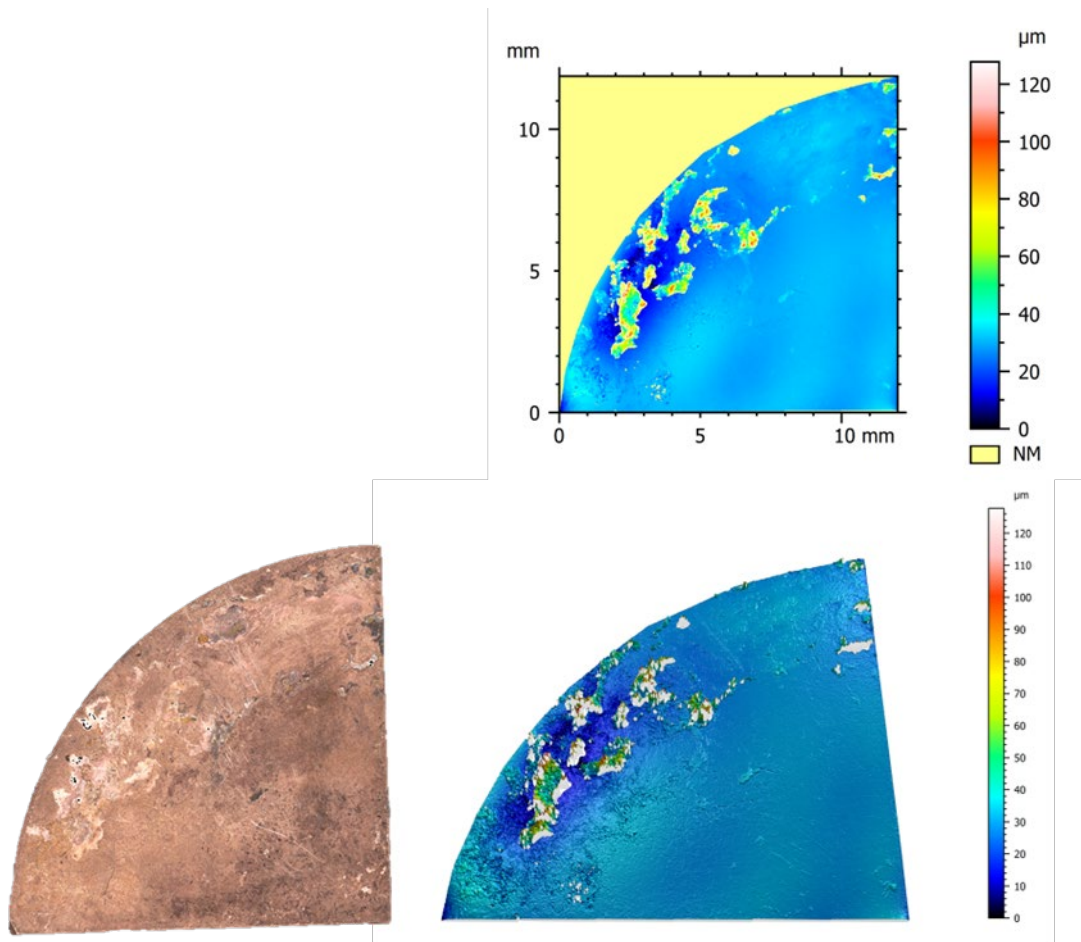


Figure 7-70. Surface characterization of exposed and pickled sample C4-1 (top side).

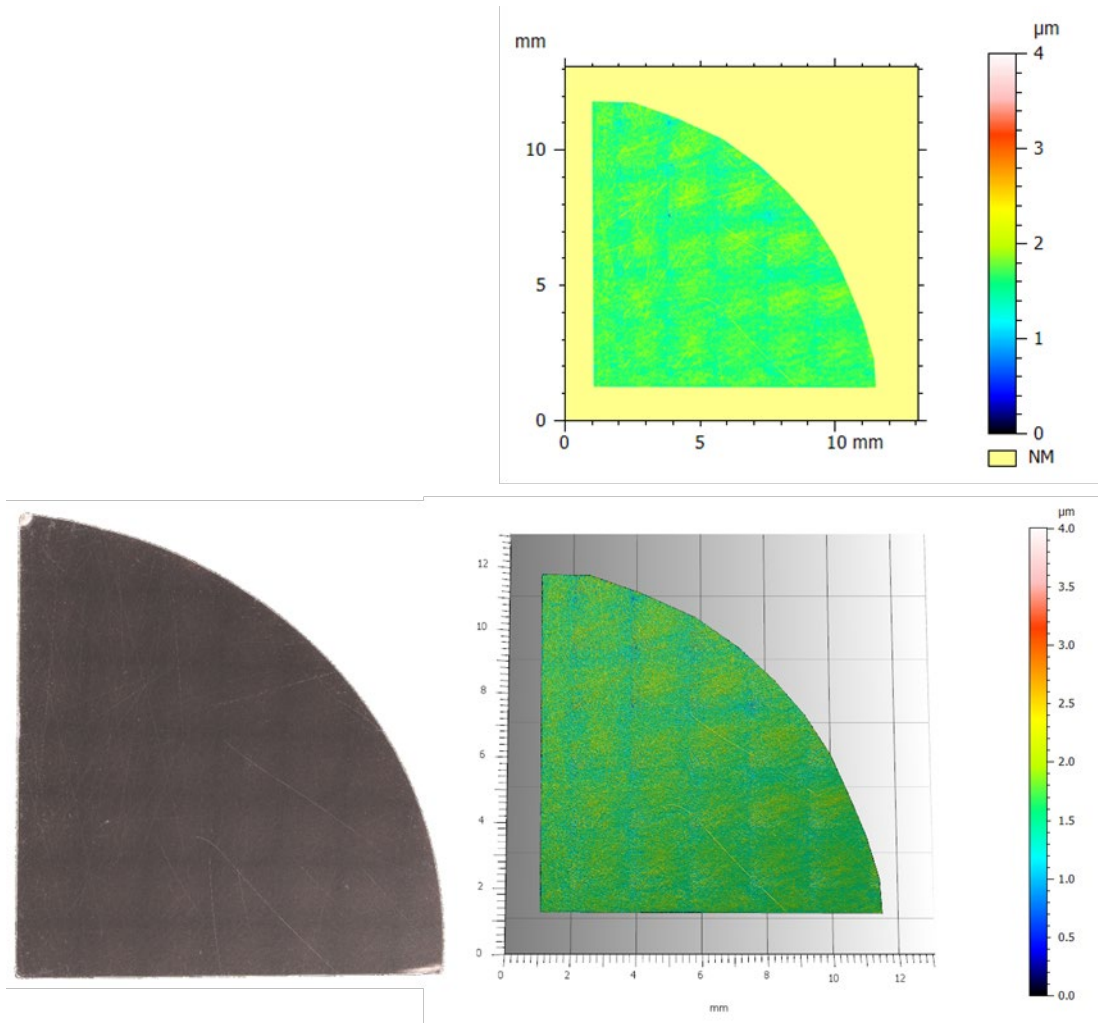


Figure 7-71. Surface characterization of non-exposed sample C4-1 (bottom side).

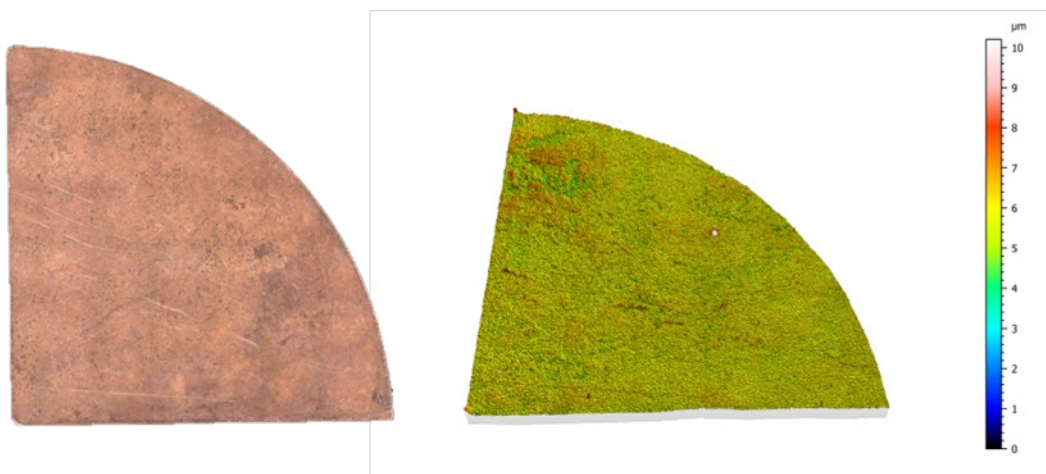
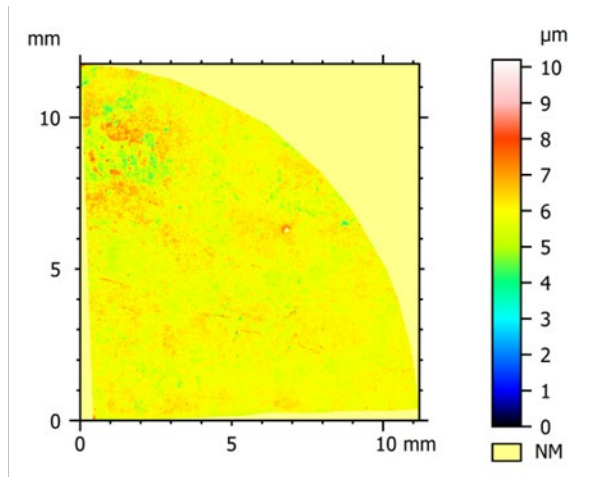


Figure 7-72. Surface characterization of exposed and pickled sample C4-1 (bottom side).

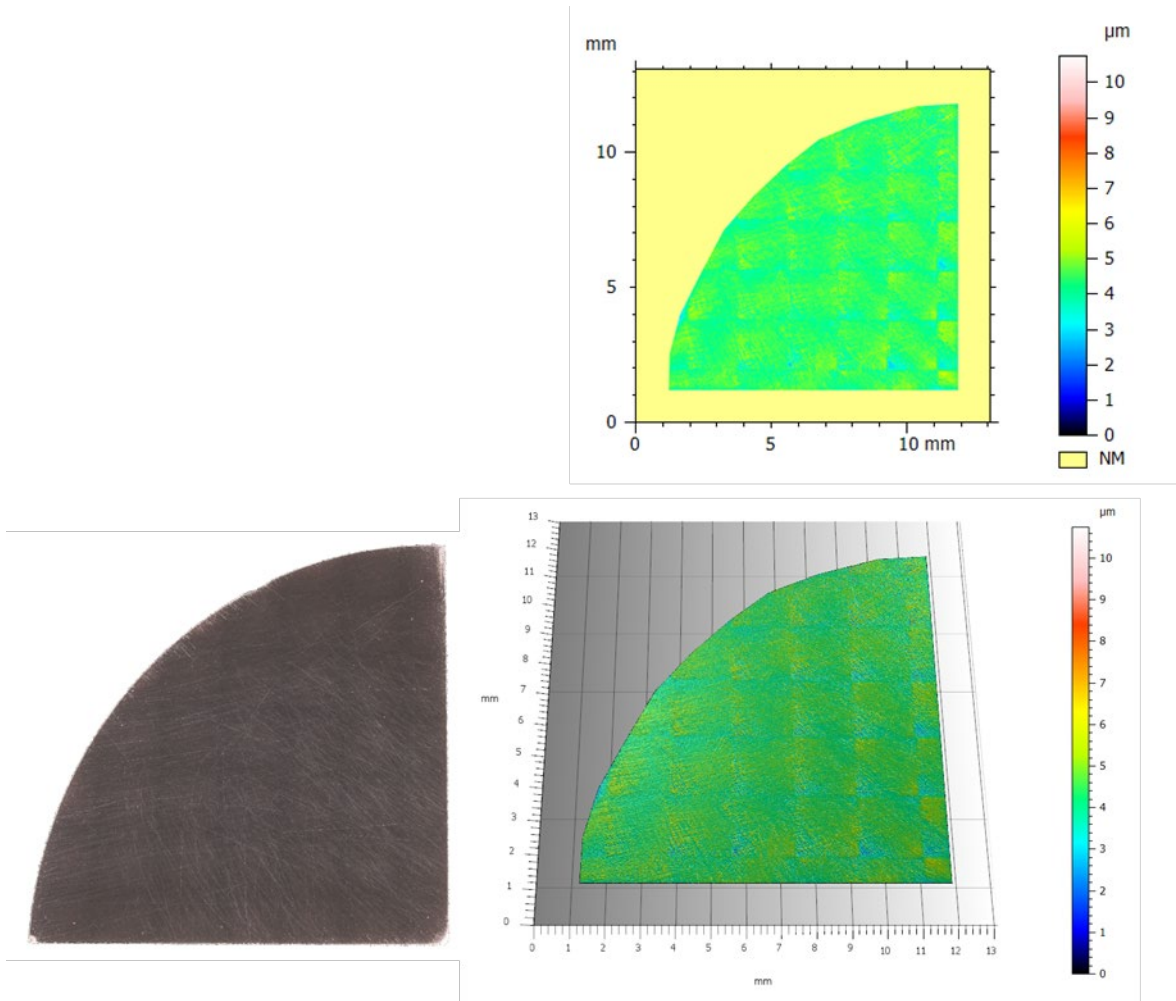


Figure 7-73. Surface characterization of non-exposed sample C5-1 (top side).

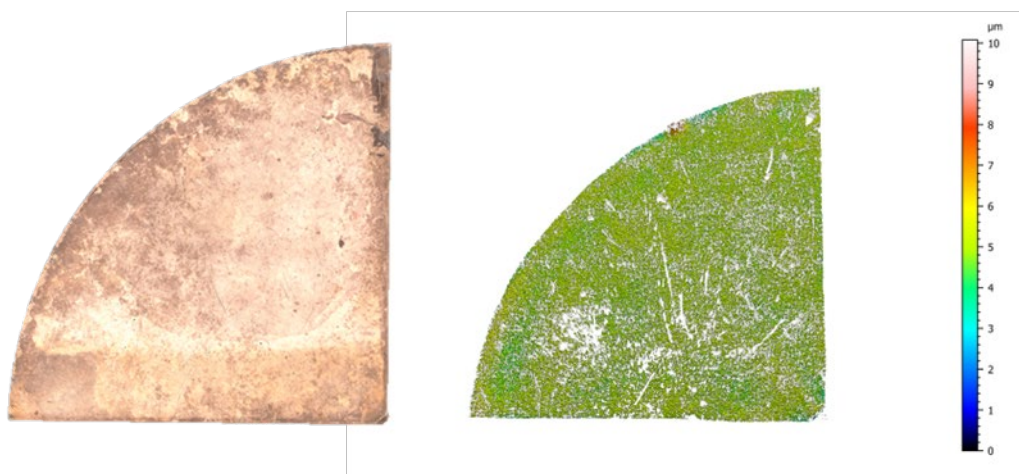
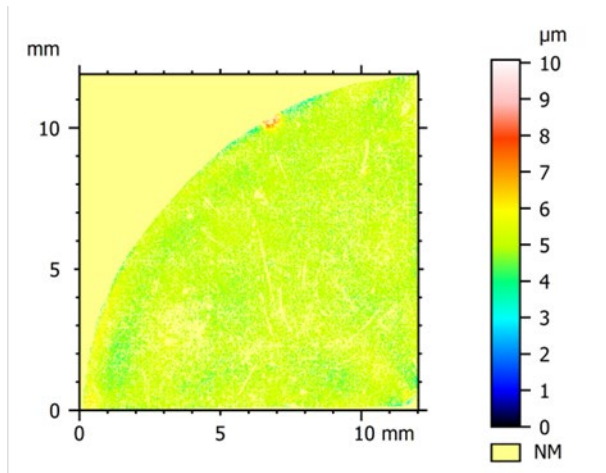


Figure 7-74. Surface characterization of exposed and pickled sample C5-1 (top side).

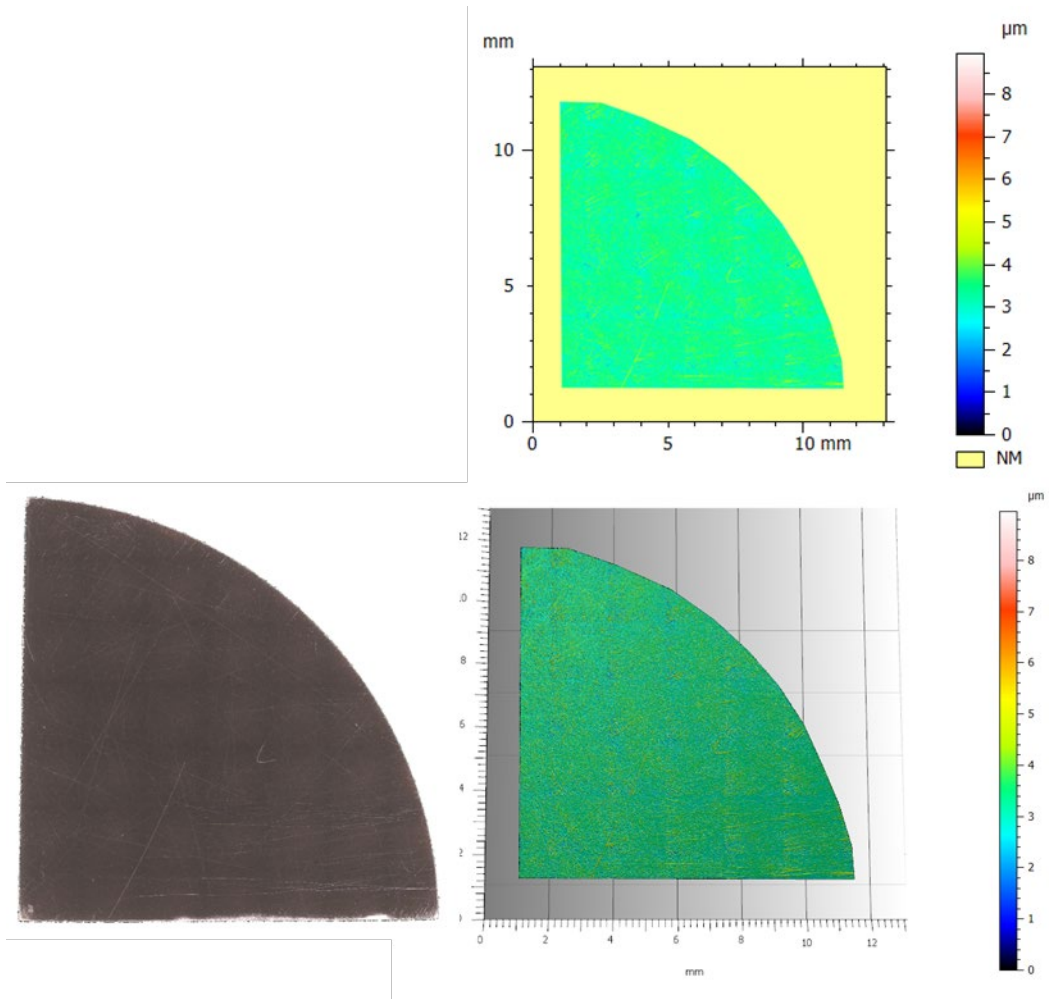


Figure 7-75. Surface characterization of non-exposed sample C5-1 (bottom side).

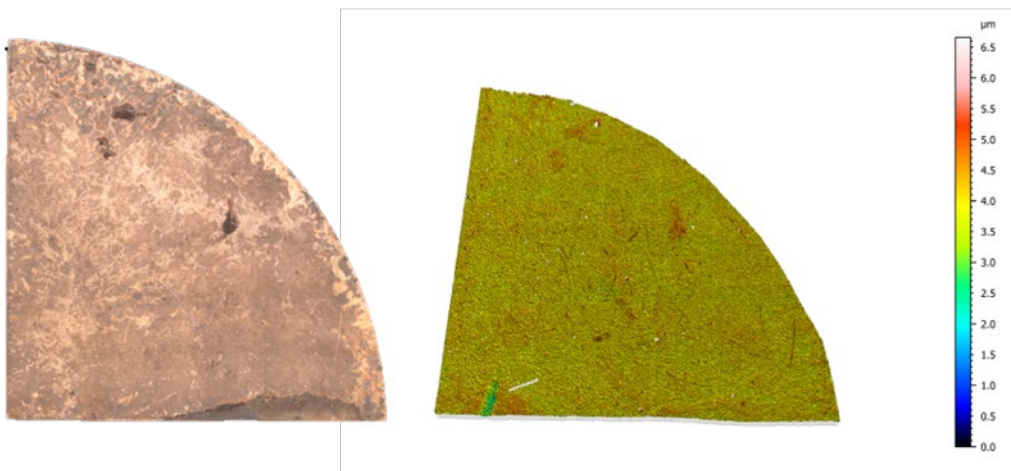
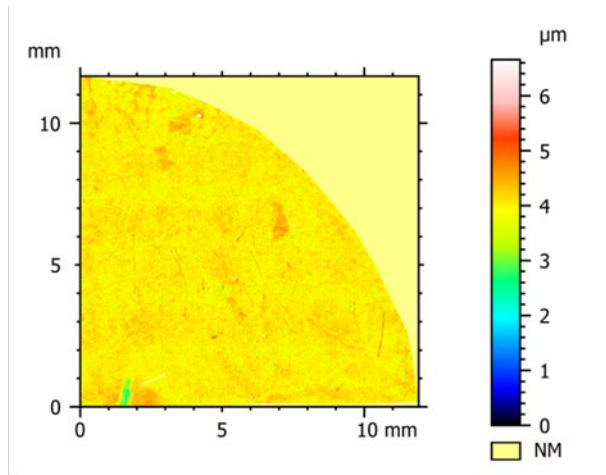


Figure 7-76. Surface characterization of exposed and pickled sample C5-1 (bottom side).

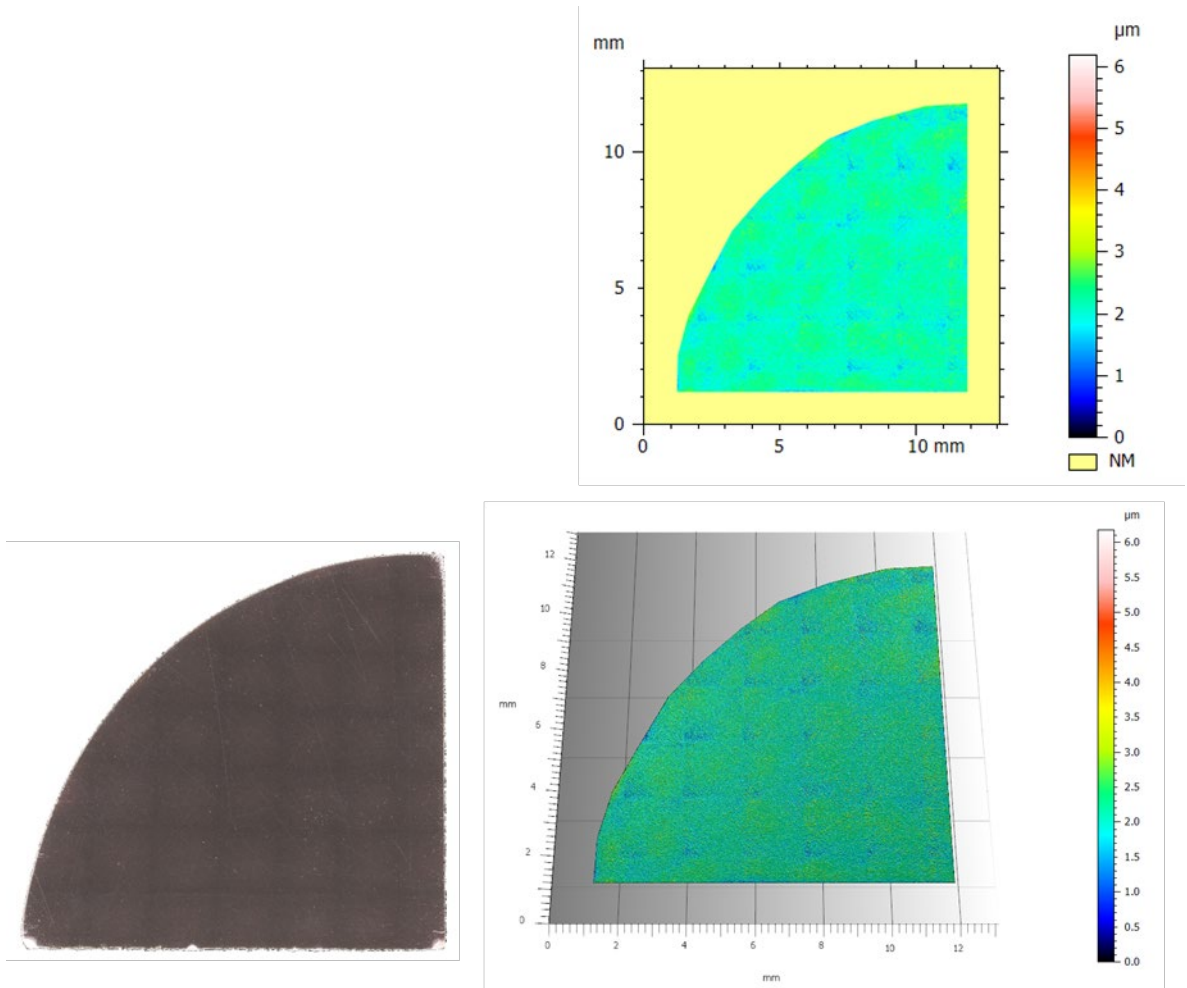


Figure 7-77. Surface characterization of non-exposed sample C6-1 (top side).

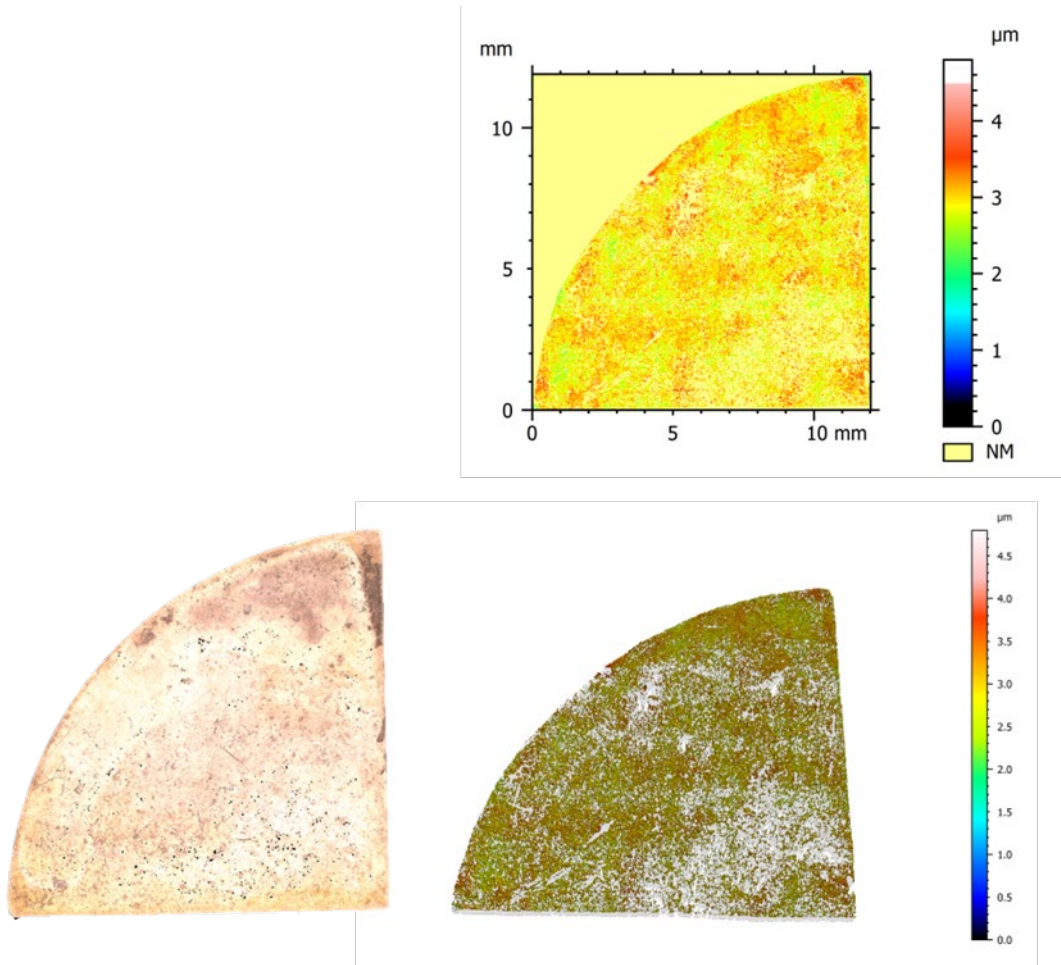


Figure 7-78. Surface characterization of exposed and pickled sample C6-1 (top side).

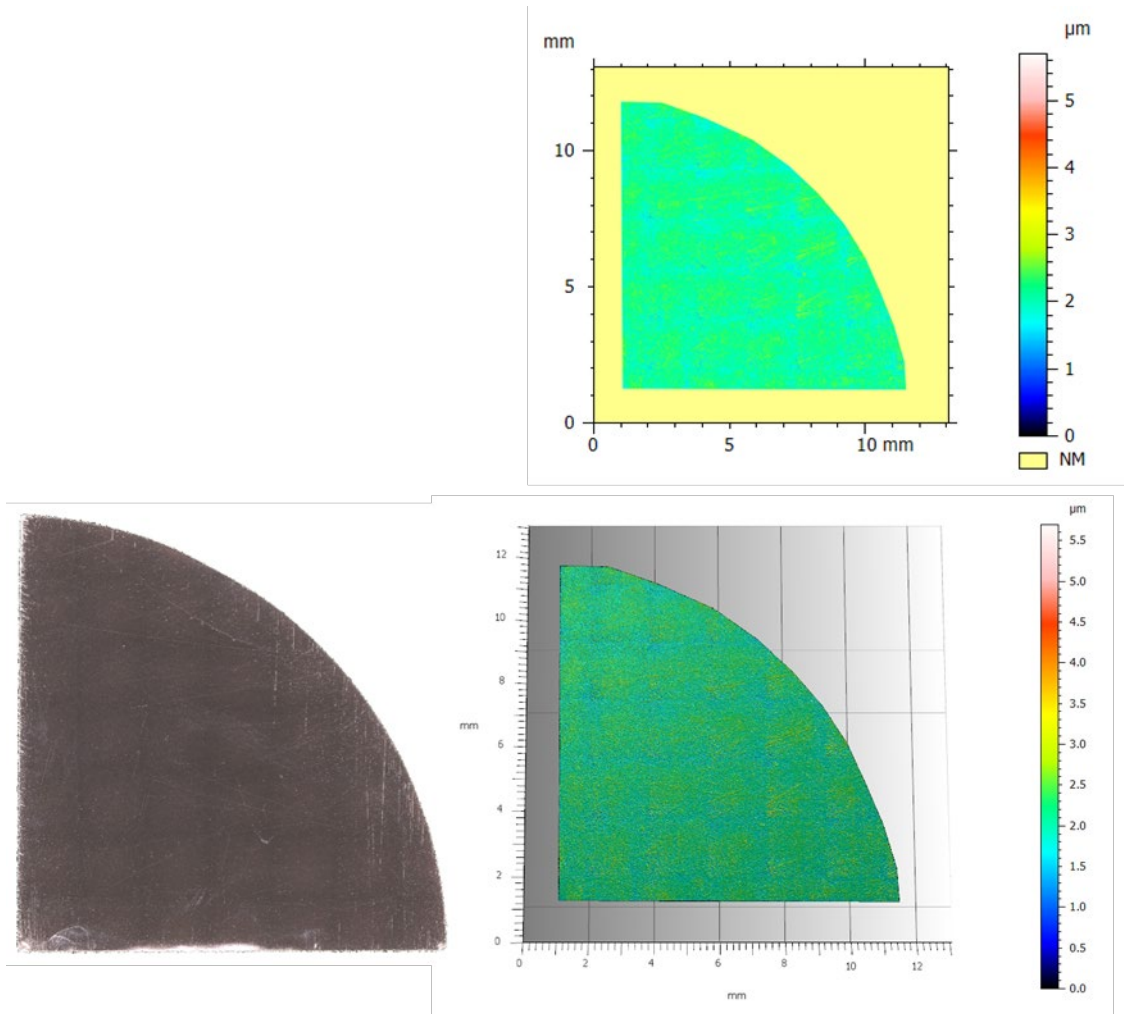


Figure 7-79. Surface characterization of non-exposed sample C6-1 (bottom side).

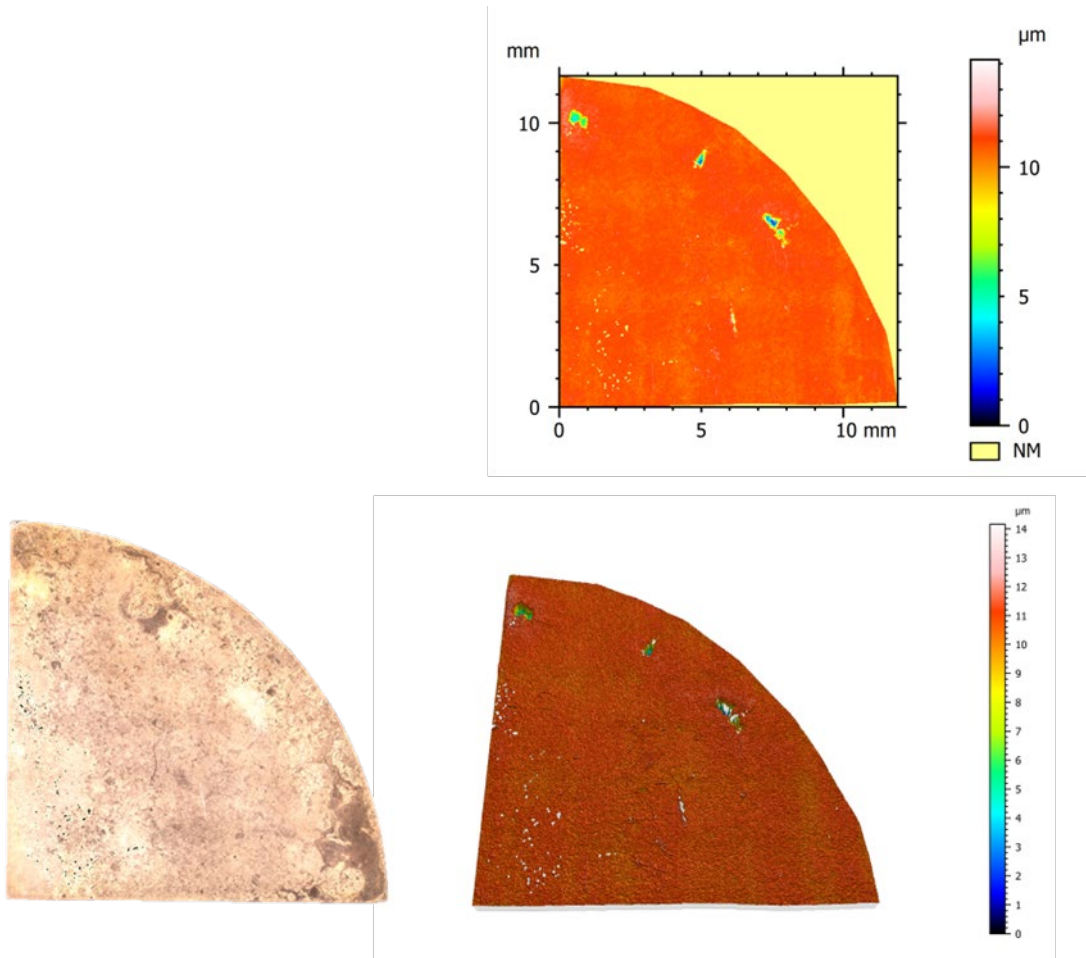


Figure 7-80. Surface characterization of exposed and pickled sample C6-1 (bottom side).

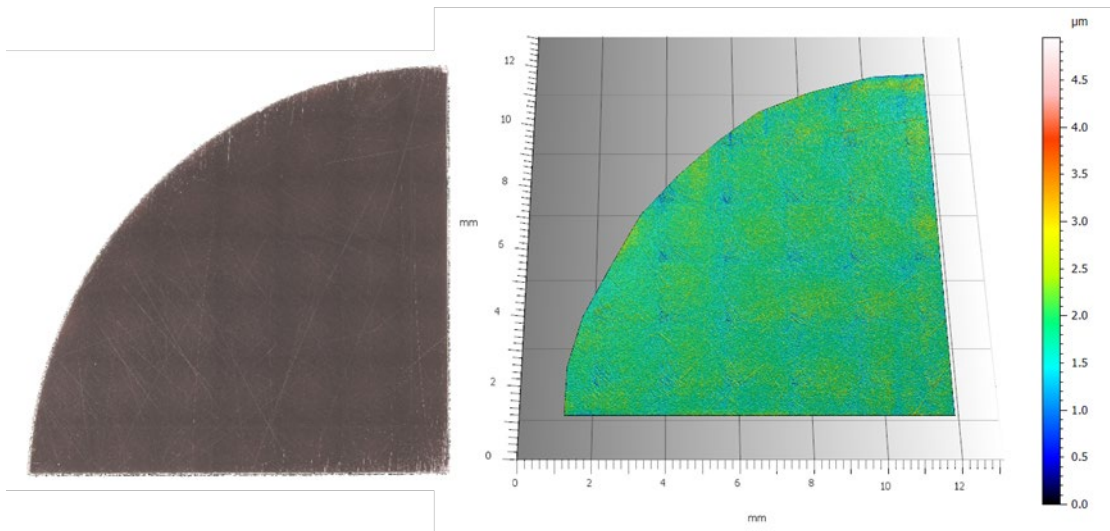
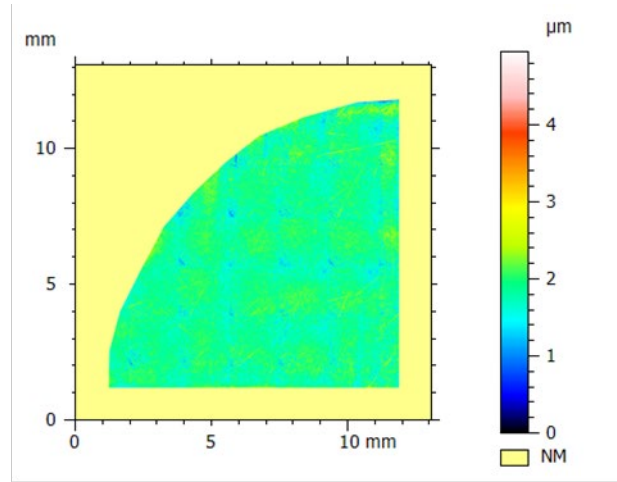


Figure 7-81. Surface characterization of non-exposed sample C7-1 (top side).

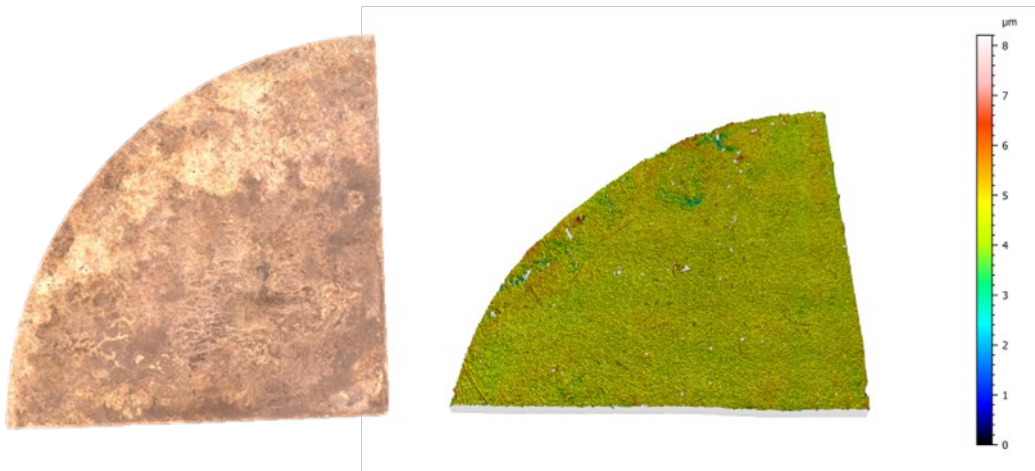
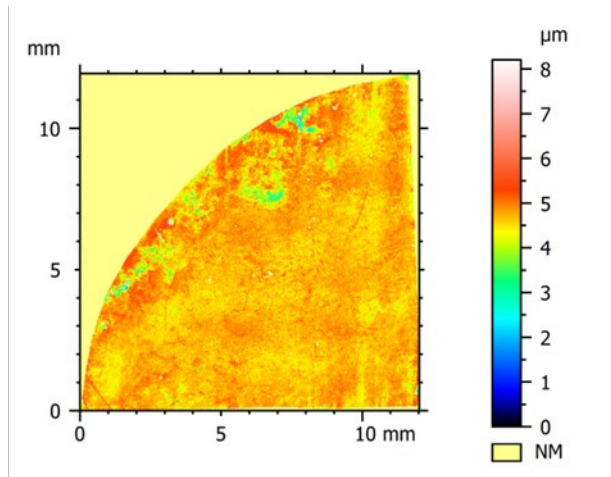


Figure 7-82. Surface characterization of exposed and pickled sample C7-1 (top side).

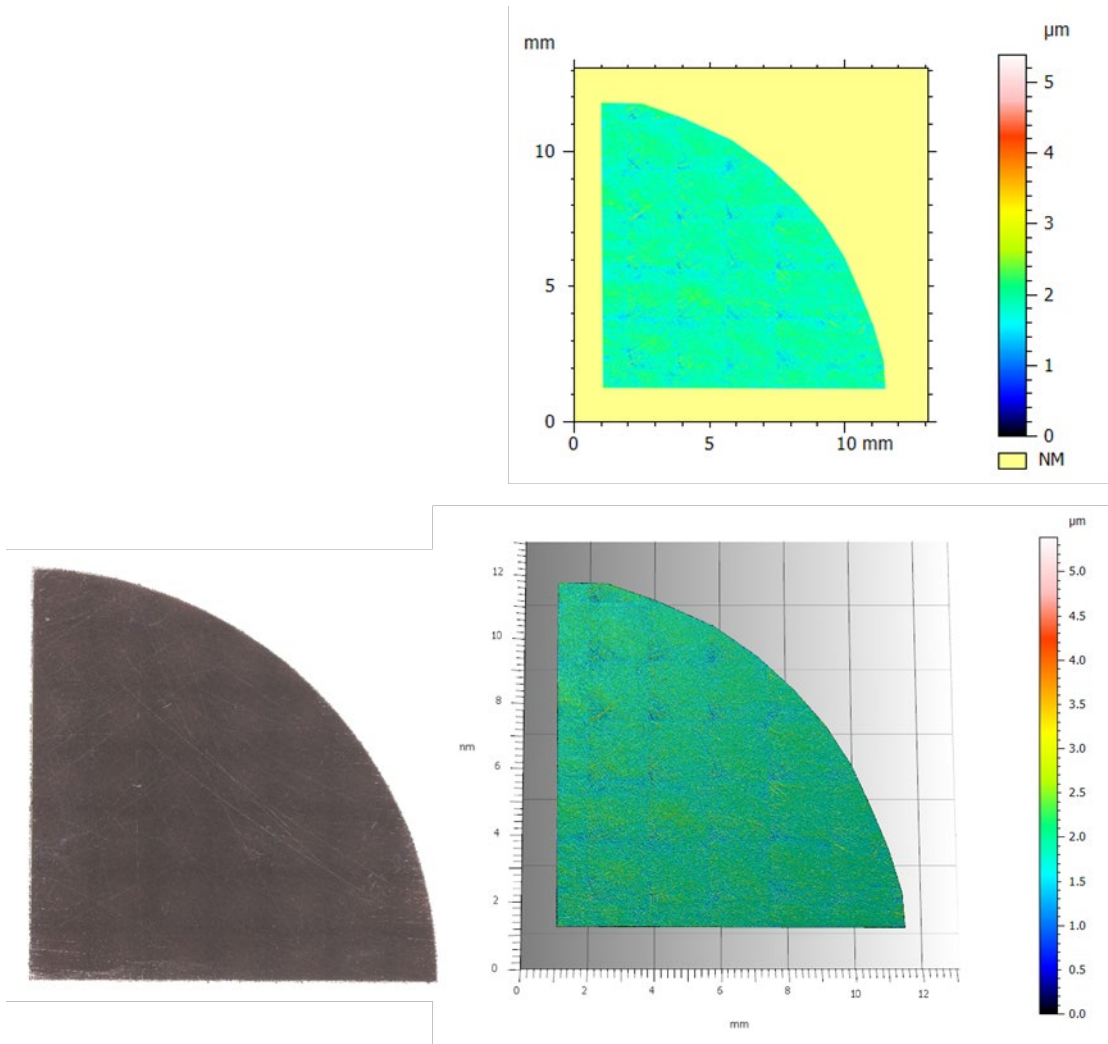


Figure 7-83. Surface characterization of non-exposed sample C7-1 (bottom side).

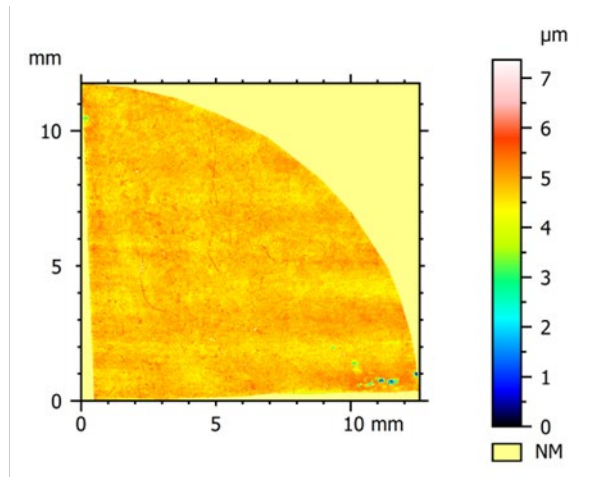


Figure 7-84. Surface characterization of exposed and pickled sample C7-1 (bottom side).

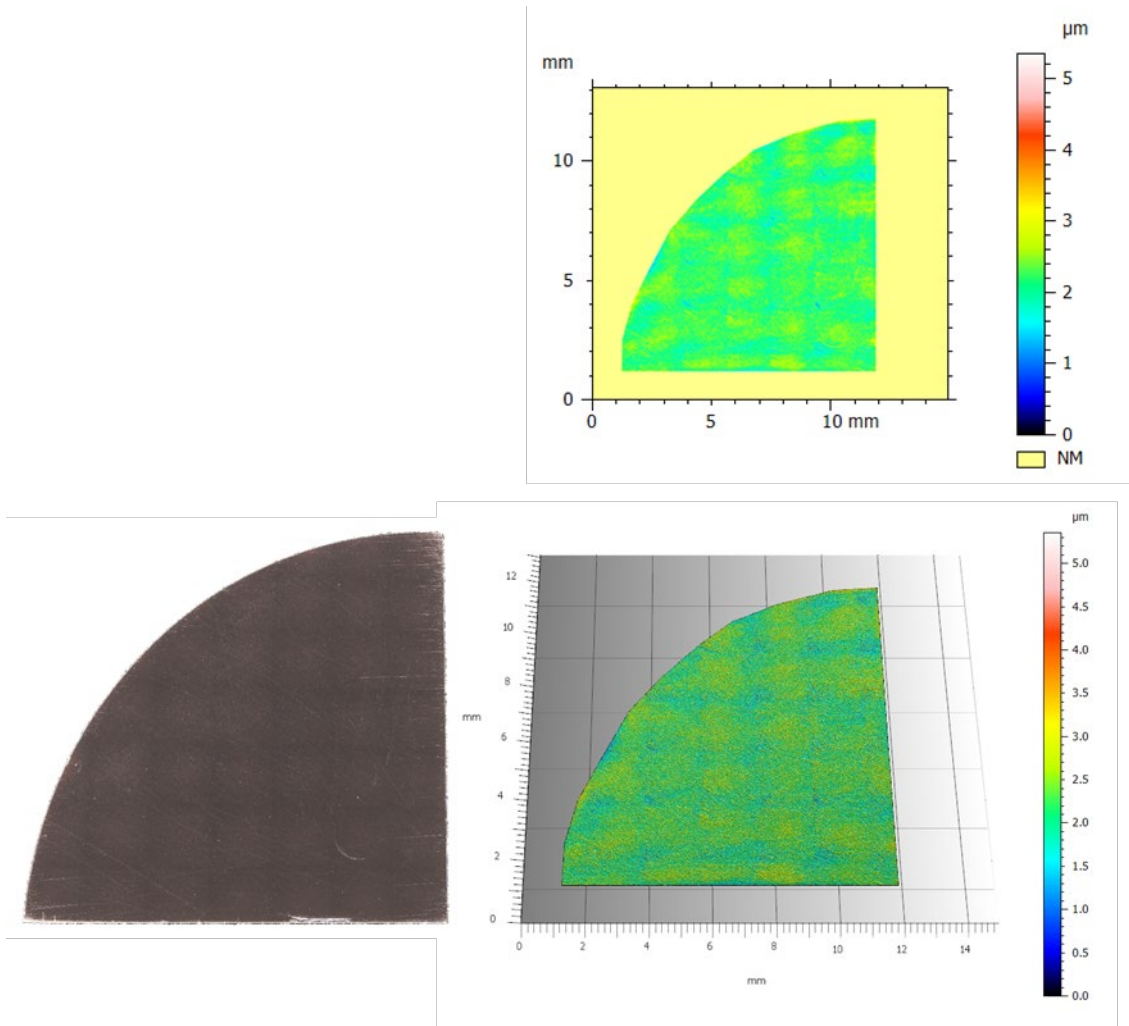


Figure 7-85. Surface characterization of non-exposed sample C8-1 (top side).

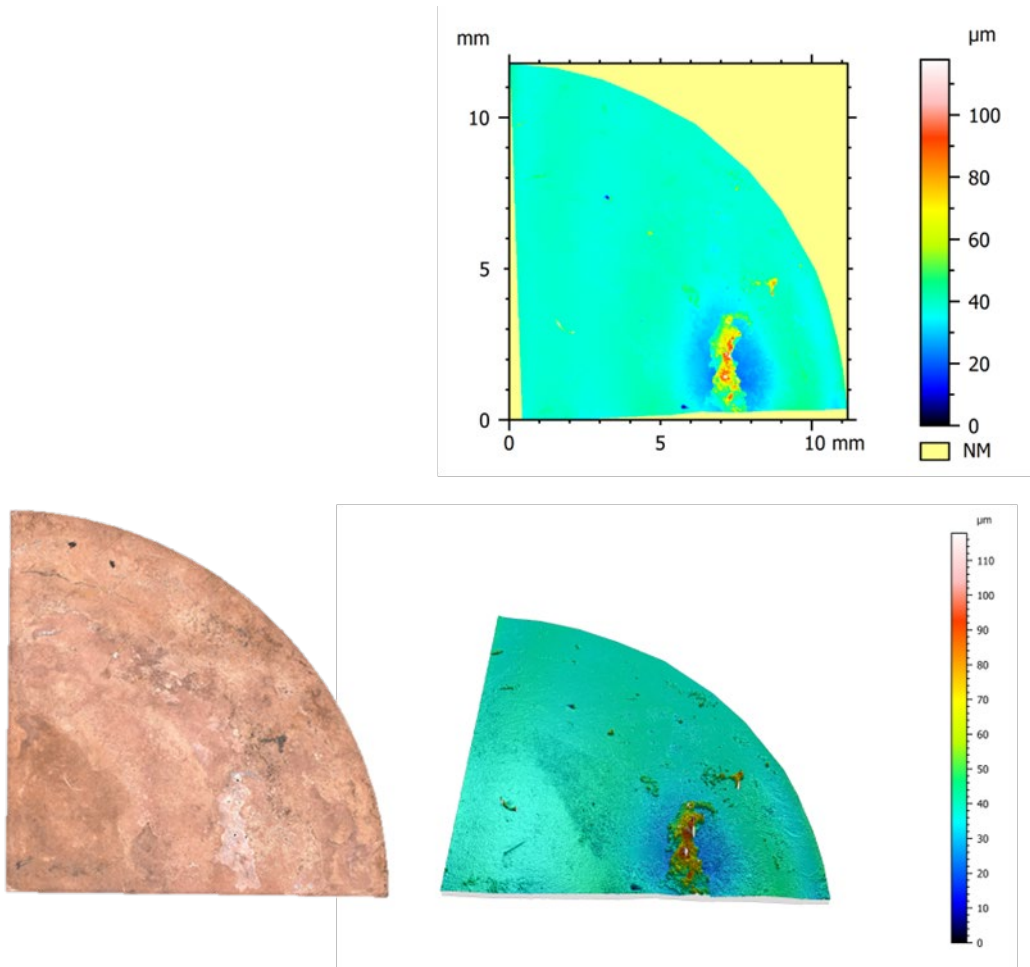


Figure 7-86. Surface characterization of exposed and pickled sample C8-1 (top side).

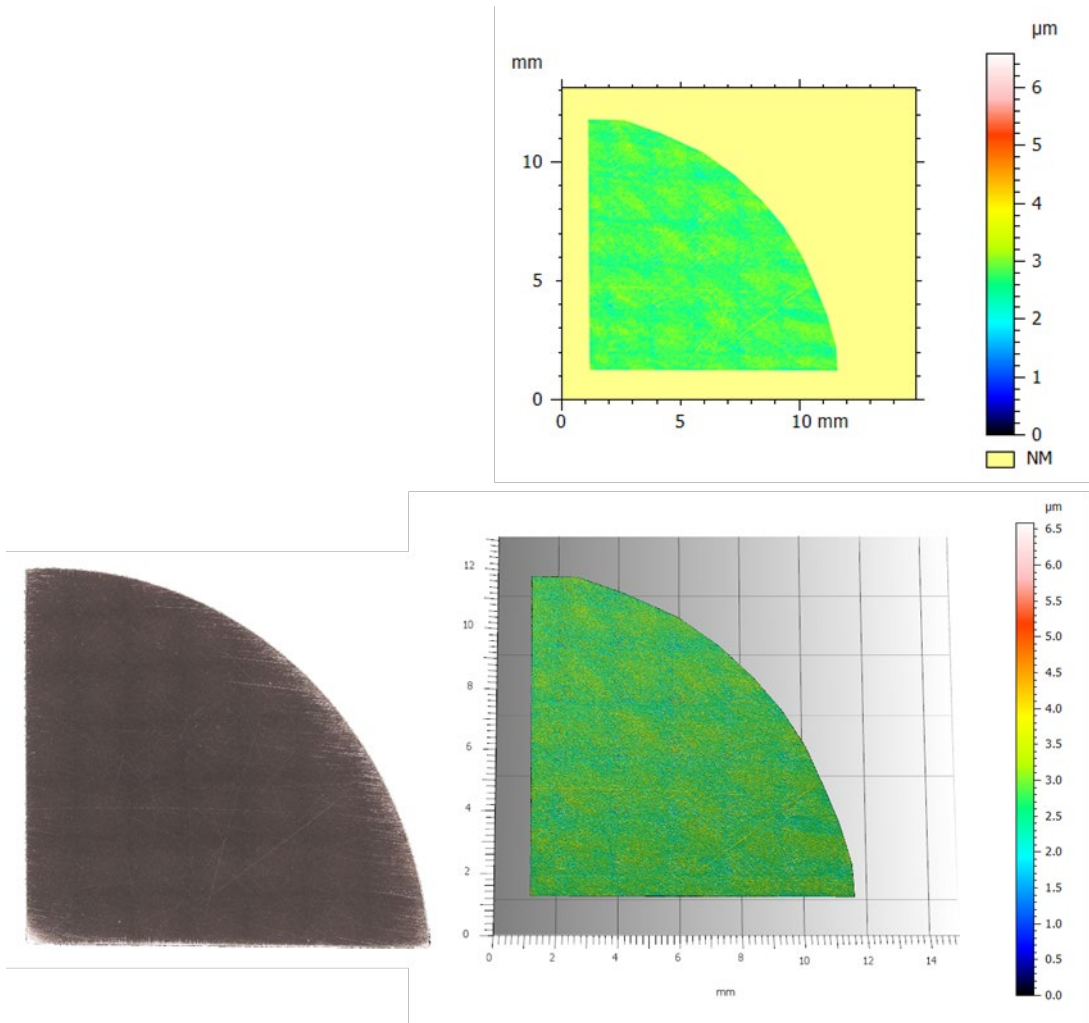


Figure 7-87. Surface characterization of non-exposed sample C8-1 (bottom side).

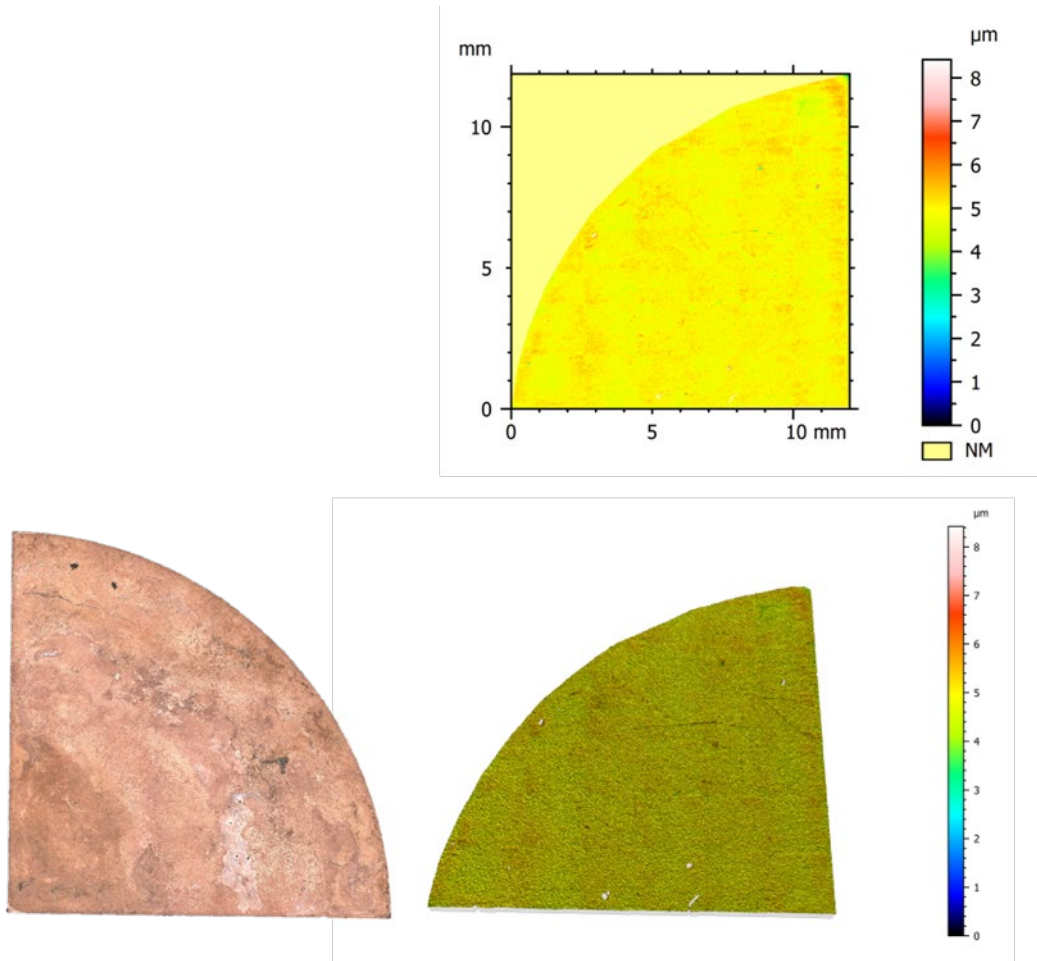


Figure 7-88. Surface characterization of exposed and pickled sample C8-1 (bottom side).

7.4 SEM/EDS Surface analysis

SEM/EDS was used to analyse the surfaces of selected copper samples.

7.4.1 Sample C1-3

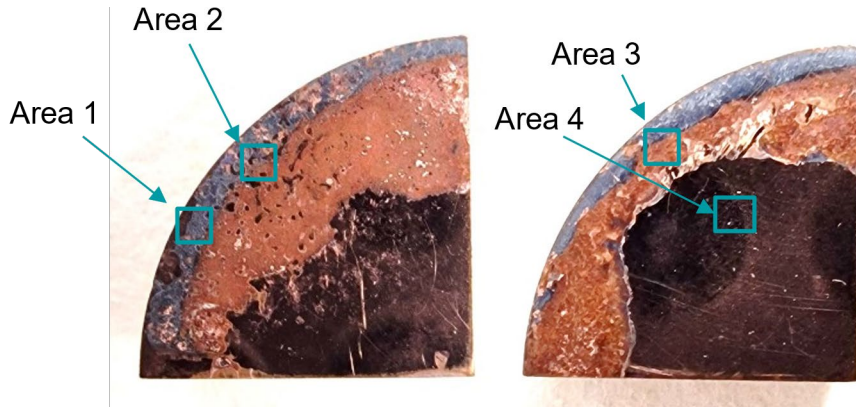


Figure 7-89. Sample C1-3. The marked areas correspond to approximately the examined sites using SEM/EDS.

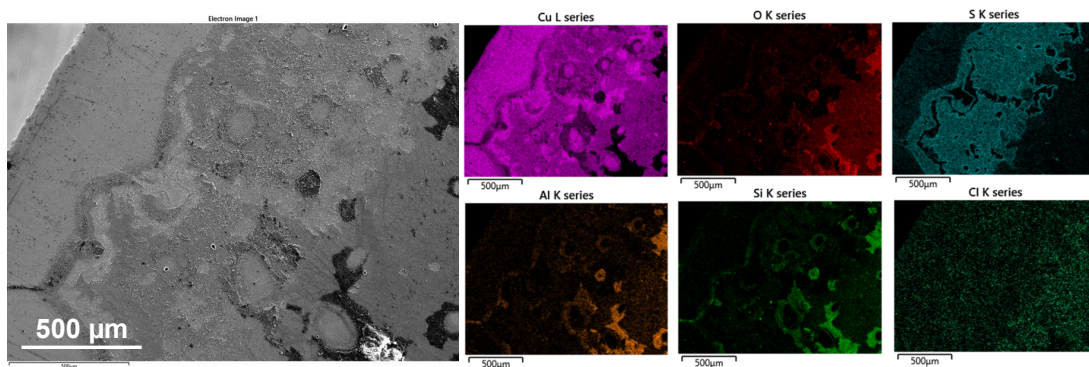


Figure 7-90. SEM and corresponding EDS maps of sample C1-3 (Area 1 from Figure 7-89).

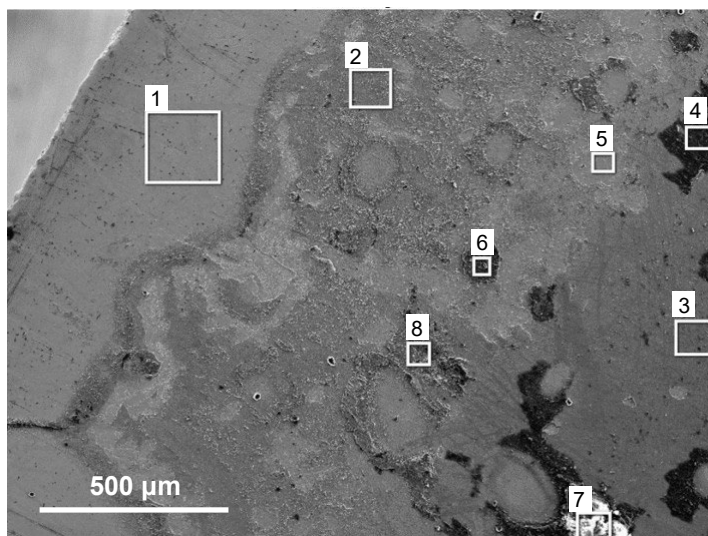


Figure 7-91. SEM of sample C1-3 (Area 1 from Figure 7-89).

Table 7-1. EDS spectra corresponding to Figure 7-91 (wt%).

Label	O	Na	Mg	Al	Si	S	Cl	K	Ca	Ti	Fe	Cu	Total
Spectrum 1	1.91			0.45	0.93	2.55						94.17	100
Spectrum 2	5.41			1.36	3.86	11.04						78.34	100
Spectrum 3	19.57			3.58	7.44	0.83	0.64				0.57	67.38	100
Spectrum 4	42.51			10.53	27.63	1.56	0.21	0.27	1.27		2.61	13.42	100
Spectrum 5						0.28						99.72	100
Spectrum 6	28.97			7.63	22.96	5.45		0.2	0.69		1.96	32.14	100
Spectrum 7	45.83	0.98	4.88	10.39	30.3	0.41		2.43	0.48	0.34	2.24	1.71	100
Spectrum 8	13.71			5.2	14.44	10.75			0.26		1.48	54.15	100

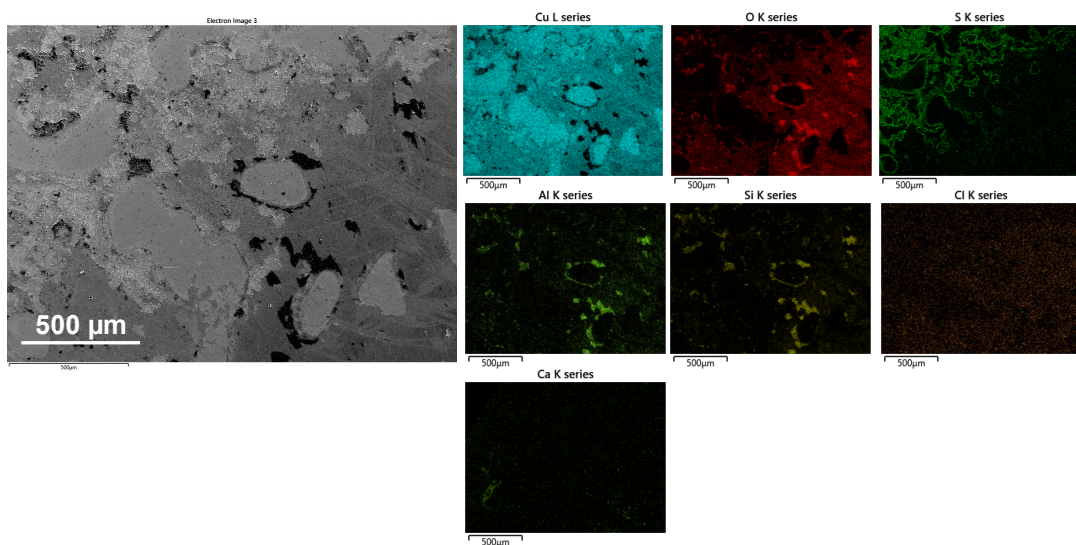


Figure 7-92. SEM and corresponding EDS maps of sample C1-3 (Area 2 from Figure 7-89).

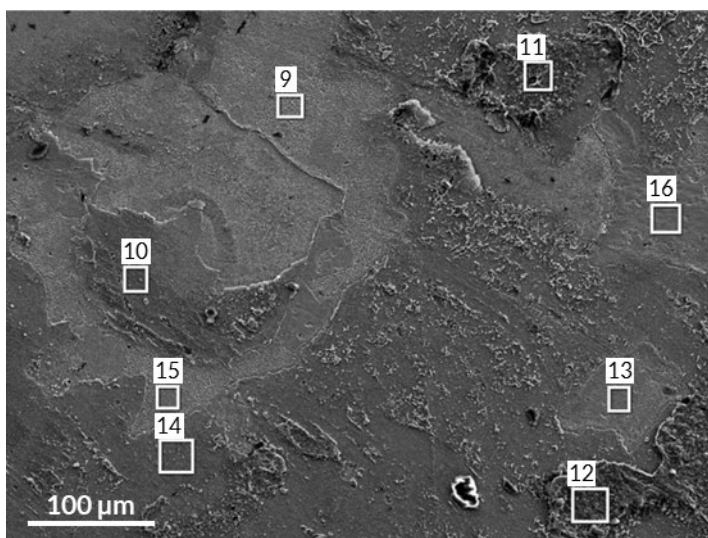


Figure 7-93. SEM of sample C1-3 (Area 1 from Figure 7-89).

Table 7-2. EDS spectra corresponding to Figure 7-93 (wt%).

Label	O	Al	Si	S	Cl	K	Ca	Fe	Cu	Total
Spectrum 9				0.71					99.29	100
Spectrum 10	4.14	1.54	4.18	11.63				0.63	77.88	100
Spectrum 11	13.51	4.58	12.92	10.37				1.31	57.31	100
Spectrum 12	13.23	5.45	15.14	10.56		0.18	0.2	1.29	53.96	100
Spectrum 13									100	100
Spectrum 14	3.89	0.85	2.26	10.73	0.25				82.03	100
Spectrum 15				1.26					98.74	100
Spectrum 16									100	100

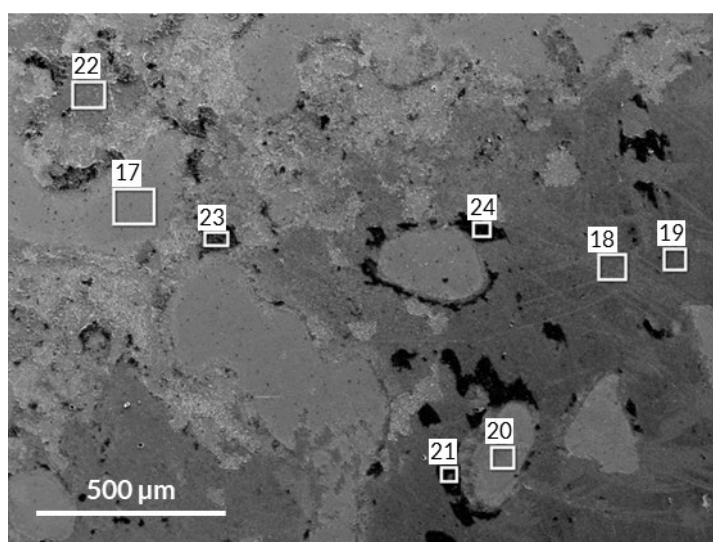


Figure 7-94. SEM of sample CI-3 (Area 2 from Figure 7-89).

Table 7-3. EDS spectra corresponding to Figure 7-94 (wt%).

Label	O	Na	Mg	Al	Si	S	Cl	K	Ca	Fe	Cu	Total
Spectrum 17	0.74					0.38					98.89	100
Spectrum 18	11.45			1.07	1.91	0.4	0.76				84.4	100
Spectrum 19	16.86			2.52	5.1	0.51	0.79			0.6	73.62	100
Spectrum 20					0.72						99.28	100
Spectrum 21	37.22	2.16		10.28	25.17	0.42	0.28	0.12	0.28	1.94	22.12	100
Spectrum 22	3.69			0.95	2.32	10.78	0.21				82.05	100
Spectrum 23	23.53			6.88	17.66	6.98	0.16	0.17	0.52	1.51	42.58	100
Spectrum 24	43.21	2.16	1.92	11.15	29.86	0.75	0.15	0.14	0.79	2.56	7.32	100

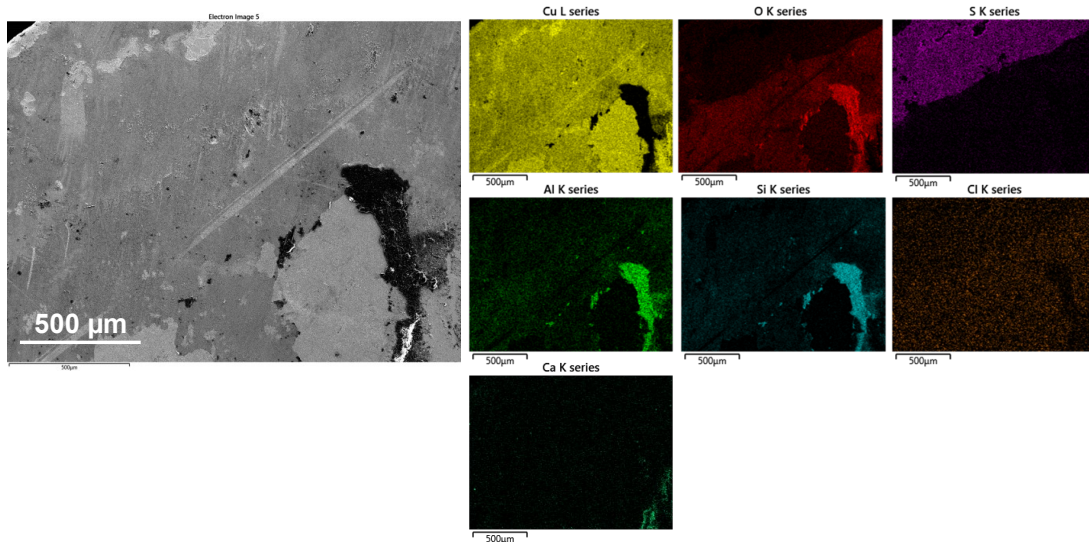


Figure 7-95. SEM and corresponding EDS maps of sample C1-3 (Area 3 from Figure 7-89).

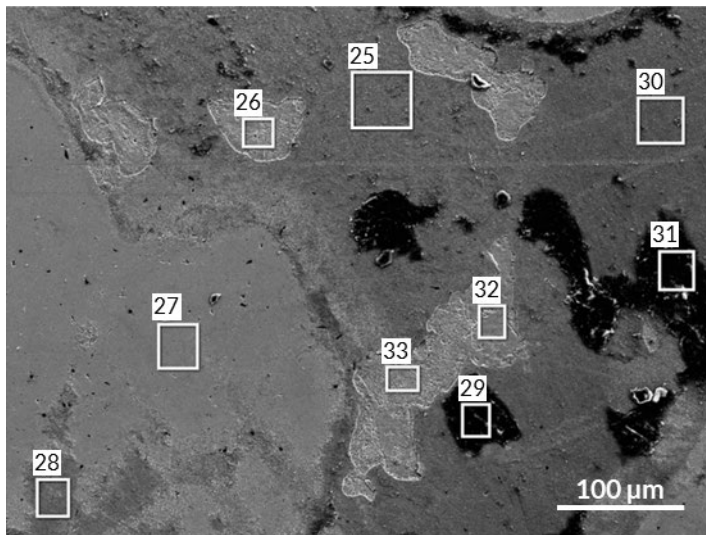


Figure 7-96. SEM of sample C1-3 (Area 2 from Figure 7-89).

Table 7-4. EDS spectra corresponding to Figure 7-96 (wt%).

Label	O	Na	Mg	Al	Si	S	Cl	K	Ca	Fe	Cu	Total
Spectrum 25	11.97			1.16	2.28	0.41	0.93				83.25	100
Spectrum 26						0.78					99.22	100
Spectrum 27											100	100
Spectrum 28	10.23			0.73	1.41	0.73	0.86				86.05	100
Spectrum 29	45.59	2.16	1.69	11.82	31.37	0.35	0.23	0.15	0.48	2.67	3.48	100
Spectrum 30	15.55			2.12	4.48	0.93	0.83				76.09	100
Spectrum 31	47.11	2.27		10.84	27.39	1.25	0.13	0.15	4.03	2.38	4.46	100
Spectrum 32						0.81					99.19	100
Spectrum 33											100	100

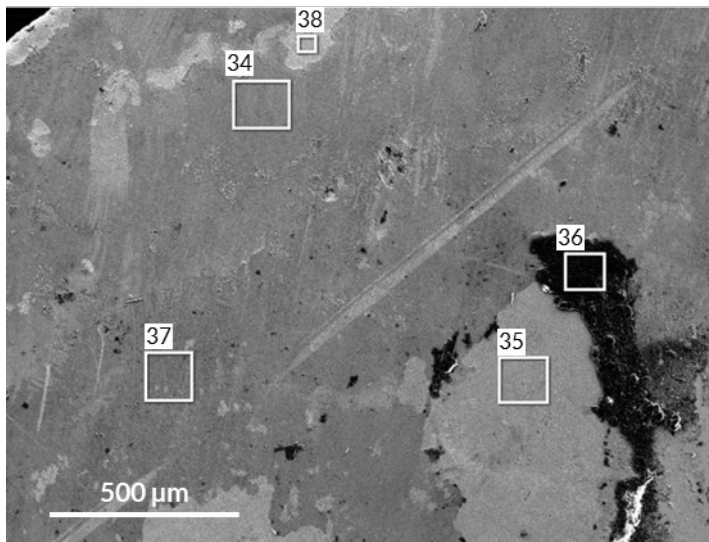


Figure 7-97. SEM of sample C1-3 (Area 3 from Figure 7-89).

Table 7-5. EDS spectra corresponding to Figure 7-97 (wt%).

Label	O	Na	Al	Si	S	Cl	K	Ca	Fe	Cu	Total
Spectrum 34	5.64		1.39	3.55	9.02	0.2			0.35	79.85	100
Spectrum 35	9.1			0.33	0.54	0.82				89.21	100
Spectrum 36	48.22	2.24	11.98	31.49			0.21	0.46	2.7	2.69	100
Spectrum 37	18.43		3.02	5.95	0.42	0.68				71.5	100
Spectrum 38					0.73					99.27	100

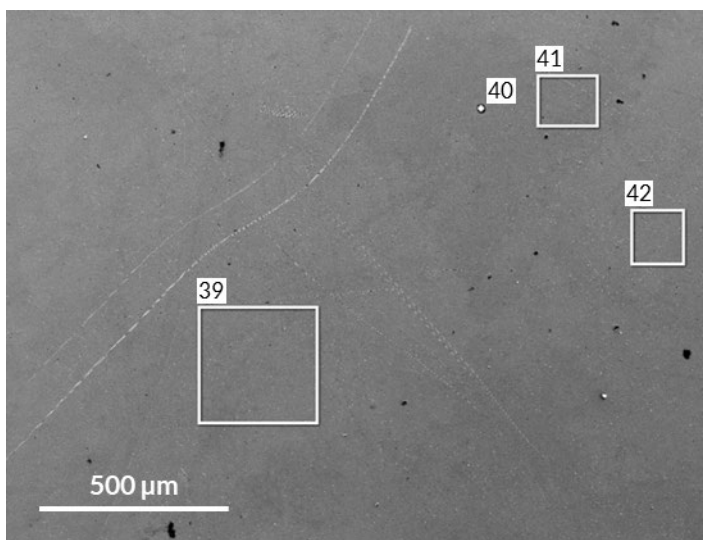


Figure 7-98. SEM of sample C1-3 (Area 4 from Figure 7-89). The surface is mostly clean.

Table 7-6. EDS spectra corresponding to Figure 7-98 (wt%).

Label	O	Na	Al	Si	K	Ca	Fe	Cu	Total
Spectrum 39								100	100
Spectrum 40	44.88	1.31	11.55	26.57	0.99	0.37	2.32	12.01	100
Spectrum 41								100	100
Spectrum 42								100	100

7.4.2 Sample C2-3

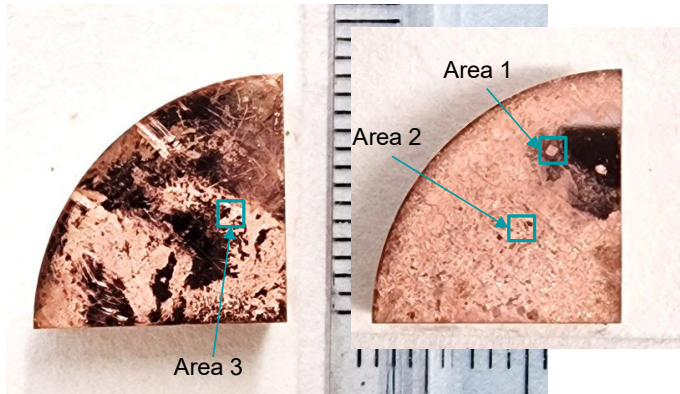


Figure 7-99. Sample C2-3. The marked areas correspond to approximately the examined sites using SEM/EDS.

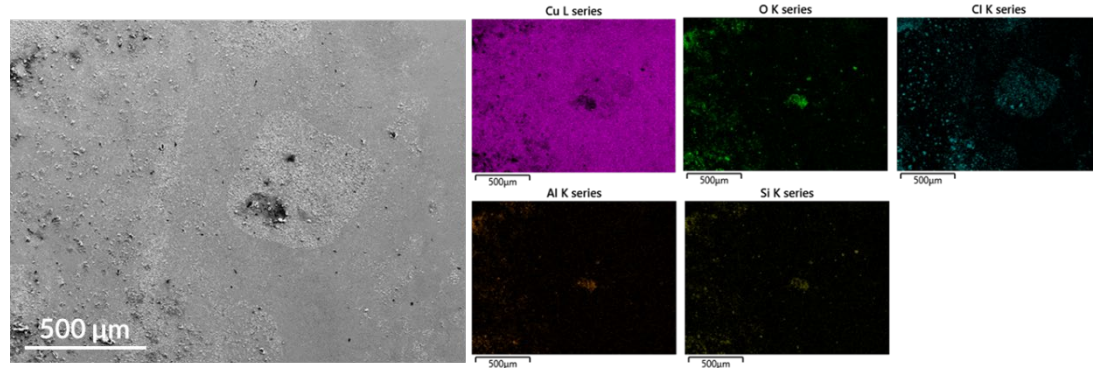


Figure 7-100. SEM and corresponding EDS maps of sample C2-3 (Area 1 from Figure 7-99).

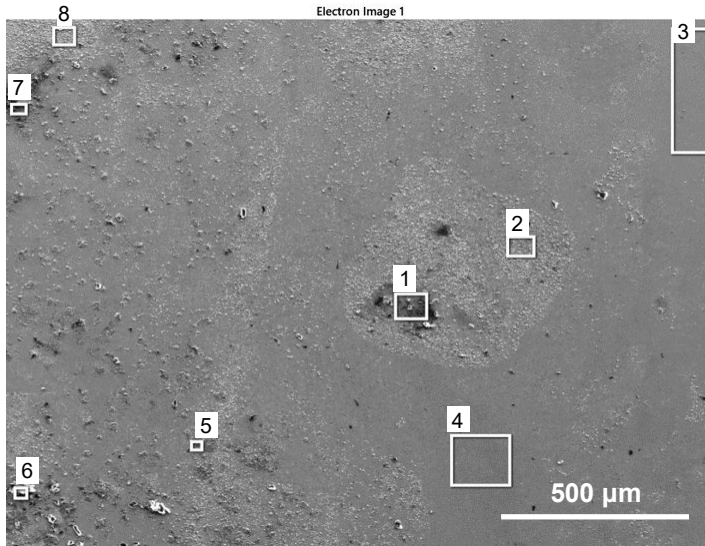


Figure 7-101. SEM of sample C2-3 (Area 1 from Figure 7-99).

Table 7-7. EDS spectra corresponding to Figure 7-101 (wt%).

Label	O	Na	Mg	Al	Si	S	Cl	K	Ca	Fe	Cu	Total
Spectrum 1	22.96			7.1	11.25		5.91			0.57	52.21	100
Spectrum 2	1.01				0.43		7.11				91.45	100
Spectrum 3											100	100
Spectrum 4	1.2			0.28	0.5						98.02	100
Spectrum 5	3.23				1.68		26.91				68.18	100
Spectrum 6	24.64		7.2	4.78	11.19	0.57	8.54	0.23	0.49	0.42	41.94	100
Spectrum 7	29.44	1.33		9.87	16.02		1.54		0.27	0.94	40.58	100
Spectrum 8	0.76				0.34		13.04				85.87	100

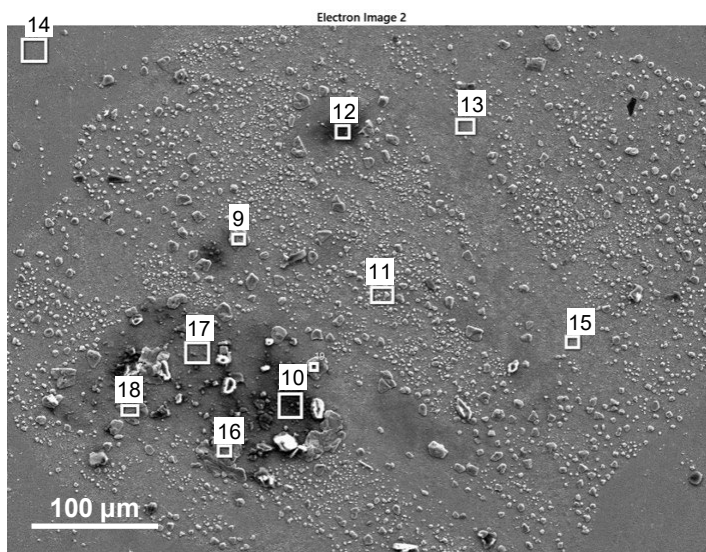


Figure 7-102. SEM of sample C2-3 (Area 1 from Figure 7-99).

Table 7-8. EDS spectra corresponding to Figure 7-102 (wt%).

Label	O	Al	Si	Cl	K	Ca	Fe	Cu	Total
Spectrum 9			0.25	32.57				67.18	100
Spectrum 10	35.65	10.95	18.7	3.22	0.2	0.26	0.75	30.27	100
Spectrum 11	0.95	0.27	0.32	11.95				86.51	100
Spectrum 12	34.79	10.19	17.19	2.92	0.14	0.36	1.12	33.29	100
Spectrum 13	0.85	0.23	0.32	1.28				97.33	100
Spectrum 14								100	100
Spectrum 15				1.57				98.43	100
Spectrum 16			0.44	33.26				66.3	100
Spectrum 17	13.72	4.02	6.03	7.26				68.97	100
Spectrum 18	0.93	0.45	0.79	33.36				64.47	100
Spectrum 19	3.96		2.44	28.21				65.4	100

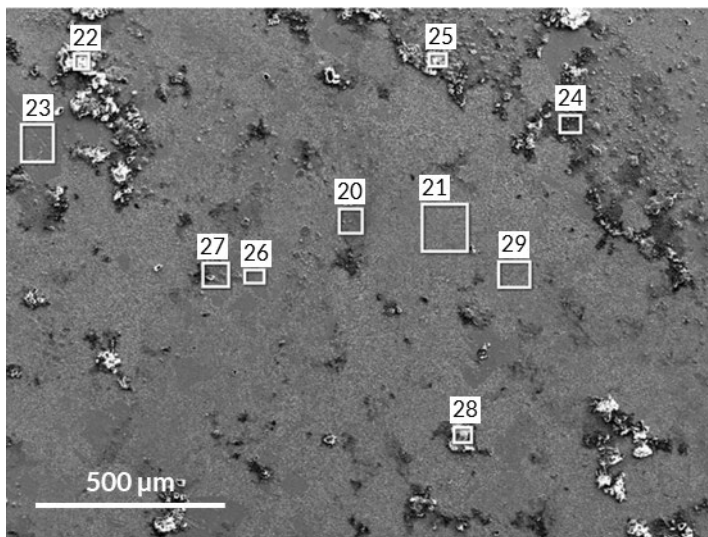


Figure 7-103. SEM of sample C2-3 (Area 2 from Figure 7-99).

Table 7-9. EDS spectra corresponding to Figure 7-103 (wt%).

Label	O	Na	Mg	Al	Si	Cl	K	Ca	Fe	Cu	Total
Spectrum 20	4.51			1.17	1.79	8.92				83.61	100
Spectrum 21						1.2				98.8	100
Spectrum 22	42.53	1.1	3.05	12.21	24.31	4.23	0.4	0.56	1.31	10.3	100
Spectrum 23					0.26	1.54				98.2	100
Spectrum 24	27.84			8.07	13.76	8.6		0.21	0.92	40.61	100
Spectrum 25	31.32			9.55	15.77	11.77		0.39	1.17	30.03	100
Spectrum 26	0.98				0.56	0.17				98.29	100
Spectrum 27	10.16		3.83	1.64	5.9	7.95				70.52	100
Spectrum 28	36.63		5.75	9.59	19.25	7.18	0.36	0.64	0.9	19.7	100
Spectrum 29	1			0.27	0.37	2.49				95.87	100

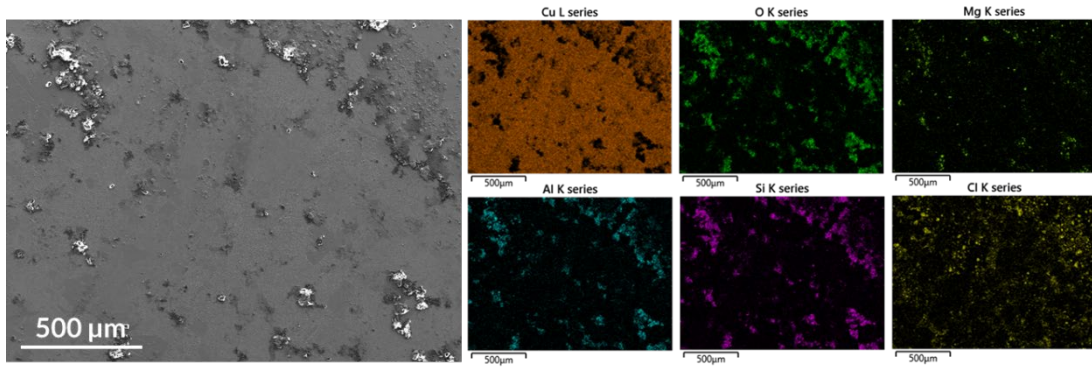


Figure 7-104. SEM and corresponding EDS maps of sample C2-3 (Area 2 from Figure 7-99).

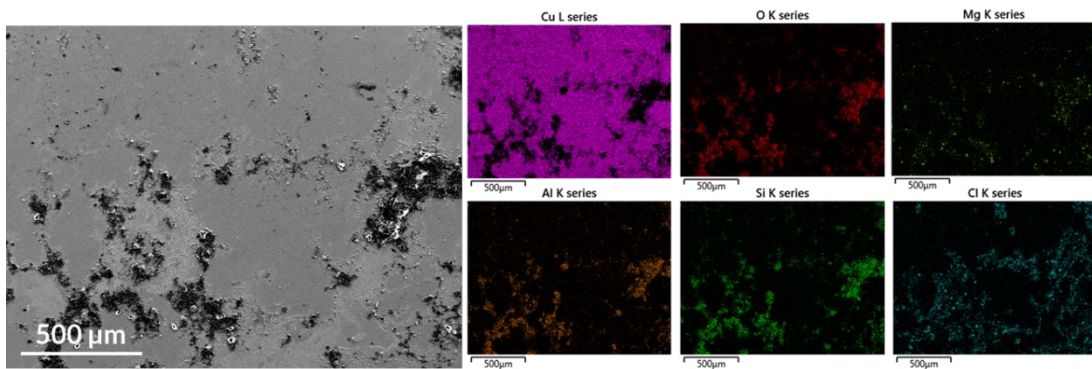


Figure 7-105. SEM and corresponding EDS maps of sample C2-3 (Area 3 from Figure 7-99).

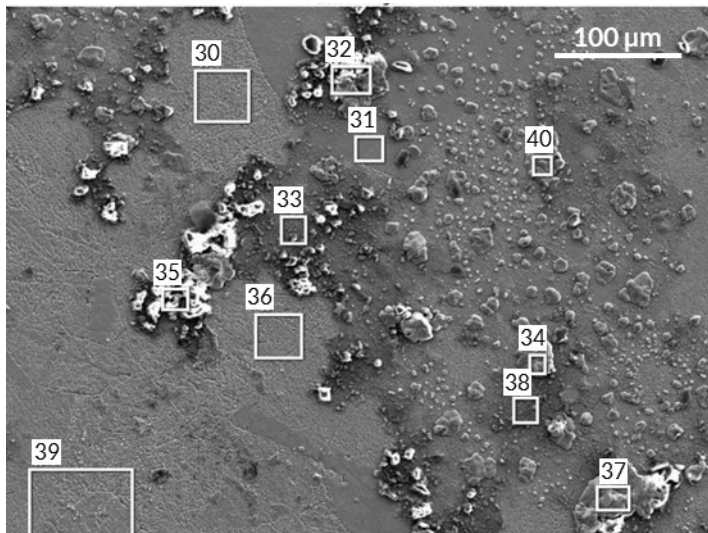


Figure 7-106. SEM of sample C2-3 (Area 2 from Figure 7-99).

Table 7-10. EDS spectra corresponding to Figure 7-106 (wt%).

Label	O	Na	Al	Si	Cl	K	Ca	Fe	Cu	Total
Spectrum 30					0.67				99.33	100
Spectrum 31									100	100
Spectrum 32	24.85		6.3	13.07	18.03		0.27	0.77	36.7	100
Spectrum 33	22.58		7.02	11.51	3.8		0.21	0.46	54.42	100
Spectrum 34	1.64			0.47	32.25				65.63	100
Spectrum 35	46.96	1.31	15.18	28.59	1.45	0.28	0.71	2.05	3.48	100
Spectrum 36					1.03				98.97	100
Spectrum 37	2.4		0.63	1.1	31.07				64.79	100
Spectrum 38	22.93		6.56	10.8	7.5			0.73	51.49	100
Spectrum 39				0.35	1.95				97.7	100
Spectrum 40				0.26	32.8				66.93	100

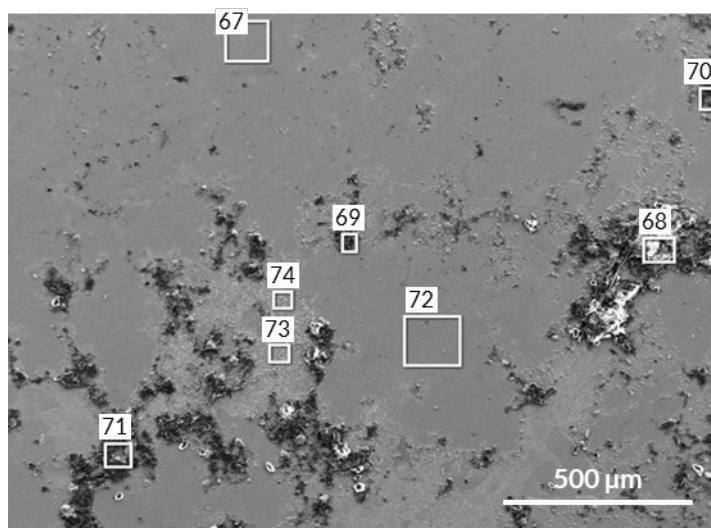


Figure 7-107. SEM of sample C2-3 (Area 3 from Figure 7-99).

Table 7-11. EDS spectra corresponding to Figure 7-107 (wt%).

Label	O	Na	Mg	Al	Si	S	Cl	K	Ca	Fe	Cu	Total
Spectrum 67	0.65										99.35	100
Spectrum 68	46.13	1.21	2.41	14	27.24		1.33	0.25	0.68	1.75	5	100
Spectrum 69	34.07	0.62	5.11	10.01	19.16	0.25	3.51	0.27	0.65	0.96	25.38	100
Spectrum 70	28.18		4.58	6.9	16.12	0.47	6.92		0.77	0.8	35.25	100
Spectrum 71	30.28			9.67	17.47		9.18		0.52	1.01	31.86	100
Spectrum 72	0.51										99.49	100
Spectrum 73	0.46						3.08				96.46	100
Spectrum 74											100	100

7.4.3 Sample C3-4

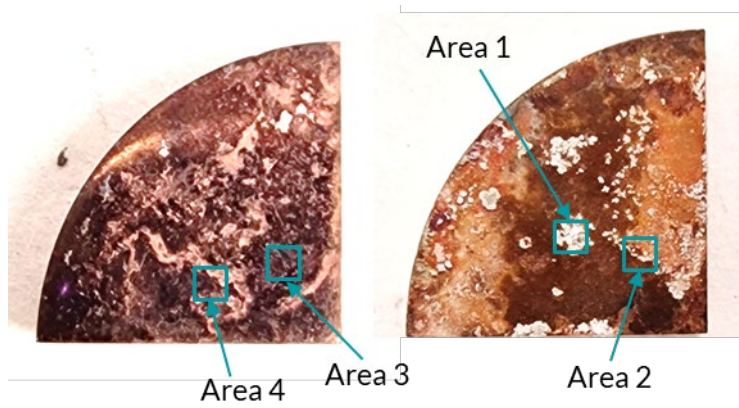


Figure 7-108. Sample C3-4. The marked areas correspond to approximately the examined sites using SEM/EDS.

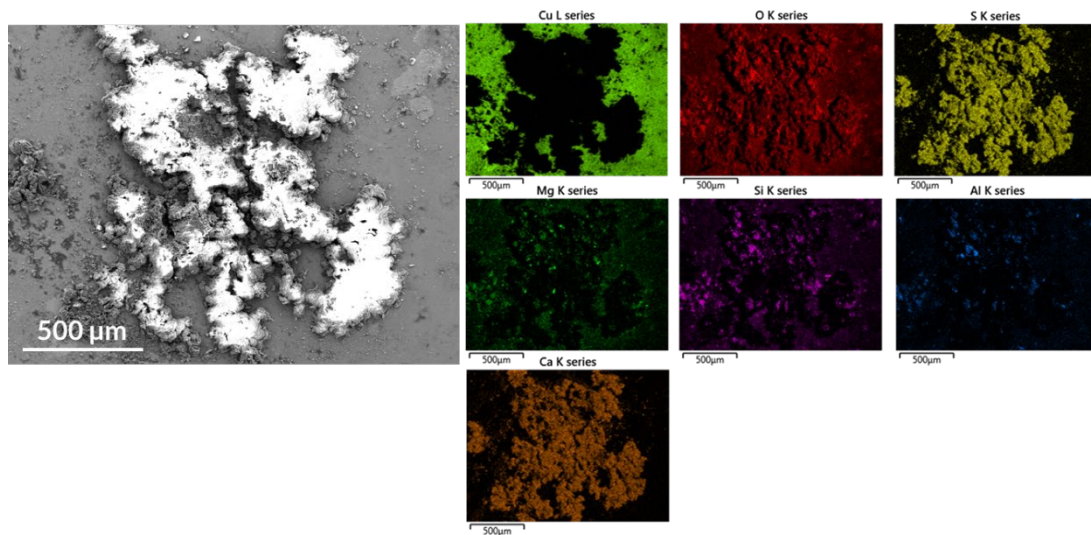


Figure 7-109. SEM and corresponding EDS maps of sample C3-4 (Area 1 from Figure 7-108).

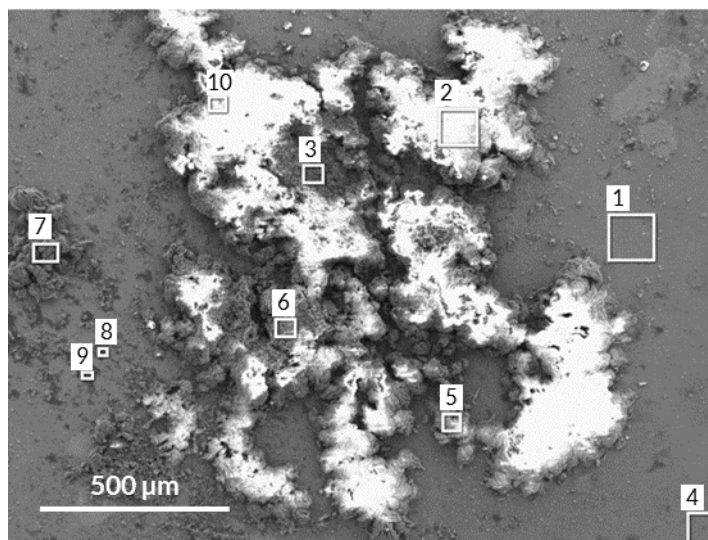


Figure 7-110. SEM of sample C3-4 (Area 1 from Figure 7-108).

Table 7-12. EDS spectra corresponding to Figure 7-110 (wt%).

Label	O	Na	Mg	Al	Si	S	Cl	K	Ca	Fe	Cu	Total
Map Sum Spectrum	23.77		2.33	1.01	4.34	9.28			11.16	0.36	47.74	100
Spectrum 1	11.33		2.39	0.92	3.65	0.75	0.19		0.31		80.47	100
Spectrum 2	45.06		1.41	0.98	4.41	19.69		0.2	26.95	0.91	0.38	100
Spectrum 3	48.59		0.99	0.4	3.05	19.86			26.14		0.97	100
Spectrum 4	9.51		1.31	1.14	3.13	0.71	0.17				84.03	100
Spectrum 5	43.26		0.21	0.14	0.86	23.1			31.88		0.55	100
Spectrum 6	41.01		0.4	0.22	0.99	24.36			32.77		0.25	100
Spectrum 7	45.76				0.75	22.44			31.05		0	100
Spectrum 8	45.36	0.41	9.13	6.05	25.98	0.45	0.21	0.58	1.88	2.85	7.11	100
Spectrum 9	47.18		8.3	7.69	28.07	0.17	0.2	0.62	1	3.46	3.31	100
Spectrum 10	49.44	0.46	4.83	5.99	21.61	5.92		0.55	7.49	3.12	0.6	100

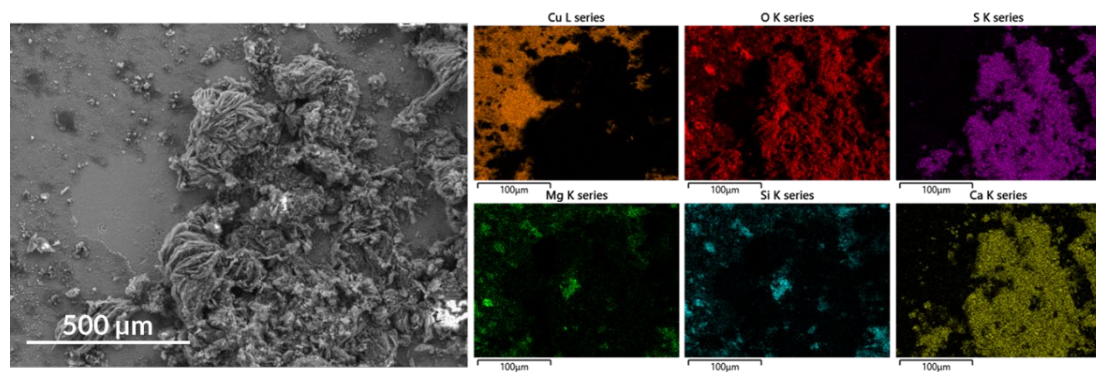


Figure 7-111. SEM and corresponding EDS maps of sample C3-4 (Area 1 from Figure 7-108).

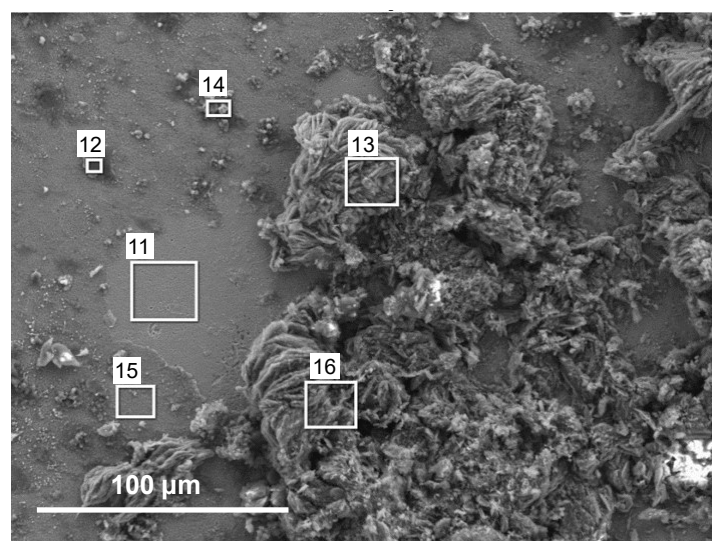


Figure 7-112. SEM of sample C3-4 (Area 1 from Figure 7-108).

Table 7-13. EDS spectra corresponding to Figure 7-112 (wt%).

Label	O	Na	Mg	Al	Si	S	Cl	K	Ca	Mn	Fe	Cu	Total
Spectrum 11						0.17			0.2			99.63	100
Spectrum 12	50.8	0.28	5.68	13.4	22.73			0.63	1.4		1.64	3.46	100
Spectrum 13	49.51		0.15		0.24	21.09			27.68			1.33	100
Spectrum 14	47.84	0.33	8.02	4.33	20.06	0.63	0.18	0.34	10.08	0.33	1.89	5.98	100
Spectrum 15	11.26			0.57	2.73	0.91			2.05			82.48	100
Spectrum 16	48.54				0.24	22.44			28.78			0	100

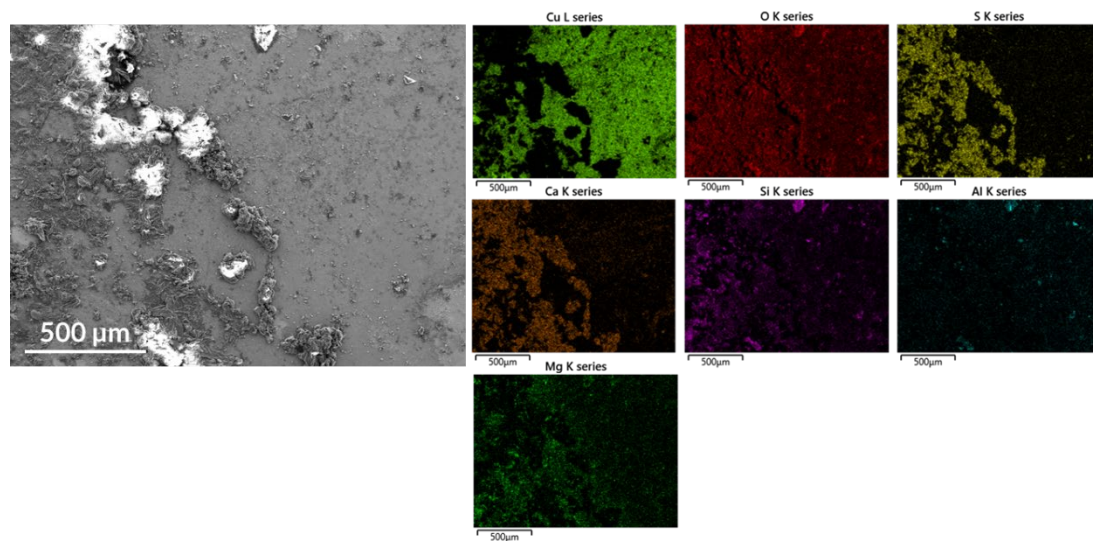


Figure 7-113. SEM and corresponding EDS maps of sample C3-4 (Area 2 from Figure 7-108).

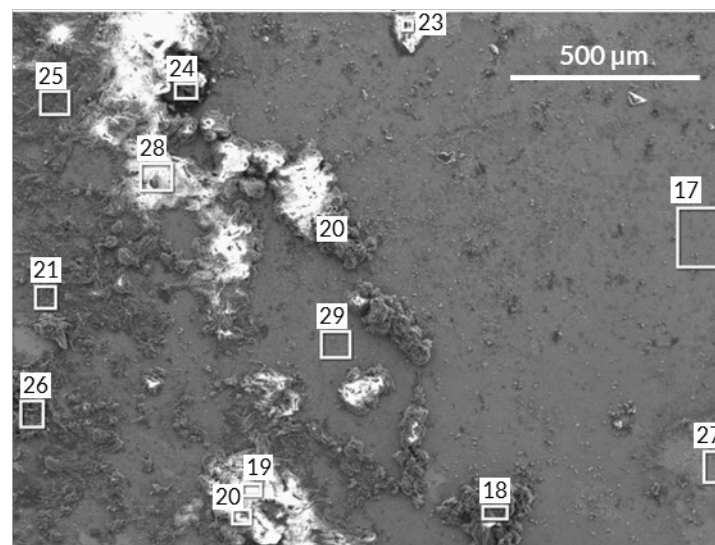


Figure 7-114. SEM of sample C3-4 (Area 2 from Figure 7-108).

Table 7-14. EDS spectra corresponding to Figure 7-114 (wt%).

Label	O	Na	Mg	Al	Si	S	Cl	K	Ca	Ti	Fe	Cu	Total
Spectrum 17	10.53			0.73	1.96	0.98	0.24		1.23			84.33	100
Spectrum 18	44.41		0.49	0.23	1.45	22.12			30.46			0.84	100
Spectrum 19	47.55		0.27		0.63	22.33			29			0.21	100
Spectrum 20	49.86	0.28	3.98	4.01	14.01	10.59		0.38	14.36		1.92	0.61	100
Spectrum 21	33.99				15.29	8.45			9.59			32.69	100
Spectrum 22	41.51				0.71	24.07			33.71			0	100
Spectrum 23	48.5	0.46	4.69	9.63	27.04	0.93	0.27	1.09	2.3	0.26	3.9	0.95	100
Spectrum 24	39.48	0.59	0.75	0.23	1.96	19.91			26.77		0.49	9.82	100
Spectrum 25	45.28		0.3	0.1	1.74	21.96			28.23			2.4	100
Spectrum 26	46.44		0.22		0.77	22.09			29.44			1.05	100
Spectrum 27	10.94				1.43	0.72	0.24		0.37			86.31	100
Spectrum 28	45.02		0.26	0.92	3.64	20.21		0.39	29.38			0.18	100
Spectrum 29	12.94				4.39	0.35	0.18		0.28			81.87	100

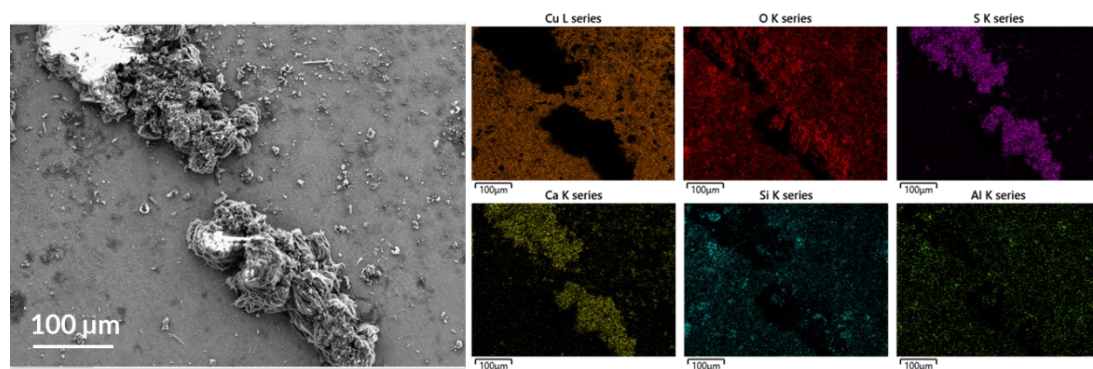


Figure 7-115. SEM and corresponding EDS maps of sample C3-4 (Area 2 from Figure 7-108).

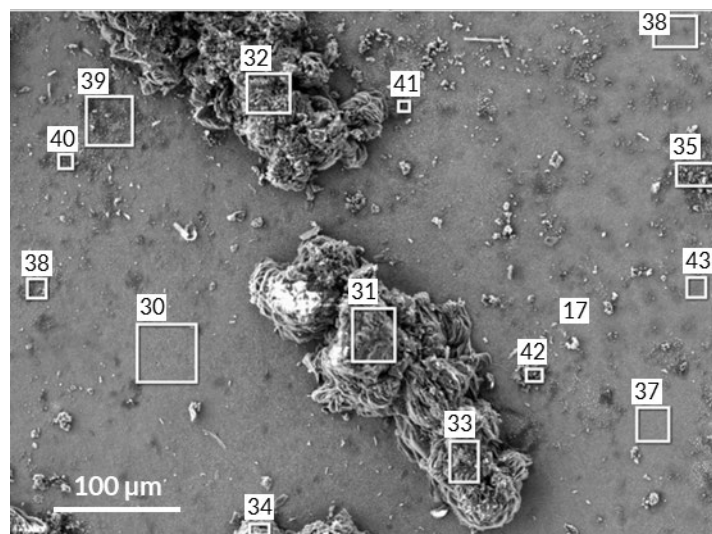


Figure 7-116. SEM of sample C3-4 (Area 2 from Figure 7-108).

Table 7-15. EDS spectra corresponding to Figure 7-116 (wt%).

Label	O	Mg	Al	Si	S	Cl	K	Ca	Fe	Cu	Total
Map Sum Spectrum	17.91			4.02	4.42			5.54	0.22	67.89	100
Spectrum 30	12.52			4.25	0.37	0.2		0.19		82.48	100
Spectrum 31	45.71	0.11		0.44	22.75			29.78		1.21	100
Spectrum 32	48.9	0.32	0.21	1.35	21.09			27.73		0.4	100
Spectrum 33	42.17	1.03	0.35	3.55	21.78			30	0.26	0.86	100
Spectrum 34	50.96	0.29		0.37	19.18			23.92		5.27	100
Spectrum 35	32.27	3.67	3.13	10.22	3.66	0.17	0.2	9.86	1.17	35.66	100
Spectrum 36	9.94		0.49	1.68	0.56	0.16		2.48		84.69	100
Spectrum 37	9.58		0.49	2.22	0.61	0.25				86.84	100
Spectrum 38	27.6	10.04	2.44	14.31	0.3	0.19	0.14	0.53	0.85	43.6	100
Spectrum 39	25.23	8.45	1.97	11.6	0.64	0.2		0.7	0.9	50.3	100
Spectrum 40	27.33	9.46	2.14	12.92	0.3	0.23		0.26	0.87	46.49	100
Spectrum 41	33.08	10	3.59	16.73	0.71	0.17	0.3	0.86	1.32	33.24	100
Spectrum 42	40.15	6.28	2.18	13.43	10.57		0.3	14.23	1.76	11.11	100
Spectrum 43	15.42		0.53	1.76	0.93	0.24		5.24		75.88	100

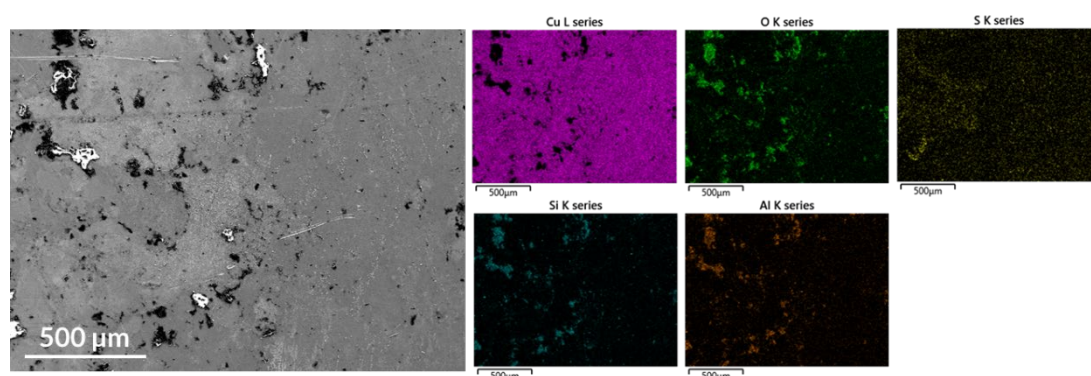


Figure 7-117. SEM and corresponding EDS maps of sample C3-4 (Area 3 from Figure 7-108).

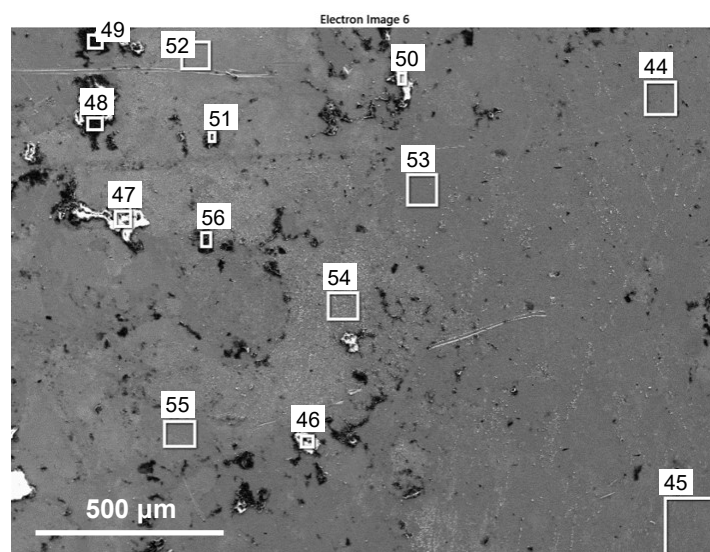


Figure 7-118. SEM of sample C3-4 (Area 3 from Figure 7-108).

Table 7-16. EDS spectra corresponding to Figure 7-118 (wt%).

Label	O	Na	Mg	Al	Si	S	K	Ca	Ti	Fe	Cu	Total
Spectrum 44	3.4			0.78	1.54	0.54					93.74	100
Spectrum 45	2.92			0.66	1.26	0.82					94.34	100
Spectrum 46	46.47		1.9	12.92	28.57	0.67	1.21	1.54		4.83	1.89	100
Spectrum 47	47.18		1.91	12.64	29.52		1.13	1.42		4.96	1.24	100
Spectrum 48	41.51		2.04	11.43	26.38	0.28	1.3	1.2	0.26	6.08	9.52	100
Spectrum 49	46.35		1.97	11.77	29.06	0.27	1.29	1.33		6.17	1.8	100
Spectrum 50	46.72	0.28	1.77	12.91	28.94		1.64	1.3	0.17	4.84	1.44	100
Spectrum 51	49.36		2.09	12.17	28.18		0.64	1.1	0.27	4.72	1.46	100
Spectrum 52	1.57			0.3	0.6	1.01					96.51	100
Spectrum 53	2.8			0.67	1.16	0.68					94.7	100
Spectrum 54	2.19			0.48	0.91	0.41					96	100
Spectrum 55	1.76			0.39	0.75	0.23					96.86	100
Spectrum 56	39.96		1.79	11.66	24.09	0.93	0.9	1.08		4.1	15.49	100

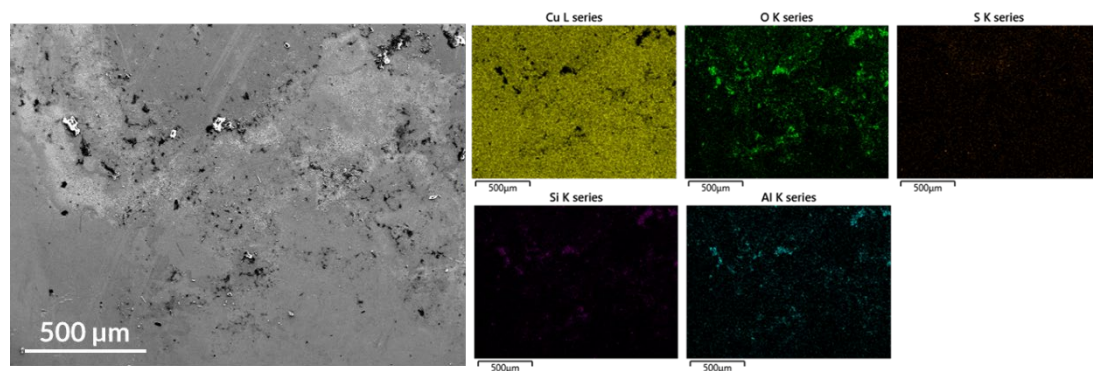


Figure 7-119. SEM and corresponding EDS maps of sample C3-4 (Area 4 from Figure 7-108).

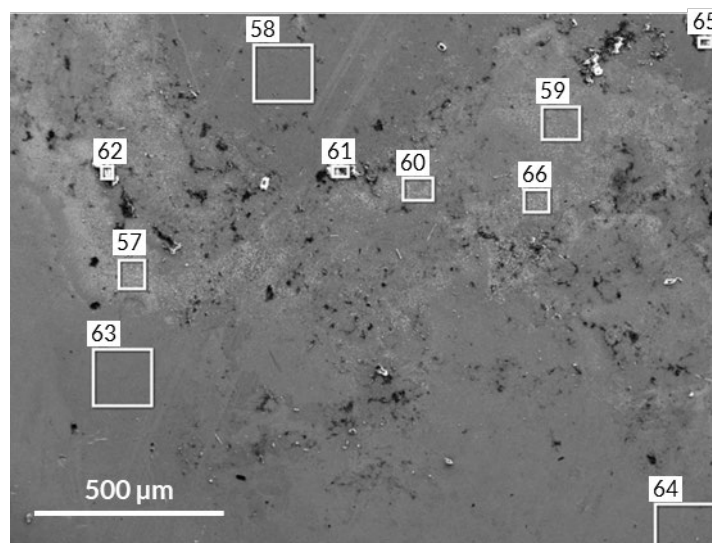


Figure 7-120. SEM of sample C3-4 (Area 4 from Figure 7-108).

Table 7-17. EDS spectra corresponding to Figure 7-120 (wt%).

Label	O	Na	Mg	Al	Si	S	K	Ca	Ti	Fe	Cu	Total
Map Sum Spectrum	3.95			1.18	2.18	0.28		0.08		0.21	92.12	100
Spectrum 57	2.22			0.47	0.94						96.36	100
Spectrum 58	4.78			1.13	2.16	0.57					91.36	100
Spectrum 59	1.31			0.28	0.58						97.82	100
Spectrum 60	1.91			0.44	0.83						96.82	100
Spectrum 61	42.89		1.72	13.61	24.07	0.5	1.26	1.34		3.29	11.32	100
Spectrum 62	47.43	0.18	2.51	13.15	27.69	0.53	1.05	1.74		4.63	1.08	100
Spectrum 63	1.03			0.26	0.4						98.31	100
Spectrum 64	0.92				0.4						98.69	100
Spectrum 65	43.22		1.92	12.48	28.27	0.49	0.8	1.71	0.16	4.91	6.06	100
Spectrum 66	1.35				0.46						98.19	100

7.4.4 Sample C4-2

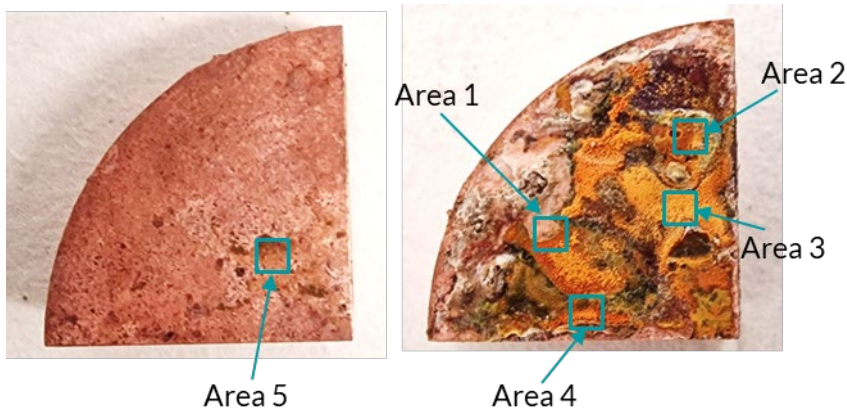


Figure 7-121. Sample C4-2. The marked areas correspond to approximately the examined sites using SEM/EDS.

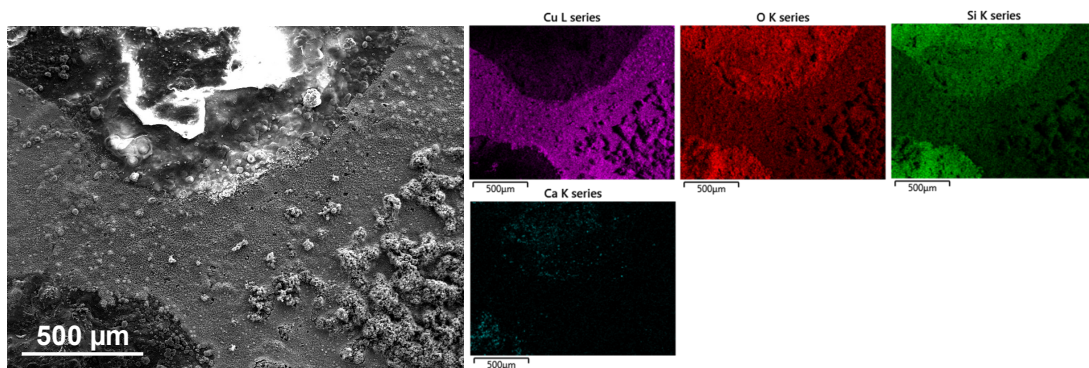


Figure 7-122. SEM and corresponding EDS maps of sample C4-2 (Area 1 from Figure 7-121).

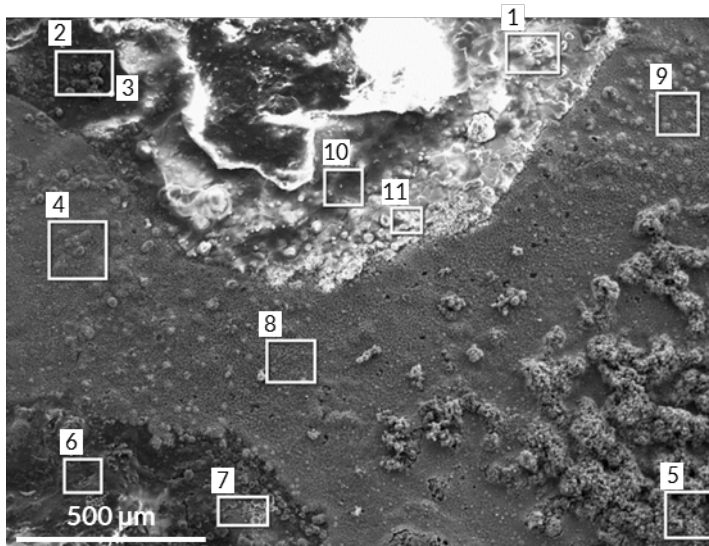


Figure 7-123. SEM of sample C4-2 (Area 1 from Figure 7-121).

Table 7-18. EDS spectra corresponding to Figure 7-123 (wt%).

Label	O	Na	Mg	Si	Ca	Cu	Total
Spectrum 1	43.64			28.84	1.14	26.37	100
Spectrum 2	48.56	1.08		38.43	1.14	10.79	100
Spectrum 3	48.11	1.1		39.32	0.24	11.23	100
Spectrum 4	25.81			19.95	0.3	53.94	100
Spectrum 5	22.18			13.06	0.2	64.57	100
Spectrum 6	46.17	0.64	2.16	30.48	11.24	9.31	100
Spectrum 7	44.83			36.28	0.52	18.37	100
Spectrum 8	23.49			17.94		58.57	100
Spectrum 9	25.15			18.86		55.99	100
Spectrum 10	42.91			28.69	0.8	27.6	100
Spectrum 11	41.35			24.57	1.55	32.53	100

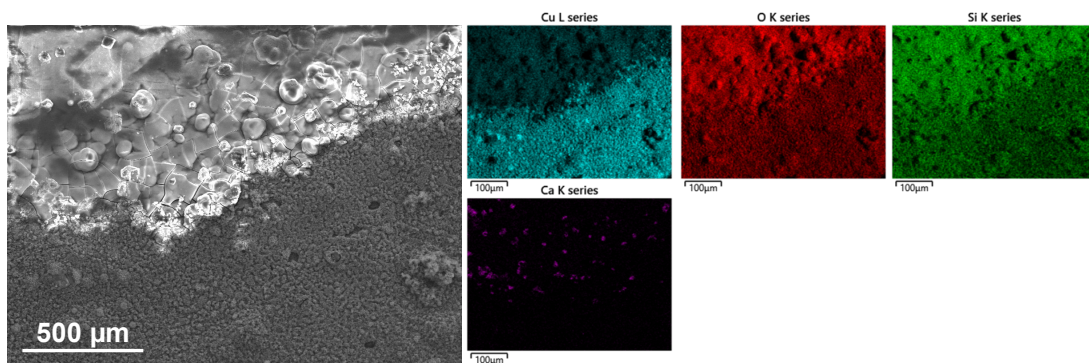


Figure 7-124. SEM and corresponding EDS maps of sample C4-2 (Area 2 from Figure 7-121).

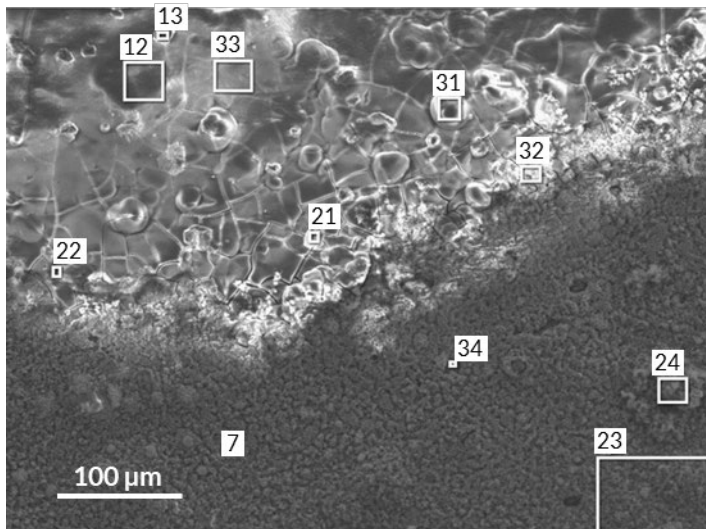


Figure 7-125. SEM of sample C4-2 (Area 1 from Figure 7-121).

Table 7-19. EDS spectra corresponding to Figure 7-125 (wt%).

Label	O	Si	Cl	Ca	Cu	Total
Spectrum 12	43.43	27.05		1.12	28.4	100
Spectrum 13	53.19	6.2		26.33	14.28	100
Spectrum 21	38.13	31.01	0.19	4.26	26.42	100
Spectrum 22	45.99	16.81		19.17	18.03	100
Spectrum 23	21.16	14.89			63.95	100
Spectrum 24	20.03	11.91			68.06	100
Spectrum 31	42.02	27.99	0.14	3.97	25.87	100
Spectrum 32	34.04	23.1		0.63	42.23	100
Spectrum 33	43.02	27.45		0.6	28.93	100
Spectrum 34	22.06	14.9			63.03	100

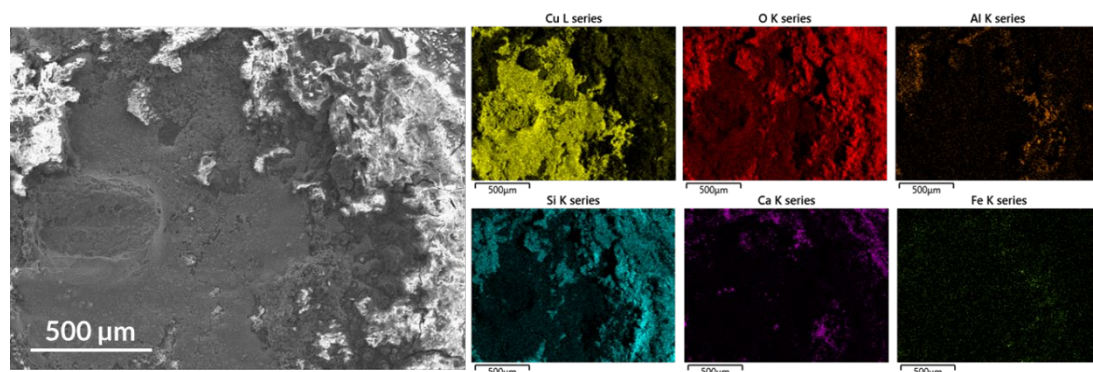


Figure 7-126. SEM of sample C4-2 (Area 2 from Figure 7-121).

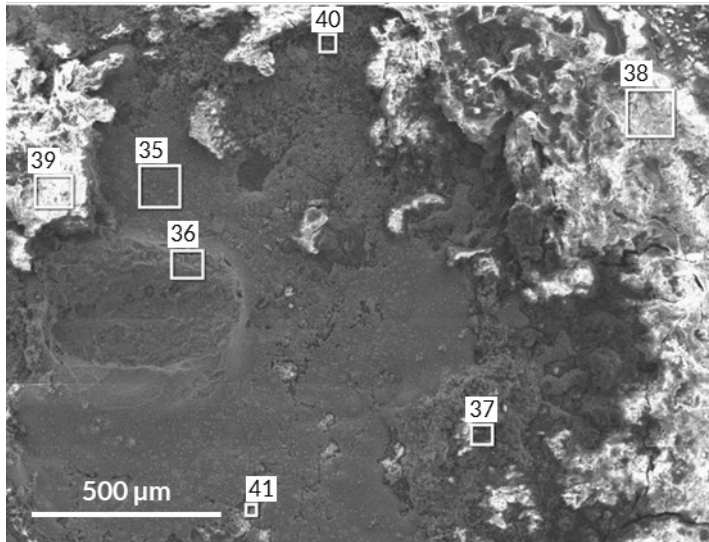


Figure 7-127. SEM of sample C4-2 (Area 2 from Figure 7-121).

Table 7-20. EDS spectra corresponding to Figure 7-127 (wt%).

Label	O	Na	Mg	Al	Si	Cl	Ca	Ti	Mn	Fe	Cu	Total
Spectrum 35	15.62				7.08						77.3	100
Spectrum 36	14.98				5.43						79.58	100
Spectrum 37	50.24	0.34	4.29	2.07	10.21		24.18	0.33	0.26	1.64	6.45	100
Spectrum 38	47.88				15.98	0.21	8.29				27.64	100
Spectrum 39	42.41			2.29	22.24		1.64			1.38	30.05	100
Spectrum 40	43.66				5.76		25.49		0.23		24.85	100
Spectrum 41	40.95				29.65	0.22	1.19				27.99	100

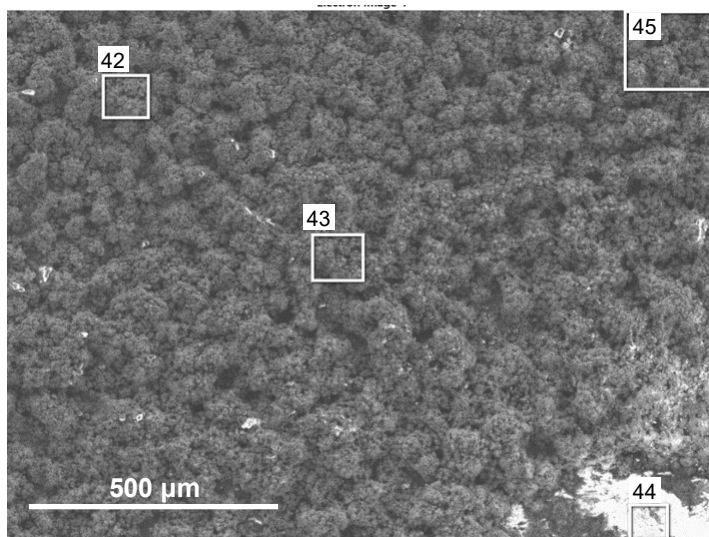


Figure 7-128. SEM of sample C4-2 (Area 3 from Figure 7-121).

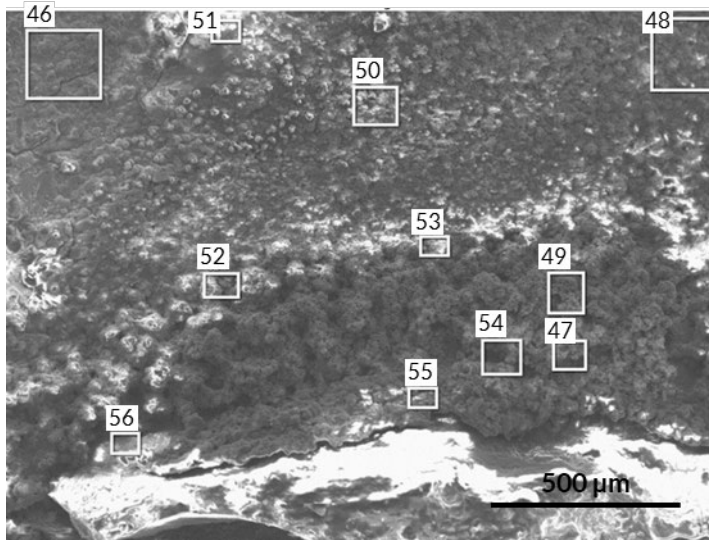


Figure 7-129. SEM of sample C4-2 (Area 4 from Figure 7-121).

Table 7-21. EDS spectra corresponding to Figure 7-129 (wt%).

Label	O	Na	Mg	Si	Ca	Cu	Total
Spectrum 46	50.45	1	1.02	44.76	0.27	2.51	100
Spectrum 47	15.33			3.84	4.15	76.68	100
Spectrum 48	51.02	0.98	0.83	40.86	2.67	3.63	100
Spectrum 49	36.9			28.25	4.23	30.62	100
Spectrum 50	51.14	1.01	0.65	44.2	0.8	2.19	100
Spectrum 51	53	1.37		44.3		1.33	100
Spectrum 52	56.44	1.13		40.46	1.61	0.36	100
Spectrum 53	51.47	0.85		41.54	3.32	2.82	100
Spectrum 54	16.79			3.28	9.12	70.81	100
Spectrum 55	55.05	0.57	3.01	29.59	11.34	0.44	100
Spectrum 56	53.91	0.23	2.19	15.02	27.95	0.7	100

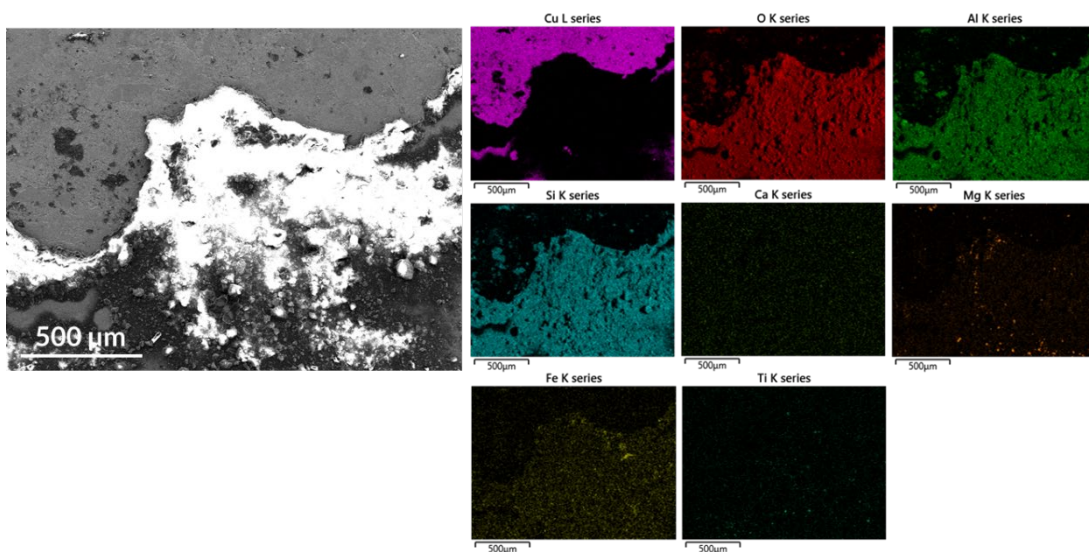


Figure 7-130. SEM and corresponding EDS maps of sample C4-2 (Area 5 from Figure 7-121).

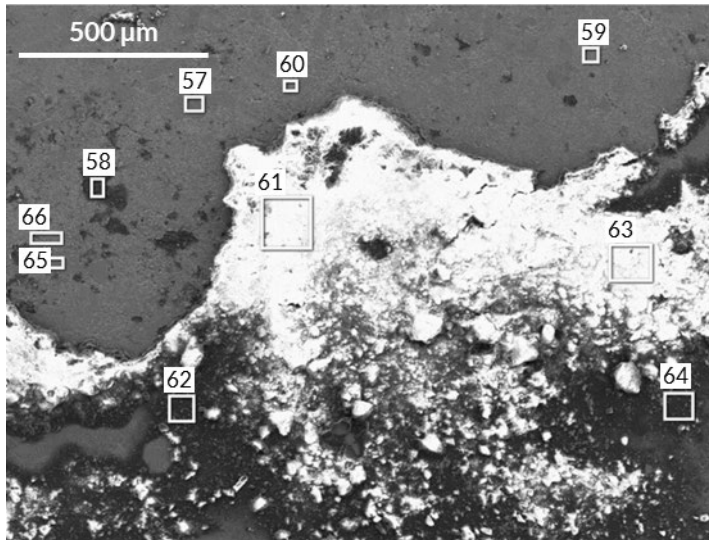


Figure 7-131. SEM of sample C4-2 (Area 5 from Figure 7-121).

Table 7-22. EDS spectra corresponding to Figure 7-131 (wt%).

Label	O	Na	Mg	Al	Si	Ca	Ti	Fe	Cu	Total
Spectrum 57	1.1			0.27	0.43				98.2	100
Spectrum 58	39.97	0.95		12.86	20.47	0.44	0.23	4.6	20.47	100
Spectrum 59	0.82				0.34				98.84	100
Spectrum 60								0.43	99.57	100
Spectrum 61	52.98	1.07	1.81	11.31	24.09	0.59	0.84	7.08	0.24	100
Spectrum 62	47.35	0.96	1.32	12.97	26.47	0.71	0.92	8.83	0.47	100
Spectrum 63	51.08	1.1	1.7	11.82	24.39	0.67	0.87	8.13	0.25	100
Spectrum 64	45.03	0.82	1.32	12.61	24.69	0.66	0.65	7.91	6.32	100
Spectrum 65	1.25			0.29	0.55				97.91	100
Spectrum 66	3.19			0.94	1.62			0.46	93.79	100

7.4.5 Sample C5-3

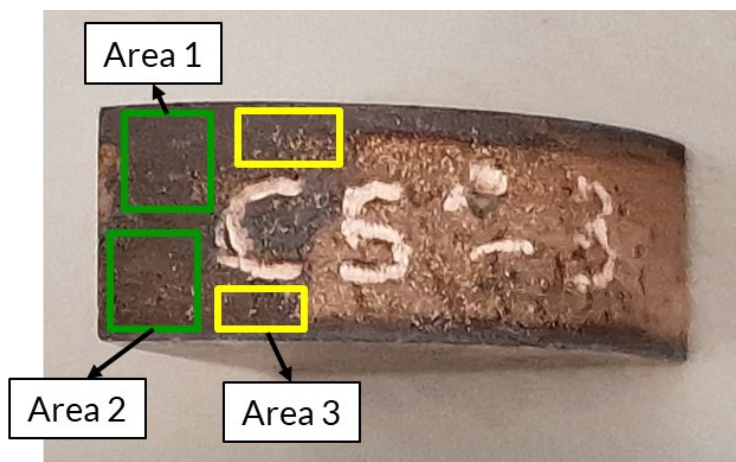


Figure 7-132. Sample C5-3 (outer rim, non pre-polished area). The marked areas correspond to approximately the examined sites using SEM/EDS.

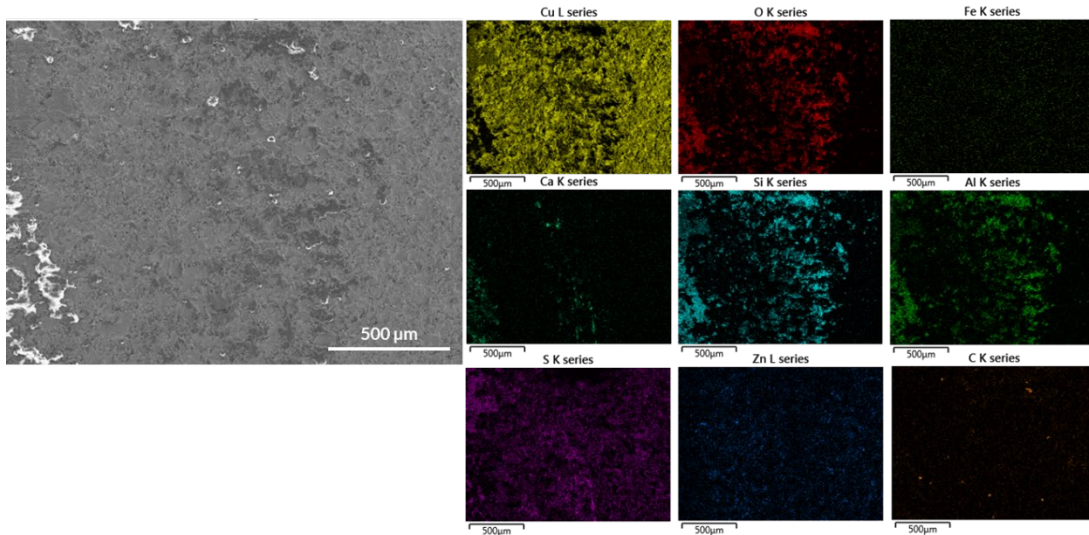


Figure 7-133. SEM and corresponding EDS maps of sample C5-3 (Area 1 from Figure 7-132).

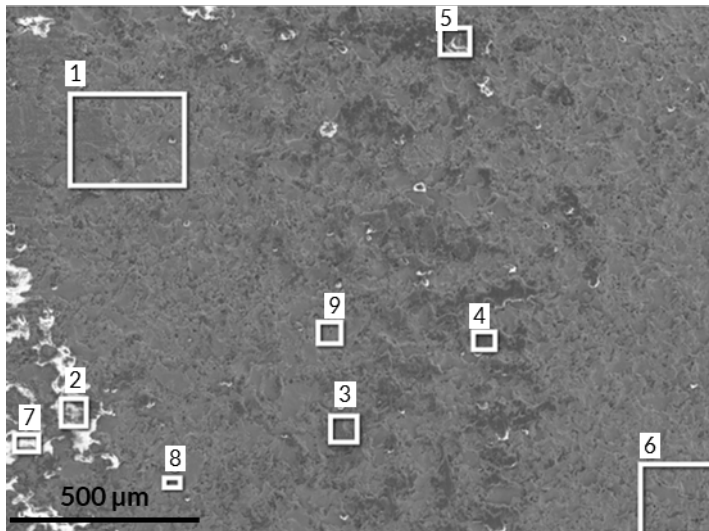


Figure 7-134. SEM of sample C5-3 (Area 1 from Figure 7-132).

Table 7-23. EDS spectra corresponding to Figure 7-134 (wt%).

Label	O	Na	Mg	Al	Si	S	K	Ca	Fe	Cu	Zn	Total
Spectrum 1	5.96			1.55	4.65	6.29		0.27		75.6	5.67	100
Spectrum 2	40.81			10.34	26.24	1.55	0.14	3.58	2.49	12.59	2.25	100
Spectrum 3	14.54			4.5	11.12	7.68		1.2	0.97	56.29	3.7	100
Spectrum 4	36.9	1.62	2.25	10.06	25.5	2.15	0.28	0.73	2.33	16.93	1.24	100
Spectrum 5	46.07	1.5	1.93	11.79	31.85	0.35	0.2	0.66	2.65	3		100
Spectrum 6	1.69					5.77				84.08	8.46	100
Spectrum 7	40.07			9.6	23.95	2.13		6.12	1.94	14.64	1.54	100
Spectrum 8	2.03				1.02	0.65				96.29		100
Spectrum 9	0.72					1.5				97.78		100

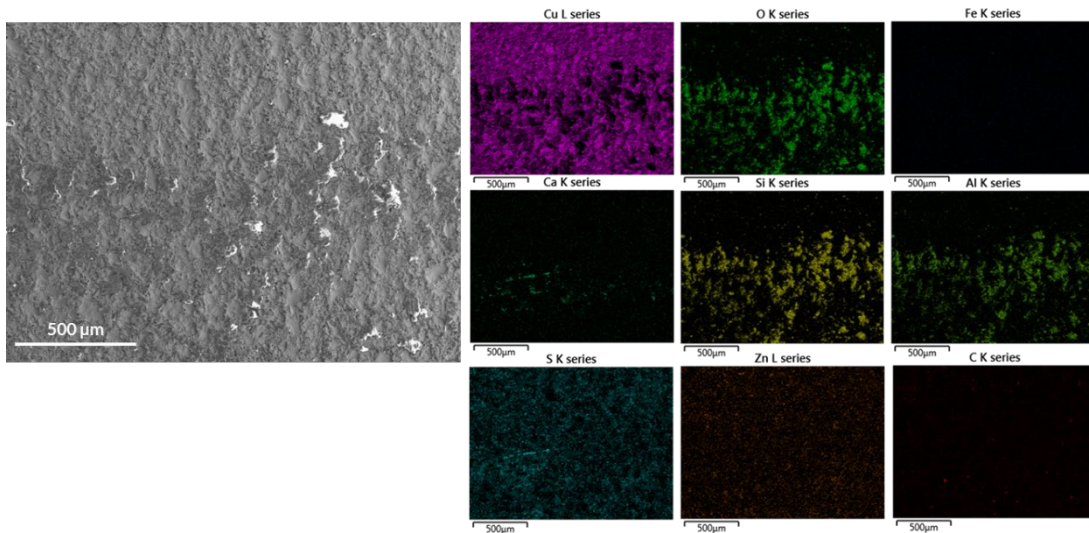


Figure 7-135. SEM and corresponding EDS maps of sample C5-3 (Area 1 from Figure 7-132).

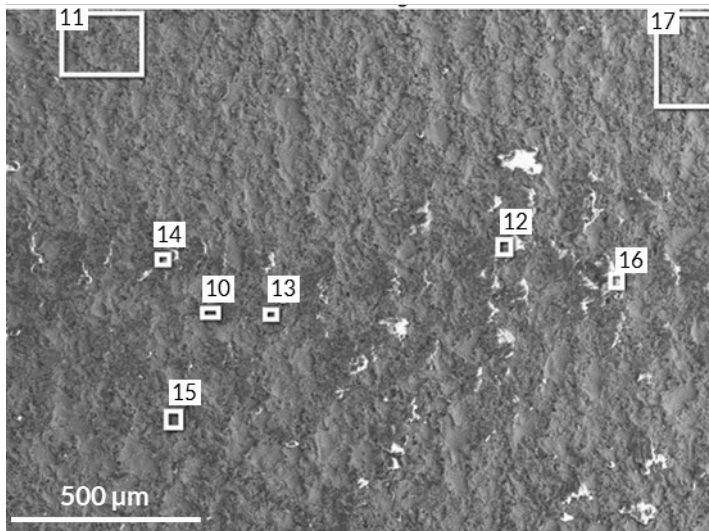


Figure 7-136. SEM of sample C5-3 (Area 1 from Figure 7-132).

Table 7-24. EDS spectra corresponding to Figure 7-136 (wt%).

Label	O	Na	Mg	Al	Si	S	K	Ca	Fe	Cu	Zn	Total
Spectrum 10	28.82			4.14	10.29	10.08		7.68	0.75	35.13	3.11	100
Spectrum 11	1.97			0.25	0.63	6.01		0.16	0.14	79.53	11.31	100
Spectrum 12	38.03	1.49		10.05	24.11	2.63	0.18	0.46	1.86	19.69	1.51	100
Spectrum 13	21.27			5.83	13.25	6.79	0.19	1.13	1.25	42.94	7.35	100
Spectrum 14	41.83			9.1	22.18	4.63	0.25	4.04	1.77	12.66	3.55	100
Spectrum 15	21.57			5.7	14.61	9.98	0.23	4.5	1.35	40.07	2.01	100
Spectrum 16	42.79	1.2	3.65	9.6	26.29	1.17	0.12	0.83	1.86	11.66	0.81	100
Spectrum 17	1.77			0.15	0.47	5.21		0.09	0	82.3	10.01	100

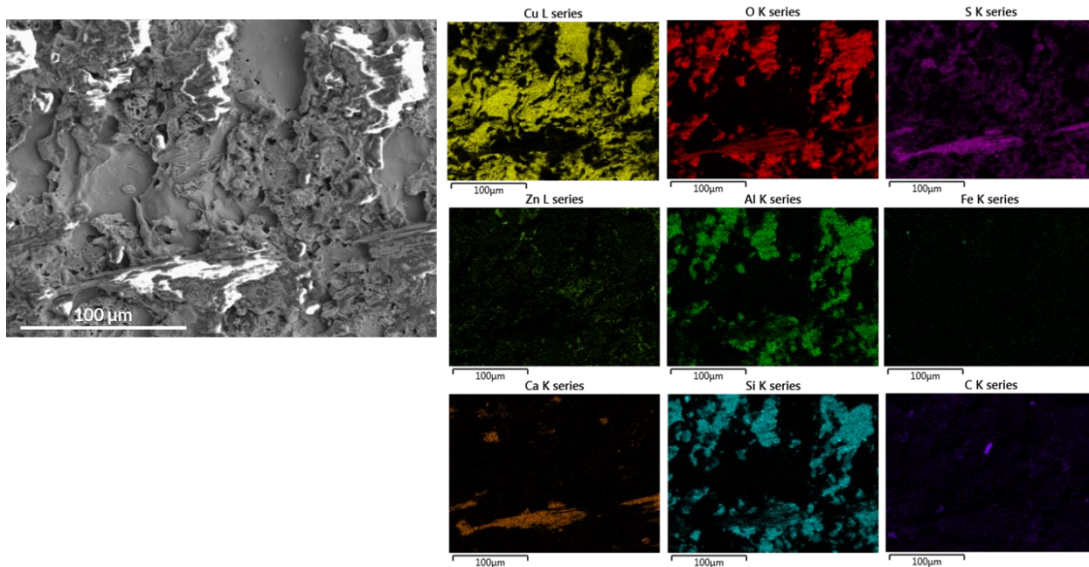


Figure 7-137. SEM and corresponding EDS maps of sample C5-3 (Area 1 from Figure 7-132).

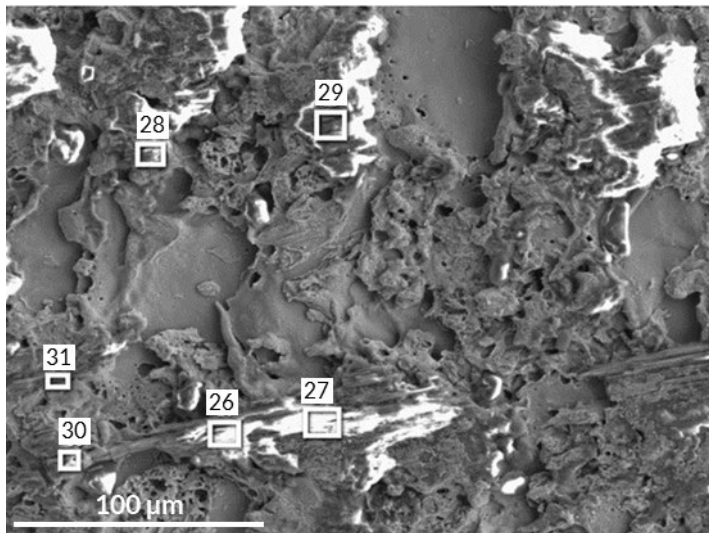


Figure 7-138. SEM of sample C5-3 (Area 1 from Figure 7-132).

Table 7-25. EDS spectra corresponding to Figure 7-138 (wt%).

Label	O	Al	Si	S	K	Ca	Fe	Cu	Total
Spectrum 26	45.77	1.11	2.92	19.75	0.15	23.16	0.29	6.86	100
Spectrum 27	43.62	1.11	3.15	20.58	0.17	24.97	0.27	6.13	100
Spectrum 28	45.93	2.28	5.83	18.22	0.18	21.31	0.47	5.78	100
Spectrum 29	45.92	10.91	28.82	4.1	0.49	4.35	2.72	2.7	100
Spectrum 30	45.23	1.29	3.66	18.8	0.11	21.14	0.29	9.49	100
Spectrum 31	42.55	1.56	3.44	17.19	0.1	19.72	0.24	15.22	100

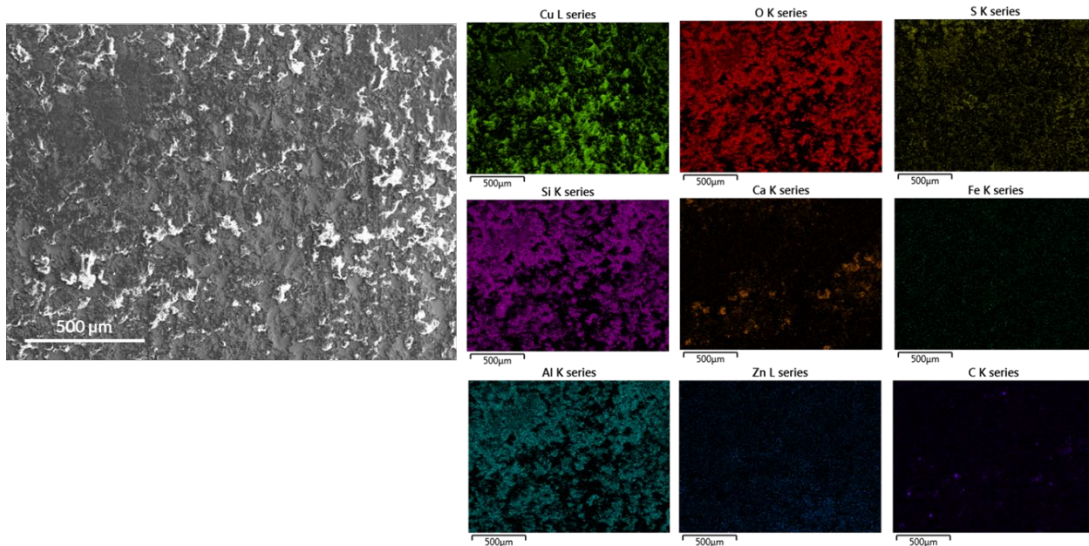


Figure 7-139. SEM and corresponding EDS maps of sample C5-3 (Area 2 from Figure 7-132).

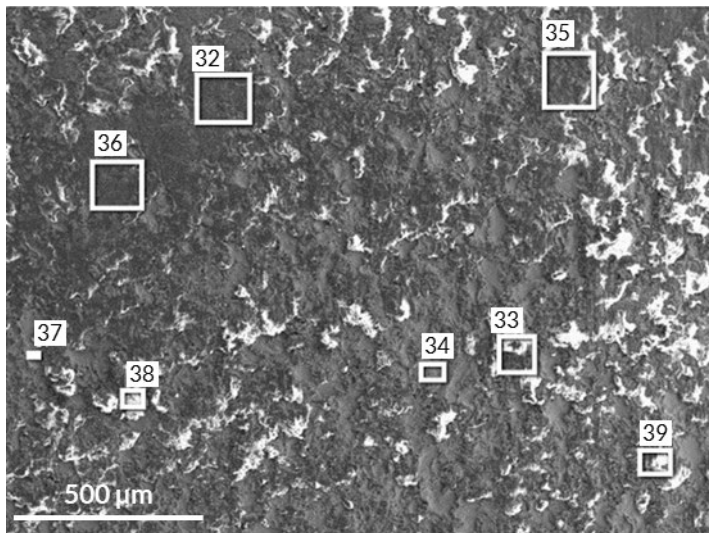


Figure 7-140. SEM of sample C5-3 (Area 2 from Figure 7-132).

Table 7-26. EDS spectra corresponding to Figure 7-140 (wt%).

Label	O	Mg	Al	Si	S	K	Ca	Fe	Cu	Zn	Total
Spectrum 32	26.3		7.72	20.61	5.57	0.15	1.5	1.59	36.55		100
Spectrum 33	38.96		6.13	15.2	2.32	0.21	12	1.29	21.79	2.09	100
Spectrum 34	1.88			0.69	3.03				85.8	8.61	100
Spectrum 35	37.91		9.98	24.19	2.57		1.23	1.94	20.6	1.58	100
Spectrum 36	29.82		8.69	22.3	4.47	0.2	1.19	1.8	31.53		100
Spectrum 37									100		100
Spectrum 38	45.48	2.41	10.07	28.36	1.53	0.31	1.3	1.97	8.58		100
Spectrum 39	35.3		9.14	22.17	2.43		1.54	2.26	22.52	4.63	100

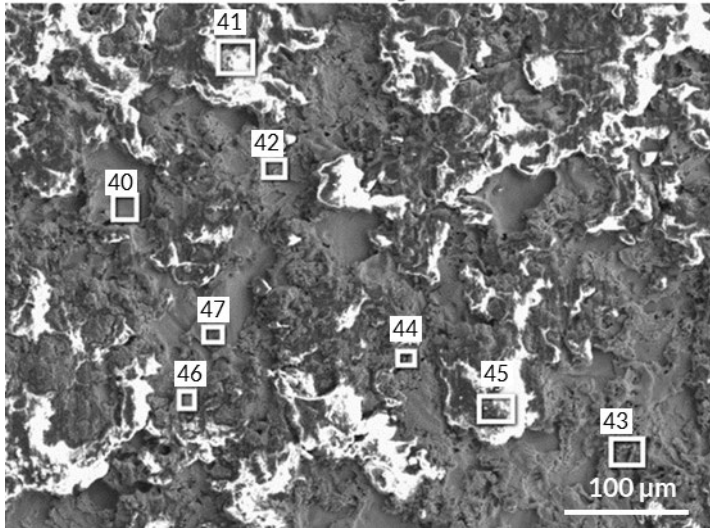


Figure 7-141. SEM of sample C5-3 (Area 2 from Figure 7-132).

Table 7-27. EDS spectra corresponding to Figure 7-141 (wt%).

Label	O	Mg	Al	Si	S	K	Ca	Ti	Fe	Cu	Zn	Total
Spectrum 40	0.95			0.22	0.36		0.18			98.29		100
Spectrum 41	41.64		10.32	26.53	2.32	0.31	1.21		2.07	15.6		100
Spectrum 42	4.58		0.61	1.35	1.65		0.42		0.41	79.71	11.27	100
Spectrum 43	19.04		5.03	11.51	2.24		0.37		0.71	53.75	7.34	100
Spectrum 44	9.03		1.07	2.2	5.66		3.42		1.11	77.5		100
Spectrum 45	42.75	1.68	9.95	25.68	2.27		3.16	0.31	2.07	12.13		100
Spectrum 46	4.67		1.12	2.88	8.58		0.33		0.36	82.07		100
Spectrum 47	2.03			0.6	1.29		0.35			95.74		100

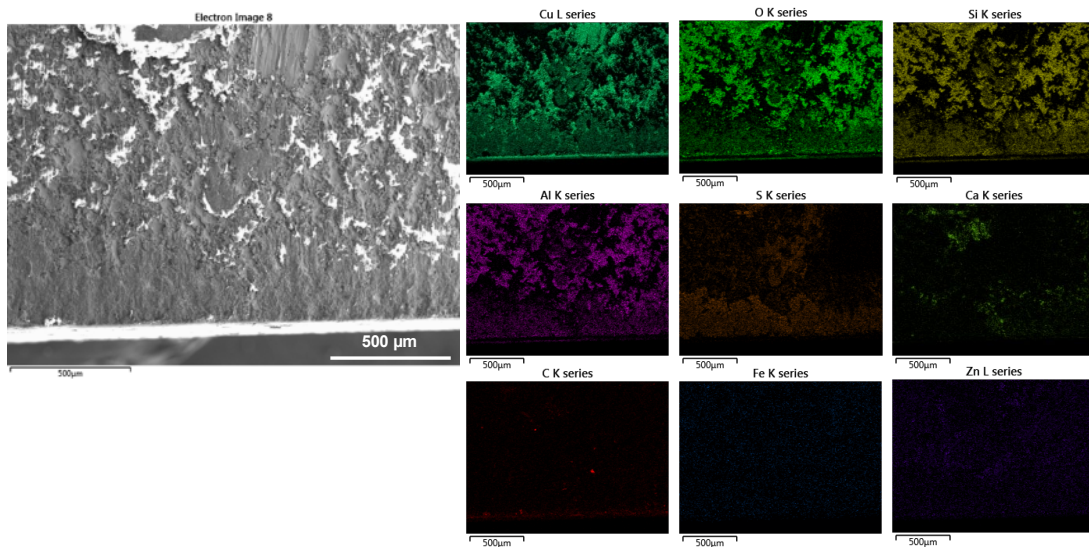


Figure 7-142. SEM and corresponding EDS maps of sample C5-3 (Area 3 from Figure 7-132).

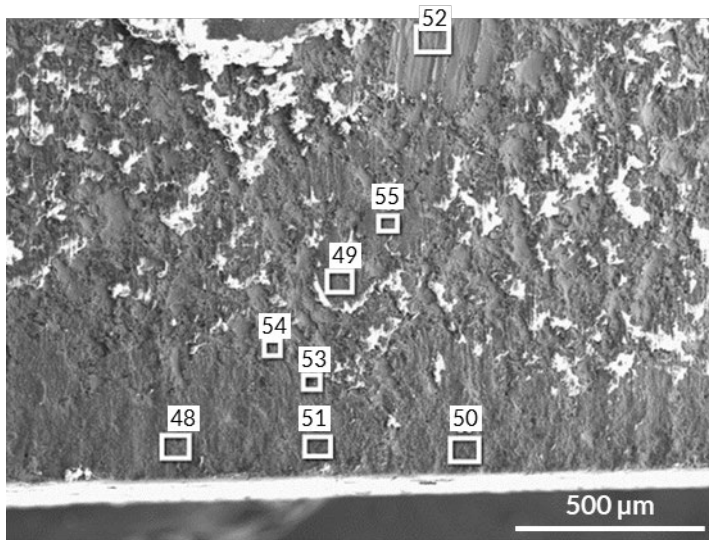


Figure 7-143. SEM of sample C5-3 (Area 3 from Figure 7-132).

Table 7-28. EDS spectra corresponding to Figure 7-143 (wt%).

Label	O	Mg	Al	Si	S	K	Ca	Fe	Cu	Zn	Total
Spectrum 48	19.63		5.95	16.08	8.42		0.96	1.38	47.57		100
Spectrum 49	16.8		5.37	14.73	8.57	0.39	0.87	1.18	49.57	2.52	100
Spectrum 50	23.5		5.93	14.91	6.09		2.93	1.51	41.89	3.23	100
Spectrum 51	19.66		6.02	15.09	6.85	0.24	0.84	1.25	46.99	3.07	100
Spectrum 52	0.86				1.4				97.74		100
Spectrum 53	17.17		1.5	4.37	14.38		10.75	0.41	51.42		100
Spectrum 54	11.02		4.03	10.87	11.91		0.68	1.11	60.39		100
Spectrum 55	12.99		4.62	11.89	11.19	0.18	0.75	0.88	57.48		100

7.4.6 Sample C6-3

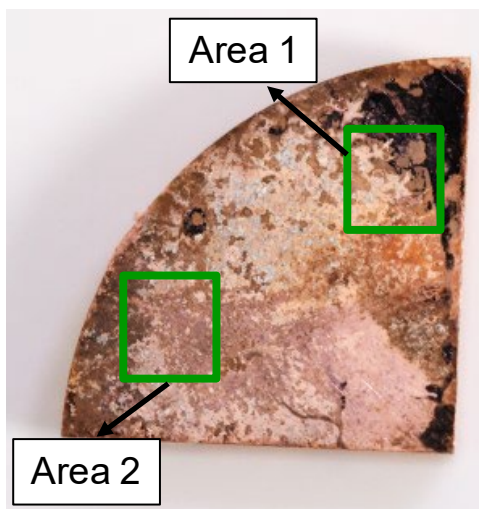


Figure 7-144. Sample C6-3. The marked areas correspond to approximately the examined sites using SEM/EDS.

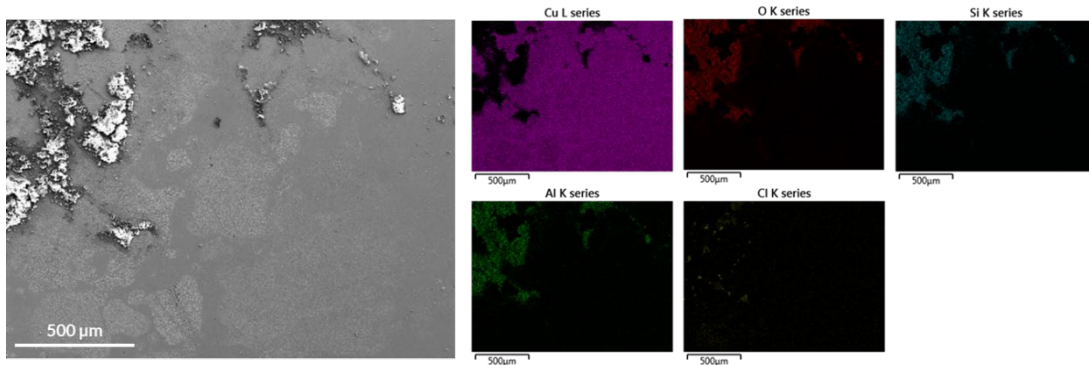


Figure 7-145. SEM and corresponding EDS maps of sample C6-3 (Area 1 from Figure 7-144).

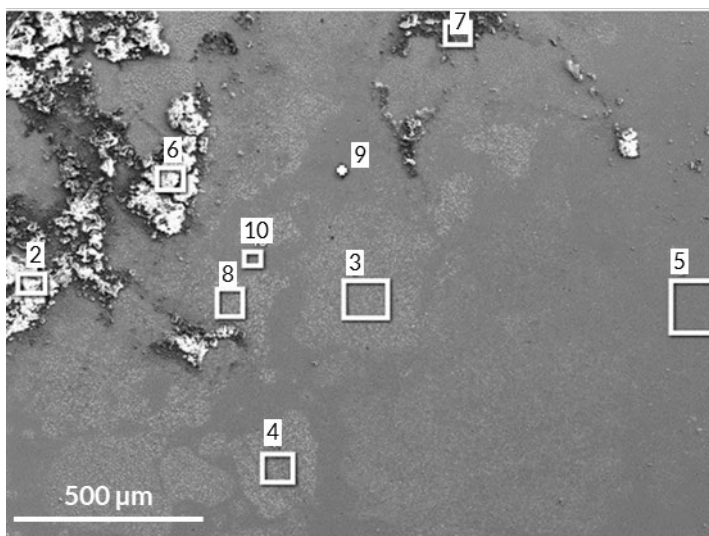


Figure 7-146. SEM of sample C6-3 (Area 1 from Figure 7-144).

Table 7-29. EDS spectra corresponding to Figure 7-146 (wt%).

Label	O	Na	Mg	Al	Si	S	Cl	K	Ca	Ti	Fe	Cu	Total
Spectrum 2	48.79	1.23	1.43	15.3	27.66		0.68		0.7		2.04	2.18	100
Spectrum 3	1.48				0.17							98.35	100
Spectrum 4	4.68			0.78	1.13		0.94					92.47	100
Spectrum 5	0.71				0.24							99.05	100
Spectrum 6	46.52	1.54	1.36	14.4	28.2		0.95	0.5	0.86	0.25	2.44	2.99	100
Spectrum 7	30.42			10.6	17.07				0.3		0.88	40.72	100
Spectrum 8	4			0.71	1.04							94.25	100
Spectrum 9	21.38			4.16	7.07	0.51			0.33			66.56	100
Spectrum 10												100	100

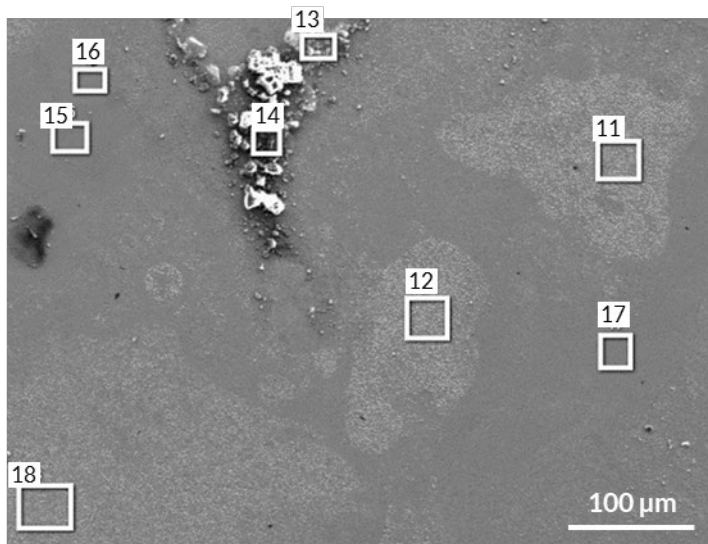


Figure 7-147. SEM of sample C6-3 (Area 1 from Figure 7-144).

Table 7-30. EDS spectra corresponding to Figure 7-147 (wt%).

Label	O	Al	Si	Ca	Fe	Cu	Total
Spectrum 11	2.2					97.8	100
Spectrum 12	1.8					98.2	100
Spectrum 13	28.89	10.31	16.73	0.26	0.93	42.87	100
Spectrum 14	33.48	13.56	24.47	0.51	1.75	26.21	100
Spectrum 15	0.83					99.17	100
Spectrum 16						100	100
Spectrum 17						100	100
Spectrum 18	1.71					98.29	100

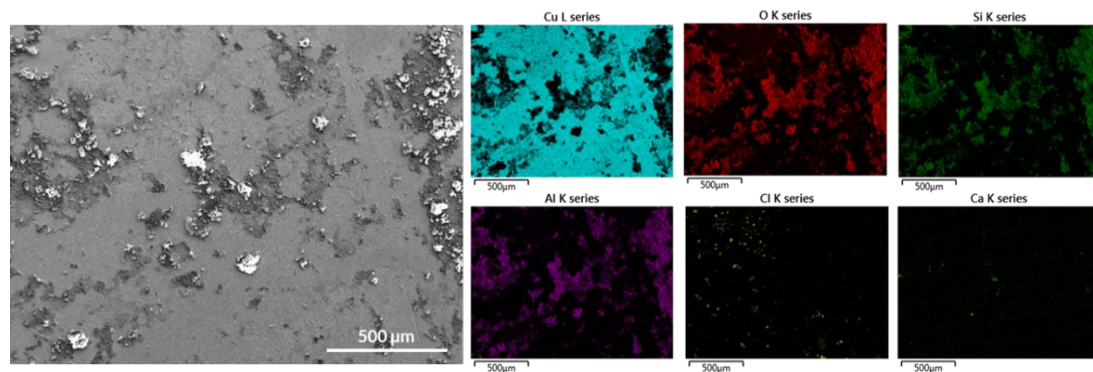


Figure 7-148. SEM and corresponding EDS maps of sample C6-3 (Area 2 from Figure 7-144).

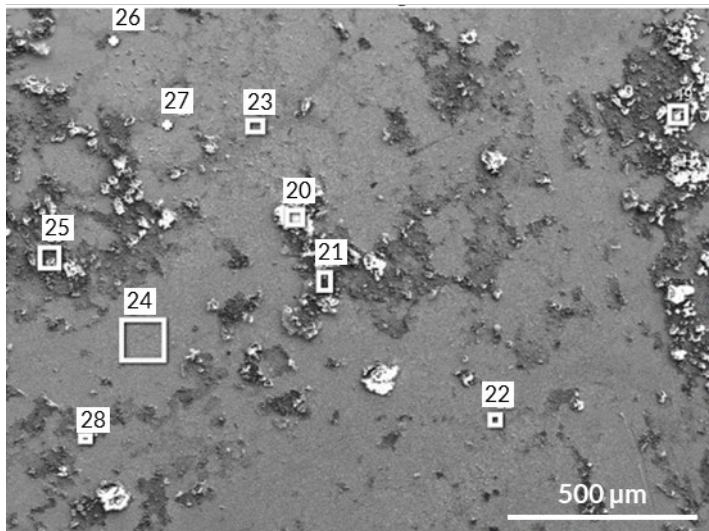


Figure 7-149. SEM of sample C6-3 (Area 2 from Figure 7-144).

Table 7-31. EDS spectra corresponding to Figure 7-149 (wt%).

Label	O	Na	Mg	Al	Si	Cl	K	Ca	Ti	Fe	Cu	Total
Spectrum 19	44.45	1.24	1.44	14.23	25.79	0.22		0.56		1.52	10.55	100
Spectrum 20	50.5	1.52	1.54	14.68	28.42	0.28	0.19	0.72		1.92	0.23	100
Spectrum 21	41.09	1.43		13.1	23.16	0.25		0.43		1.42	19.13	100
Spectrum 22	5.67			1.49	2.2	0.21					90.43	100
Spectrum 23	7.49			1.76	2.73						88.02	100
Spectrum 24	1.96				0.37	0.54					97.13	100
Spectrum 25	35.25			12.11	20.46	0.28		0.42		0.95	30.52	100
Spectrum 26						37.59					62.41	100
Spectrum 27	6.98			1.26	1.87	31.47					58.42	100
Spectrum 28	18.45			5.85	8.94	0.14				0.43	66.19	100

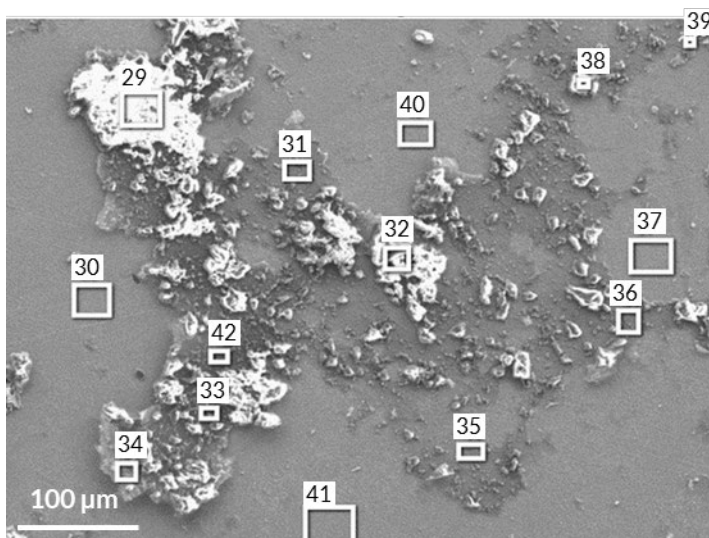


Figure 7-150. SEM of sample C6-3 (Area 2 from Figure 7-144).

Table 7-32. EDS spectra corresponding to Figure 7-150 (wt%).

Label	O	Na	Mg	Al	Si	Cl	K	Ca	Fe	Cu	Total
Spectrum 29	50.03	1.48	1.6	14.68	28.74	0.26	0.2	0.67	1.96	0.37	100
Spectrum 30	1.5				0.41					98.09	100
Spectrum 31	20.82			6.45	10.47	0.17		0.34		61.75	100
Spectrum 32	51.38	1.34	1.41	15.06	27.62	0.18	0.17	0.49	1.59	0.75	100
Spectrum 33	42.38	1.45		12.82	23.11	0.18		0.46	1.32	18.28	100
Spectrum 34	38.68	1.23		11.73	20.13	0.26	0.14	0.39	1.14	26.3	100
Spectrum 35	17.15			5.39	8.27	0.18			0.45	68.57	100
Spectrum 36	25.21			8.03	12.67			0.23	0.68	53.18	100
Spectrum 37	0.85									99.15	100
Spectrum 38	47.81	1.14	1.4	16.53	30.14			0.63	1.46	0.89	100
Spectrum 39	18.12			5.6	8.69			0.16		67.42	100
Spectrum 40	2.31				0.54					97.14	100
Spectrum 41										100	100
Spectrum 42	38.82			11.69	20.04	0.26	0.13	0.32	1.15	27.59	100

7.4.7 Sample C7-3

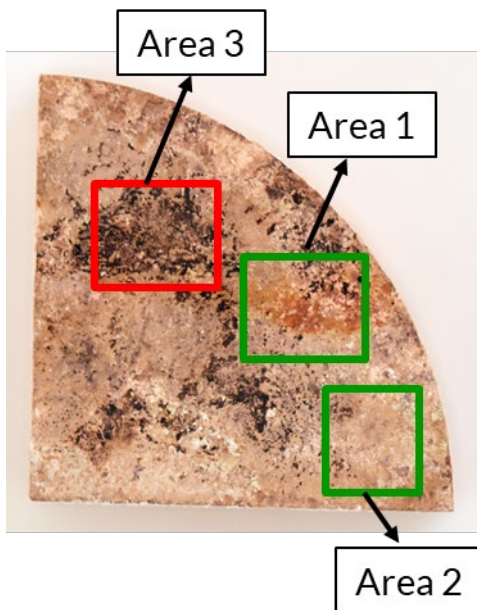


Figure 7-151. Sample C7-3. The marked areas correspond to approximately the examined sites using SEM/EDS.

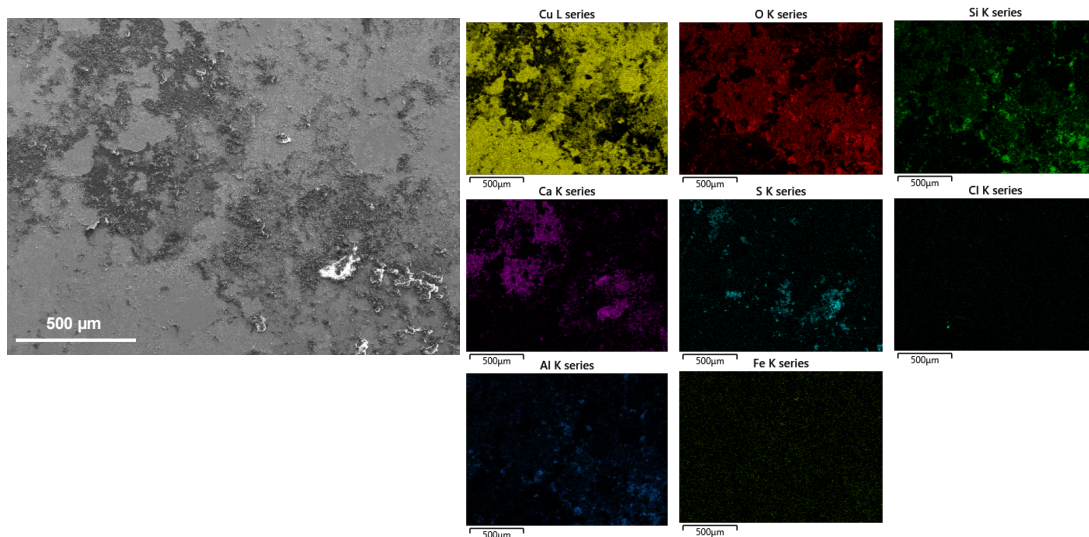


Figure 7-152. SEM and corresponding EDS maps of sample C7-3 (Area 1 from Figure 7-151).

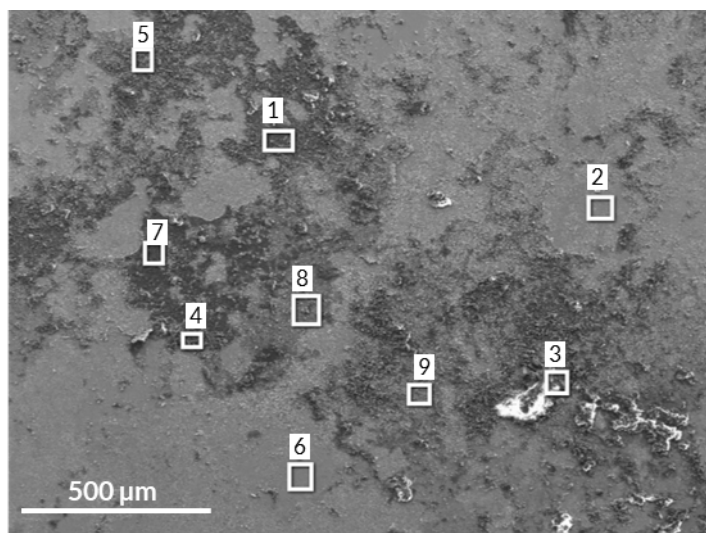


Figure 7-153. SEM of sample C7-3 (Area 1 from Figure 7-151).

Table 7-33. EDS spectra corresponding to Figure 7-153 (wt%).

Label	O	Na	Mg	Al	Si	S	Cl	K	Ca	Fe	Cu	Total
Spectrum 1	37.79		3.16	1.47	3.74	0.62	0.71		24.6	0.79	27.12	100
Spectrum 2											100	100
Spectrum 3	44.86	10.51	0.65	1.26	2.95	16.83	0.44		16.67	0.5	5.34	100
Spectrum 4	31.61	18.27		0.6	1.5	16.06			7.88		24.09	100
Spectrum 5	22.14	10.08		1.03	2.45	8.64	0.5		5.9	0.47	48.8	100
Spectrum 6						0.25					99.75	100
Spectrum 7	44.79	1.02	3.56	1.2	3.67	0.77	0.83		31.26		12.9	100
Spectrum 8	19.49			2.35	5.03	2.1	0.56		2.16	0.69	67.62	100
Spectrum 9	15.7		1.88	2.56	5.96	0.84	0.31	0.18	0.43	0.99	71.15	100

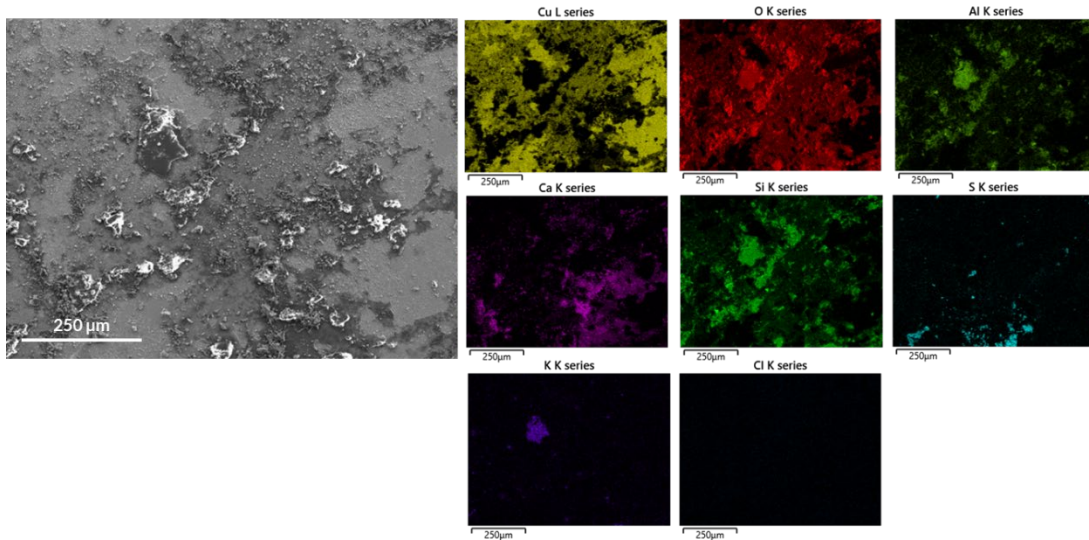


Figure 7-154. SEM and corresponding EDS maps of sample C7-3 (Area 1 from Figure 7-151).

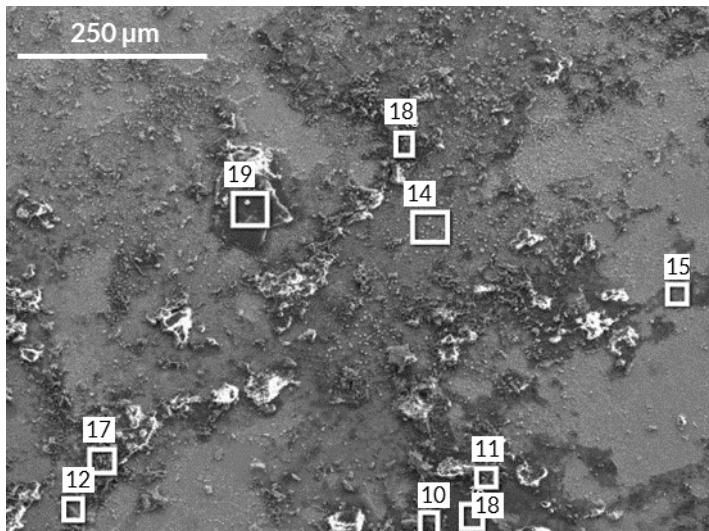


Figure 7-155. SEM of sample C7-3 (Area 1 from Figure 7-151).

Table 7-34. EDS spectra corresponding to Figure 7-155 (wt%).

Label	O	Na	Mg	Al	Si	S	Cl	K	Ca	Ti	Fe	Cu	Total
Spectrum 10	44.26	10.41	0.27	0.47	1.15	22.38			20.7			0.36	100
Spectrum 11	44.75	2.43	0.66	0.96	2.61	19.51			26.5		0.32	2.26	100
Spectrum 12	24.54	11.59			1.84	12.47			8.87			40.71	100
Spectrum 13	44.77		1.67	14.82	24.62			9.07		0.41	3.19	1.44	100
Spectrum 14	16.85			2.44	5.41	0.46	0.23		0.39		0.6	73.63	100
Spectrum 15	23.84			1.5	3.46	0.95			11.41			58.85	100
Spectrum 16	34.83			2.84	7.71	0.61	0.24		13.95		1.04	38.78	100
Spectrum 17	49.43	1.65	1.32	1.88	5.53	2.01	0.33		33.18		1.27	3.4	100
Spectrum 18	45.22	2.92	4.3	9.88	25.68		1	0.59	0.57		4.4	5.44	100

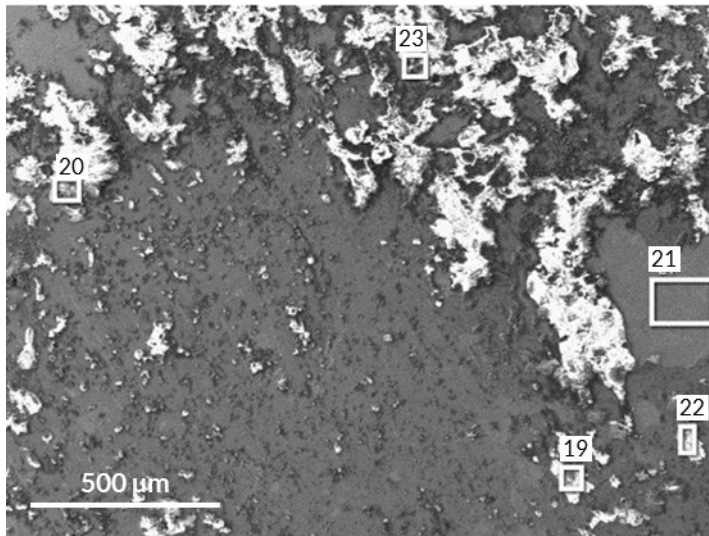


Figure 7-156. SEM of sample C7-3 (Area 2 from Figure 7-151).

Table 7-35. EDS spectra corresponding to Figure 7-156 (wt%).

Label	O	Na	Mg	Al	Si	S	K	Ca	Fe	Cu	Total
Map Sum Spectrum	24.25		3.11	4.47	10.62	2.53	0.34	5.42	1.46	47.81	100
Spectrum 19	47.2	0.31	0.32	0.29	0.89	21.48		28.7		0.81	100
Spectrum 20	45.14	0.28	0.63	1.79	3.55	19.32	0.51	28.09	0.47	0.22	100
Spectrum 21	0.58									99.42	100
Spectrum 22	47.09	0.26	0.67	0.55	1.56	19.74		29.77		0.35	100
Spectrum 23	46.54	0.22	0.39	0.73	2.02	20.31		27.78	0.57	1.44	100

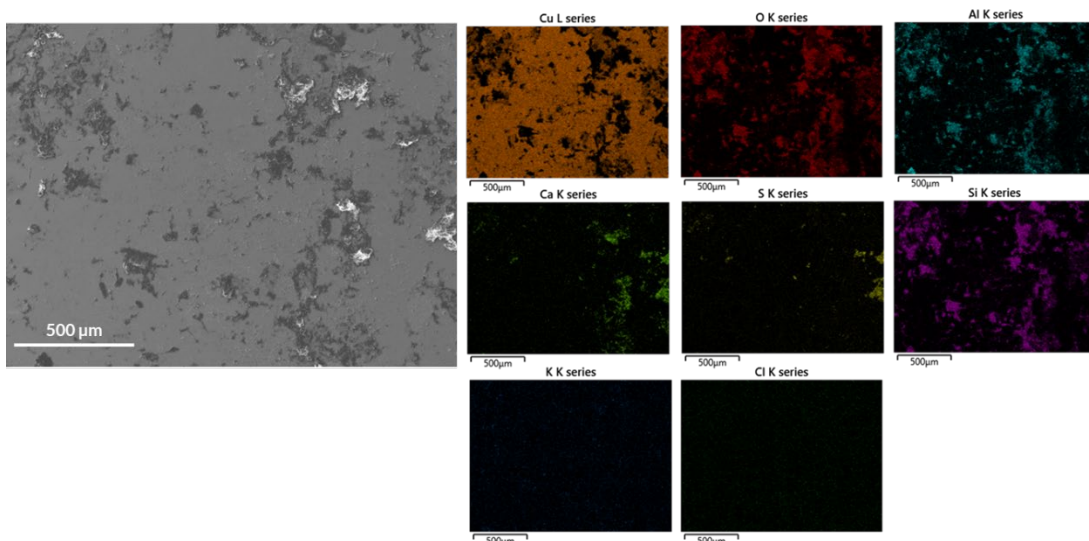


Figure 7-157. SEM and corresponding EDS maps of sample C7-3 (Area 3 from Figure 7-151).

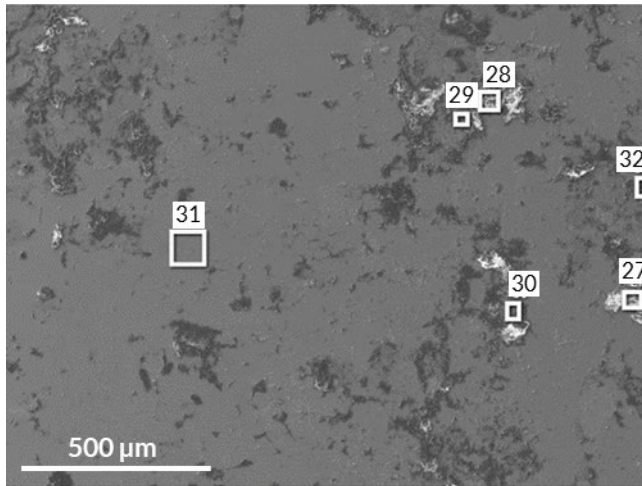


Figure 7-158. SEM of sample C7-3 (Area 3 from Figure 7-151).

Table 7-36. EDS spectra corresponding to Figure 7-158 (wt%).

Label	O	Na	Mg	Al	Si	S	Cl	K	Ca	Mn	Fe	Cu	Zn	Total
Spectrum 27	48	0.82	0.45	1.71	3.38	18.05		0.29	24.43		0.68	2.19		100
Spectrum 28	48.68	1.24	3.07	6.76	16.17	0.63	0.44	0.66	14.87	0.4	3.55	2.94	0.59	100
Spectrum 29	41.45		1.57	1.97	4.77	0.56	0.32		28.15		0.83	20.37		100
Spectrum 30	29.95		4.92	3.98	8.93	0.58	0.24	0.3	12		1.63	37.47		100
Spectrum 31	1.53				0.78							97.69		100
Spectrum 32	44.55	0.79	0.32	0.68	1.96	19.92			25.26		0.37	6.15		100

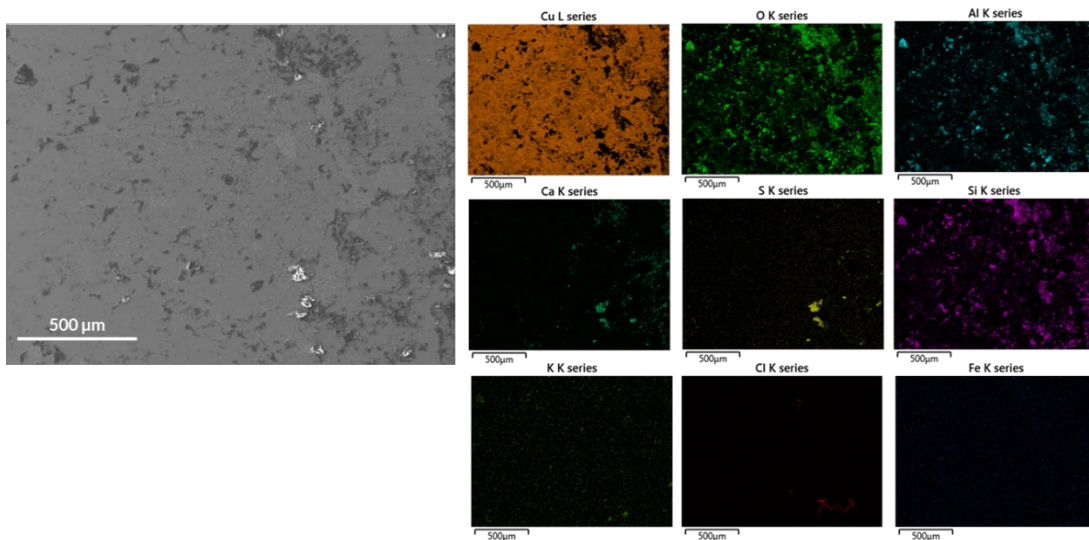


Figure 7-159. SEM and corresponding EDS maps of sample C7-3 (Area 3 from Figure 7-151).

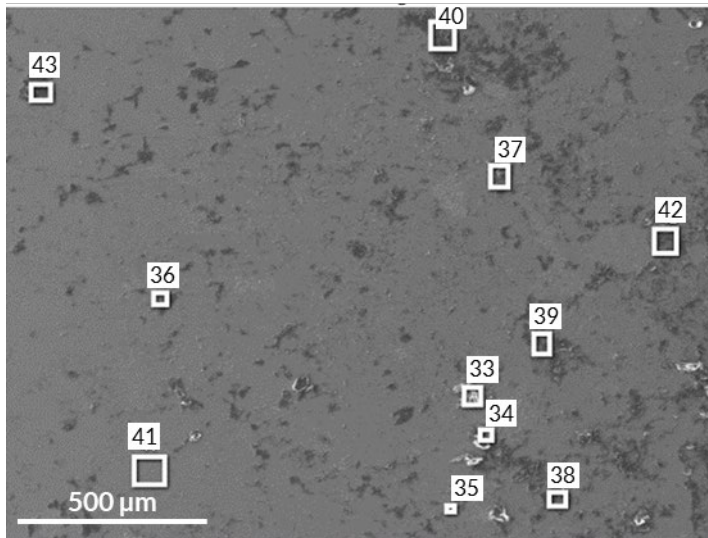


Figure 7-160. SEM of sample C7-3 (Area 3 from Figure 7-151).

Table 7-37. EDS spectra corresponding to Figure 7-160 (wt%).

Label	O	Na	Mg	Al	Si	S	Cl	K	Ca	Fe	Cu	Total
Spectrum 33	54.08				1.07	40.94	0.35				3.55	100
Spectrum 34	48.33				2.58	37.09	1.73				10.27	100
Spectrum 35	42.62	0.64			0.14	23.67	0.11		30.33		2.49	100
Spectrum 36	20.38			5.97	10.92	0.39	0.39	0.34	0.22	2.85	58.54	100
Spectrum 37	27.35	2.28	2.4	7.43	16.26	0.65	1.12	0.55	1.94	2.77	37.26	100
Spectrum 38	22.65		1.08	12.19	14.69	0.49	0.32	3.05	0.82	1.32	43.39	100
Spectrum 39	23.05			5.79	12.14	0.64	0.36	0.35	0.49	1.92	55.26	100
Spectrum 40	30.55			8.47	18.34	0.37	0.5	0.64	0.75	3.23	37.15	100
Spectrum 41	3.29			0.65	1.34	0.28	0.13				94.31	100
Spectrum 42	27.39		2.85	6.27	11.58	1.29	0.33	0.87	7	1.86	40.57	100
Spectrum 43	42.24	1.21	1.25	14.53	21.38	0.75	0.46	2.51	1.62	2.32	11.73	100

7.4.8 Sample C8-3



Figure 7-161. Sample C8-3. The marked areas correspond to approximately the examined sites using SEM/EDS.

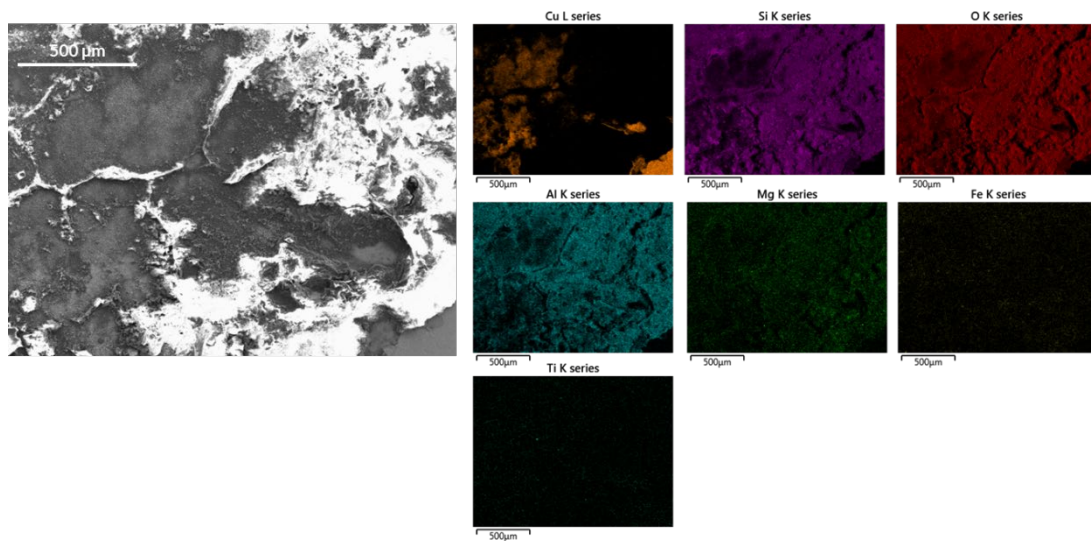


Figure 7-162. SEM and corresponding EDS maps of sample C8-3 (Area 1 from Figure 7-161).

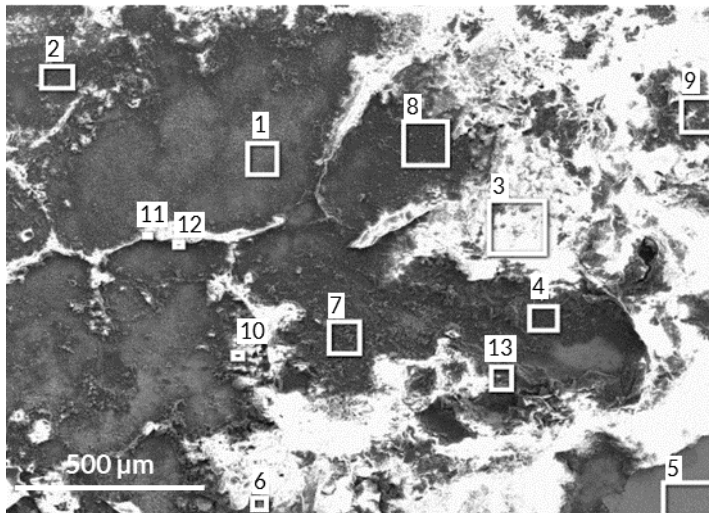


Figure 7-163. SEM of sample C8-3 (Area 1 from Figure 7-161).

Table 7-38. EDS spectra corresponding to Figure 7-163 (wt%).

Label	O	Na	Mg	Al	Si	S	K	Ca	Ti	Fe	Cu	Total
Spectrum 1	25.96			4.92	10.92			0.51		1.73	55.97	100
Spectrum 2	44.43		1.52	8.64	26.76			0.7	0.34	4.01	13.6	100
Spectrum 3	53.23		1.63	10.44	30.67			0.49	0.19	3.36	0	100
Spectrum 4	51.44	1.13	1.58	10.79	30.1		0.12	0.51	0.21	3.88	0.23	100
Spectrum 5	1.21					0.14					98.65	100
Spectrum 6	42.66		1.24	9.28	40.03			0.65		6.14	0	100
Spectrum 7	46.26	0.92		7.23	33.27		0.11	0.31	0.17	2.3	9.42	100
Spectrum 8	48.62	1.53		11.61	29.97			0.63	0.22	4.65	2.78	100
Spectrum 9	51.34	1.1	1.56	10.09	31.18			0.55	0.26	3.71	0.21	100
Spectrum 10	43.4	0.98		8.46	38.81			0.9		4.2	3.25	100
Spectrum 11	26.03		1.16	8.34	16.78			1.1	1.71	41.41	3.46	100
Spectrum 12	38.74			10.17	20.26			0.75		7.6	22.49	100
Spectrum 13	52.7		2.27	5.76	37.16			0.3		1.81	0	100

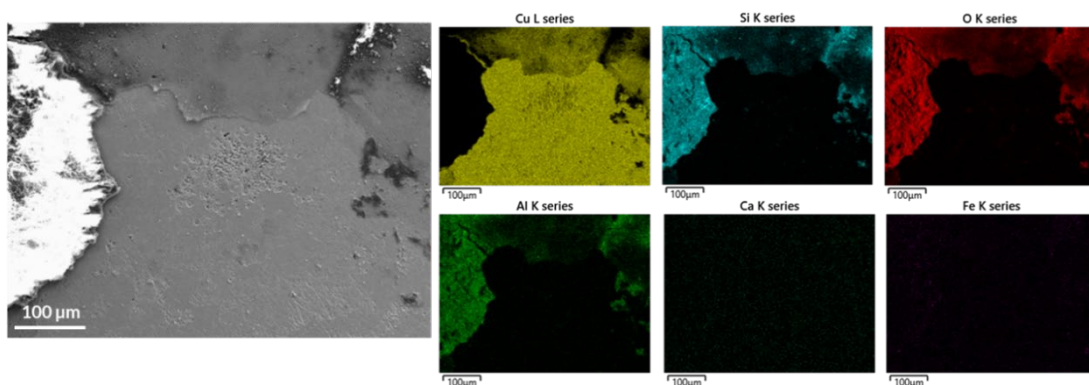


Figure 7-164. SEM and corresponding EDS maps of sample C8-3 (Area 1 from Figure 7-161).

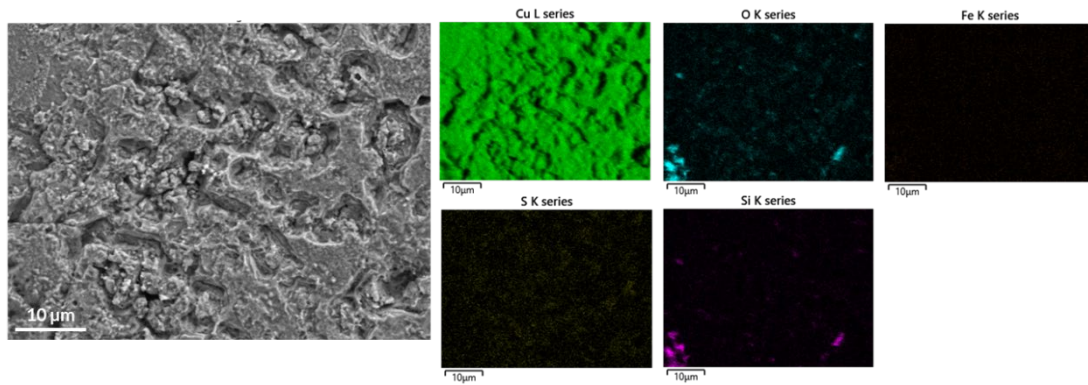


Figure 7-165. SEM and corresponding EDS maps of sample C8-3 (Area 1 from Figure 7-161).

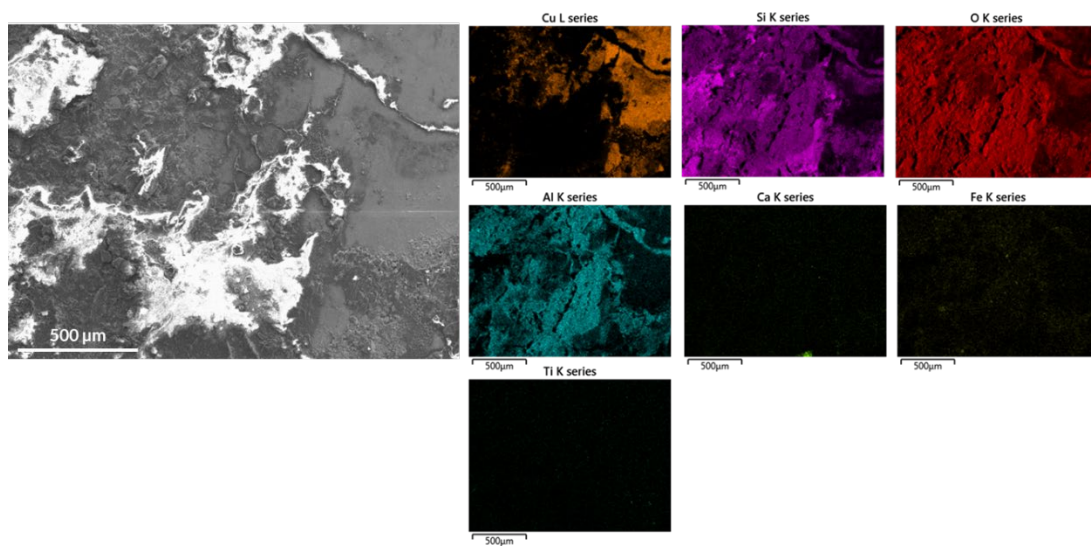


Figure 7-166. SEM and corresponding EDS maps of sample C8-3 (Area 2 from Figure 7-161).

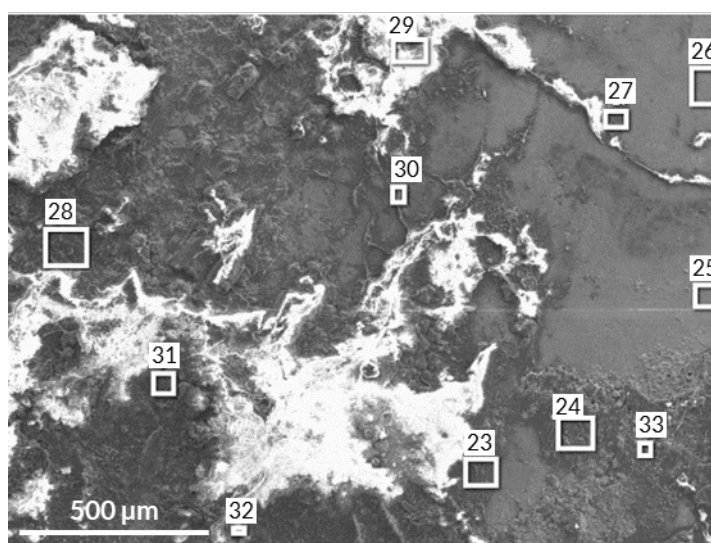


Figure 7-167. SEM of sample C8-3 (Area 2 from Figure 7-161).

Table 7-39. EDS spectra corresponding to Figure 7-167 (wt%).

Label	O	Na	Mg	Al	Si	S	K	Ca	Ti	Fe	Cu	Total
Spectrum 23	46.6		1.03	5.9	33.32			0.46		1.76	10.93	100
Spectrum 24	39.89		1.17	8.47	25.78			0.65	0.93	6.39	16.71	100
Spectrum 25	12.21			2.12	5.4	0.2				0.67	79.41	100
Spectrum 26	11.33			2.77	4.8	0.29		0.15		0.88	79.79	100
Spectrum 27	38.73		1.46	10.12	20.18	0.22		0.5	0.37	4.81	23.61	100
Spectrum 28	51.31			1.48	42.05			0.18		1.15	3.83	100
Spectrum 29	53.7	0.94	1.7	11.49	25.6			0.64	0.8	5.12	0	100
Spectrum 30	41.92			7.38	21.31			0.34	0.23	17.64	11.19	100
Spectrum 31	44.55			7.58	22.73		0.6	0.73	0.41	19.14	4.26	100
Spectrum 32	48.3	0.8		9.29	18.66			0.6	0.53	21.62	0.2	100
Spectrum 33	34.04		1.04	7.61	15.99			0.4	2.92	7.58	30.42	100

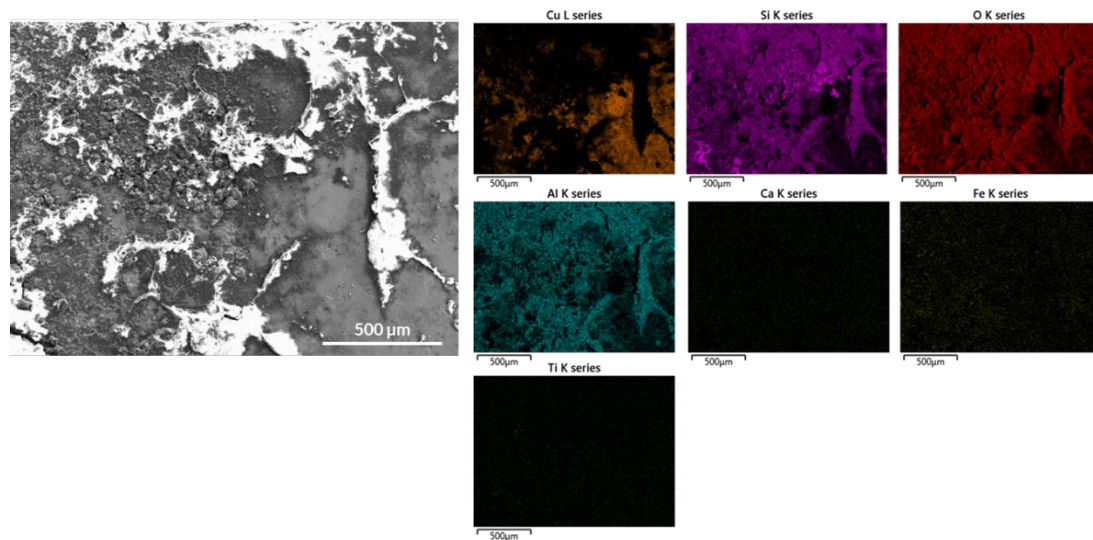


Figure 7-168. SEM and corresponding EDS maps of sample C8-3 (Area 2 from Figure 7-161).

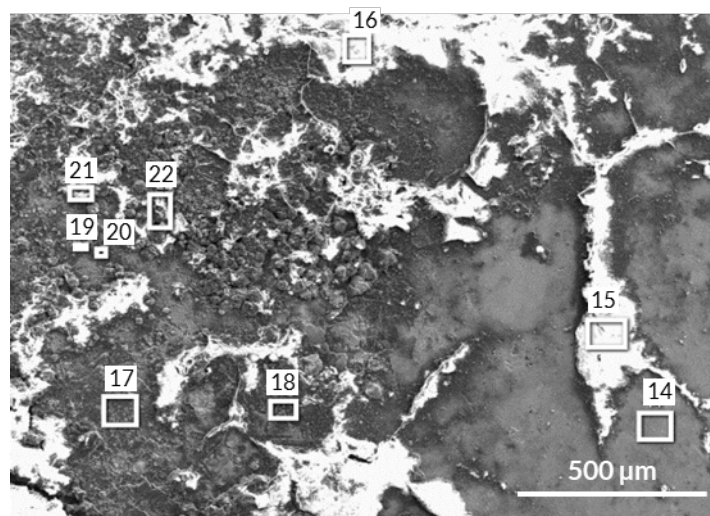


Figure 7-169. SEM of sample C8-3 (Area 2 from Figure 7-161).

Table 7-40. EDS spectra corresponding to Figure 7-169 (wt%).

Label	O	Na	Mg	Al	Si	K	Ca	Ti	Fe	Cu	Total
Spectrum 14	13.29			3.24	6.24		0.14		0.68	76.42	100
Spectrum 15	51.03	0.88	1.87	11.69	27.89		0.71	0.52	5.23	0.18	100
Spectrum 16	52.53	1.01	1.74	11.34	29.25	0.1	0.59	0.22	3.09	0.13	100
Spectrum 17	30.08			6.57	18.04		0.46	0.51	4.7	39.63	100
Spectrum 18	37.37		1.66	9.53	21.83		0.48	0.27	4.55	24.31	100
Spectrum 19	30.55			4.48	15.58		0.19		1.56	47.63	100
Spectrum 20	35.15			6.96	18.31		0.41	0.16	7.08	31.93	100
Spectrum 21	43.87	0.73	1.85	10.35	23.42		0.69	0.5	8.99	9.6	100
Spectrum 22	43.83	0.68	2.07	9.98	23.11		0.67	2.39	6.58	10.68	100

7.5 Cross section analysis (SEM/EDS)

Complementary results corresponding to the cross sectional analysis of specimen C4-2 are shown in this section.

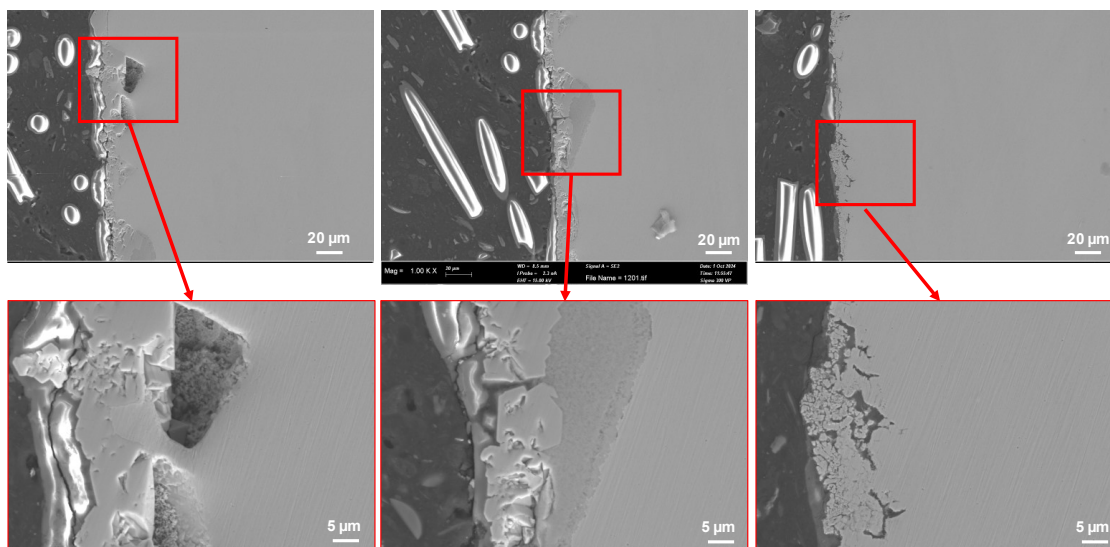


Figure 7-170. SEM images (Secondary Electrons) of cross section of specimen C4-2, corresponding to the top side in Figure 3-8. Generally, more pit-like features were observed on the cross section of the top side of specimen C4-2, which was heavily covered in bentonite deposits.

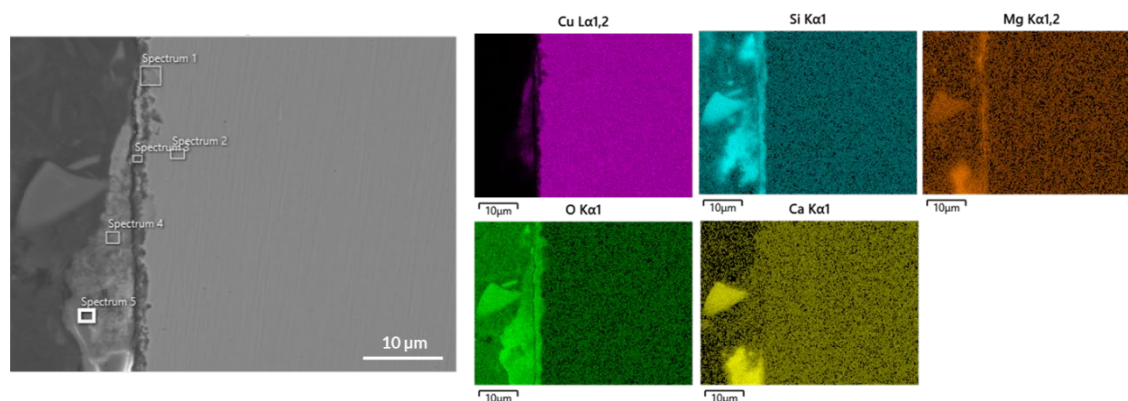


Figure 7-171. SEM image (Secondary Electrons) of cross section of specimen C4-2 (top side in Figure 3-8) and corresponding EDS maps. EDS spectra shown in Table 7-41.

Table 7-41. EDS spectra corresponding to Figure 7-171 (wt%).

Label	O	Na	Mg	Si	Ca	Cu	Total
Spectrum 1	10.2	-	-	5.7	0.3	83.8	100
Spectrum 2	-	-	-	-	-	100	100
Spectrum 3	22.7	-	-	19.7	0.6	57.1	100
Spectrum 4	21.5	-	-	16.7	0.2	61.6	100
Spectrum 5	51.2	0.2	4.7	8.6	32.5	2.8	100

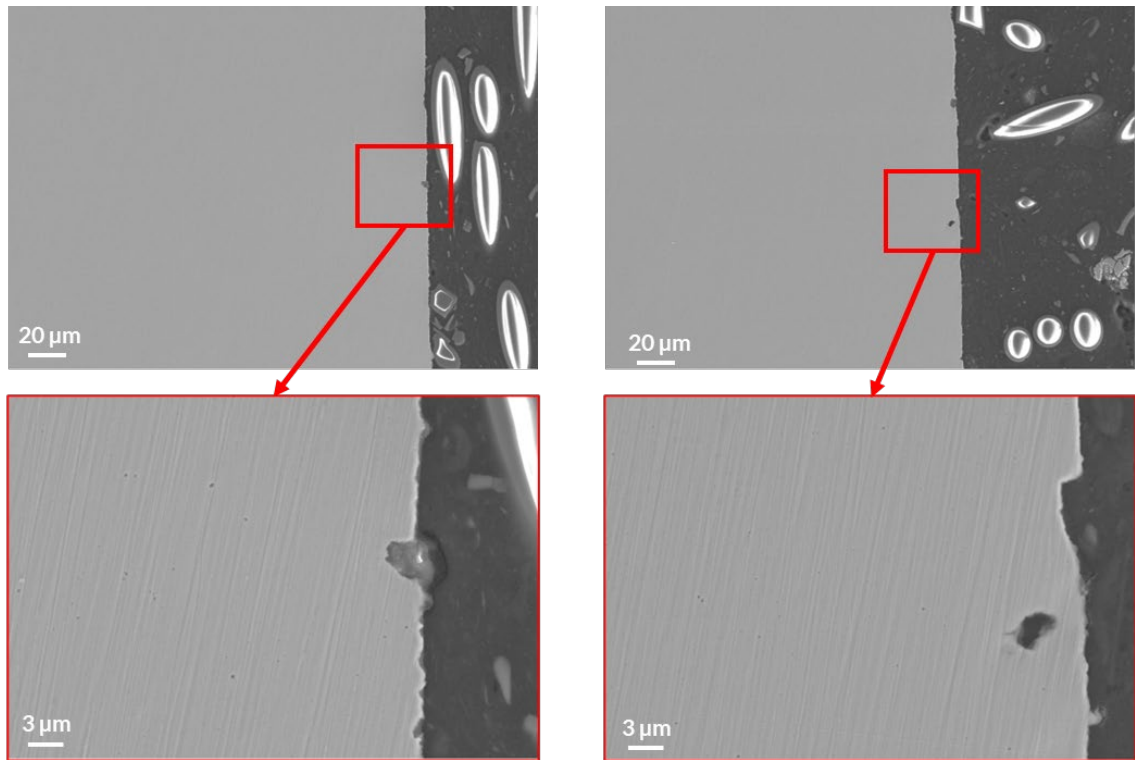


Figure 7-172. SEM images (Secondary Electrons) of cross section of specimen. C4-2, corresponding to the bottom side in Figure 3-8. Generally, fewer pit-like features (which can be even attributed to sample preparation or defects prior to the exposure) were observed in comparison to the “top” side of C4-2.

7.6 Complementary Raman Results

The nine (9) studied areas and their respective Raman spectrum are described in the following paragraphs.

The studied area 1 is shown in Figure 7-173. Both observed peaks at 277 rel.cm with a shoulder peak at around 350 rel.cm and 610 rel.cm can be attributed to CuO. As can be seen from literature these bands are characteristic for CuO and may have shifts depending on the structure (Sriyutha Murthy et al. 2011, Deng et al. 2016).

The studied area 2 is shown in Figure 7-174. The observed peaks at 150 rel.cm, 219 rel.cm and 615 rel.cm can be attributed to Cu₂O. As can be seen from literature these bands are characteristic for Cu₂O and may have shifts depending on the structure (Deng et al. 2016, Ravichandiran et al. 2019). However, both peaks at around 215 rel.cm and 110–120 rel.cm can be also characteristic for CuCl₂·2H₂O (Medeiros et al. 2018). In that case also a wide weak band is observed at around 400 rel.cm. Thus, there is a possibility that both of these chemical complexes are possible to be formed on the surface.

The studied area 3 is shown in Figure 7-175. The observed peaks at 150 rel.cm (weak), 220 rel.cm and 614 rel.cm can be attributed to Cu₂O. As can be seen from literature these bands are characteristic for Cu₂O and may have shifts depending on the structure (Deng et al. 2016, Ravichandiran et al. 2019). However, both peaks at around 215 rel.cm and 110–120 rel.cm can be also characteristic for CuCl₂·2H₂O (Medeiros et al. 2018).

The studied area 4 is shown in Figure 7-176. The observed peaks at 147 rel.cm (weak), 218 rel.cm and 619 rel.cm can be attributed to Cu₂O. As can be seen from literature these bands are characteristic for Cu₂O and may have shifts depending on the structure (Deng et al. 2016, Ravichandiran et al. 2019). However, both peaks at around 215 rel.cm and 110–120 rel.cm can be also characteristic for CuCl₂·2H₂O (Medeiros et al. 2018).

The studied area 5 is shown in Figure 7-177. The observed peaks at 148 rel.cm (weak), 218 rel.cm and 619 rel.cm can be attributed to Cu₂O. As can be seen from literature these bands are characteristic for Cu₂O and may have shifts depending on the structure (Deng et al. 2016, Ravichandiran et al. 2019). However, both peaks at around 215 rel.cm and 110–120 rel.cm can be also characteristic for CuCl₂·2H₂O (Medeiros et al. 2018).

The studied area 6 is shown in Figure 7-178. The observed peaks at 221 rel.cm and 606 rel.cm can be attributed to Cu₂O or most likely CuCl₂·2H₂O since there is no peak at around 150 rel.cm.

The studied area 7 is shown in Figure 7-179. The observed peaks at 218 rel.cm and 619 rel.cm can be attributed to Cu₂O. As can be seen from literature these bands are characteristic for Cu₂O and may have shifts depending on the structure (Deng et al. 2016, Ravichandiran et al. 2019). However, both peaks at around 215 rel.cm and 110–120 rel.cm can be also characteristic for CuCl₂·2H₂O (Medeiros et al. 2018).

The studied area 8 is shown in Figure 7-180. The observed peaks at 148 rel.cm (strong), 217 rel.cm and 619 rel.cm can be attributed to Cu₂O. As can be seen from literature these bands are characteristic for Cu₂O and may have shifts depending on the structure (Deng et al. 2016, Ravichandiran et al. 2019). However, both peaks at around 215 rel.cm and 110–120 rel.cm can be also characteristic for CuCl₂·2H₂O (Medeiros et al. 2018).

The studied area 9 is shown in Figure 7-181. The observed peaks at 148 rel.cm, 217 rel.cm and 616 rel.cm can be attributed to Cu₂O. As can be seen from literature these bands are characteristic for Cu₂O and may have shifts depending on the structure (Deng et al. 2016, Ravichandiran et al. 2019). However, both peaks at around 215 rel.cm and 110–120 rel.cm can be also characteristic for CuCl₂·2H₂O (Medeiros et al. 2018).

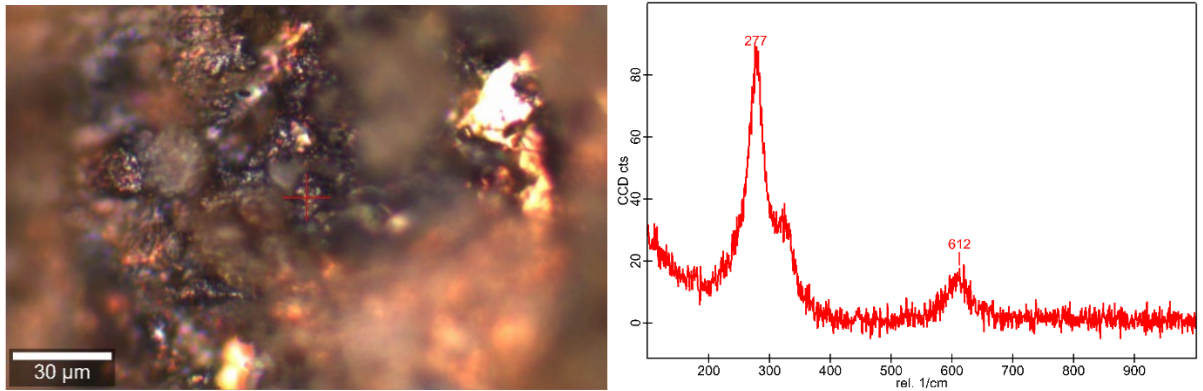


Figure 7-173. Area 1. Left: Optical image showing the area were the Raman spectrum was measured (red cross). Right: Measured Raman spectrum.

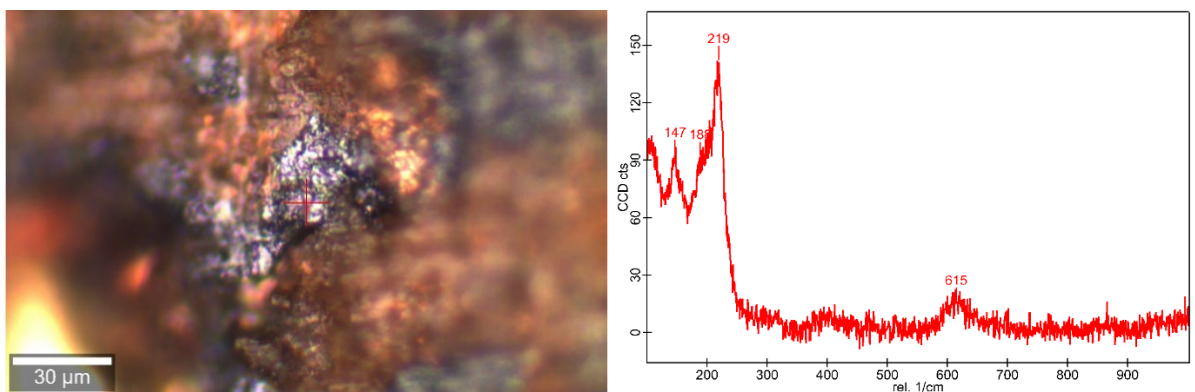


Figure 7-174. Area 2. Left: Optical image showing the area were the Raman spectrum was measured (red cross). Right: Measured Raman spectrum.

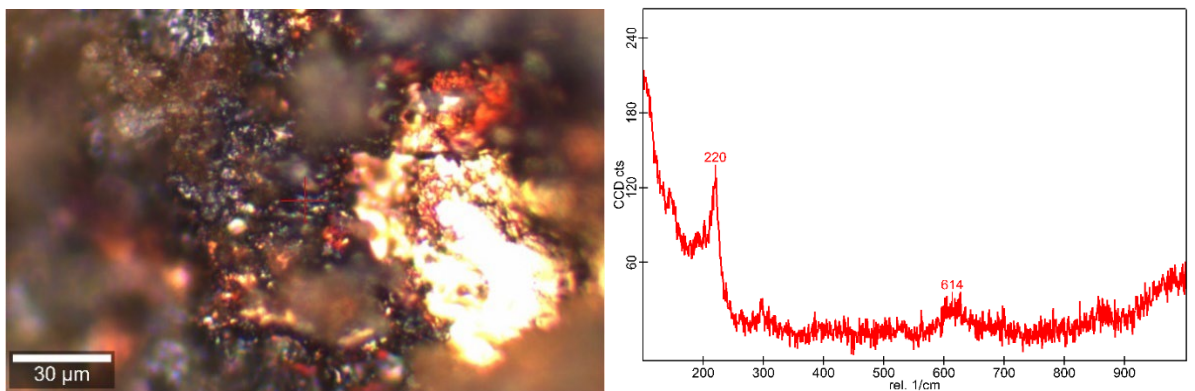


Figure 7-175. Area 3. Left: Optical image showing the area were the Raman spectrum was measured (red cross). Right: Measured Raman spectrum.

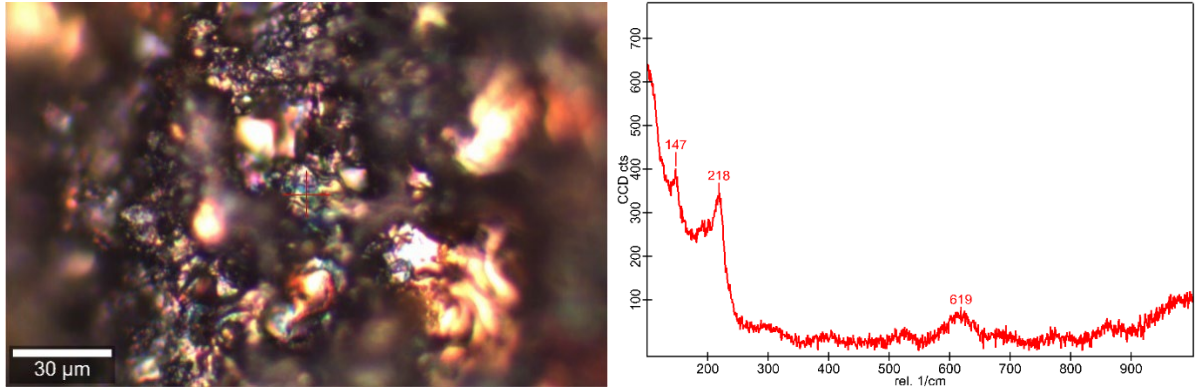


Figure 7-176. Area 4. Left: Optical image showing the area were the Raman spectrum was measured (red cross). Right: Measured Raman spectrum.

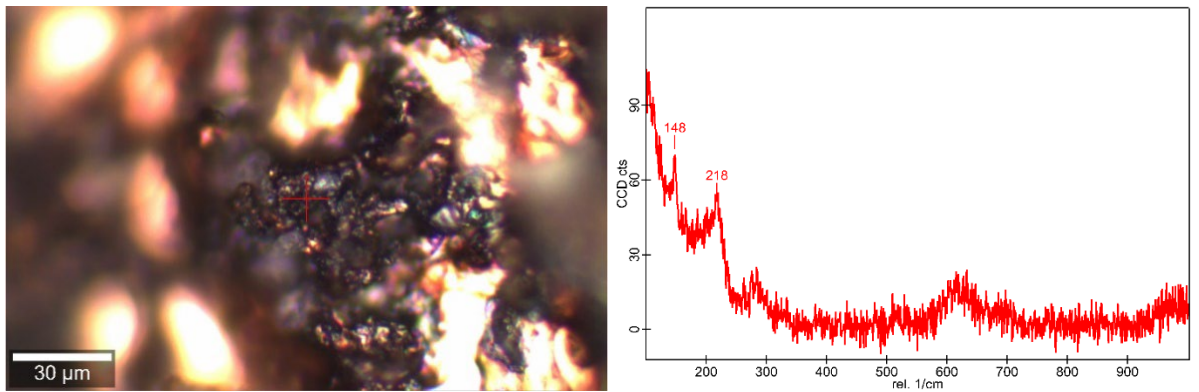


Figure 7-177. Area 5. Left: Optical image showing the area were the Raman spectrum was measured (red cross). Right: Measured Raman spectrum.

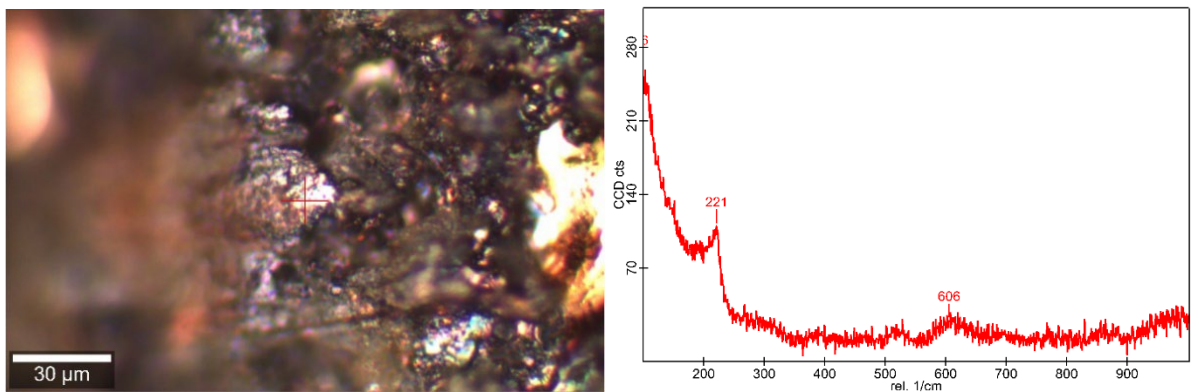


Figure 7-178. Area 6. Left: Optical image showing the area were the Raman spectrum was measured (red cross). Right: Measured Raman spectrum.

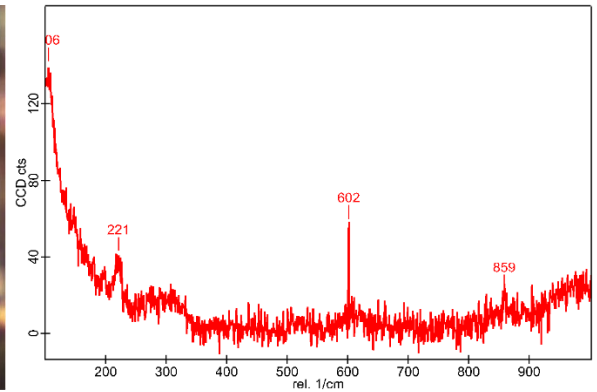
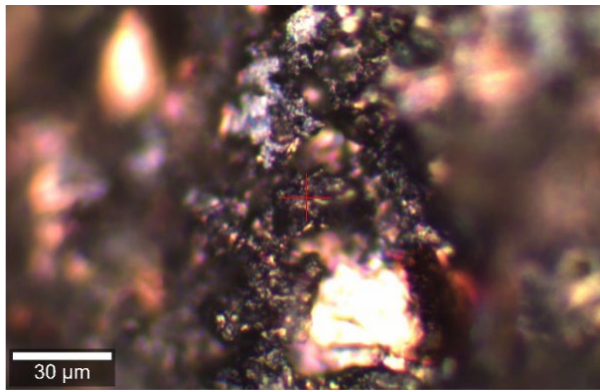


Figure 7-179. Area 7. Left: Optical image showing the area were the Raman spectrum was measured (red cross). Right: Measured Raman spectrum.

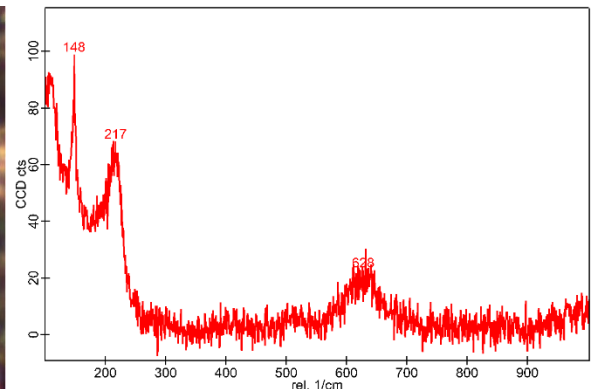
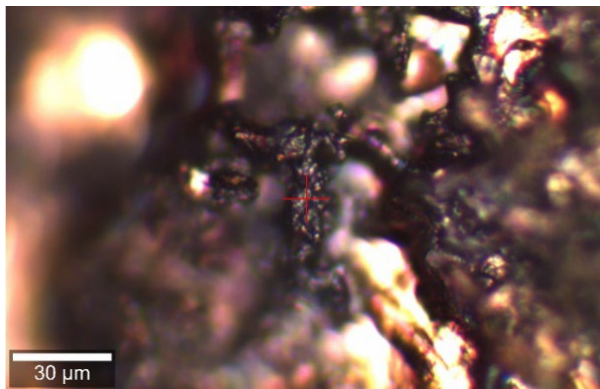


Figure 7-180. Area 8. Left: Optical image showing the area were the Raman spectrum was measured (red cross). Right: Measured Raman spectrum.

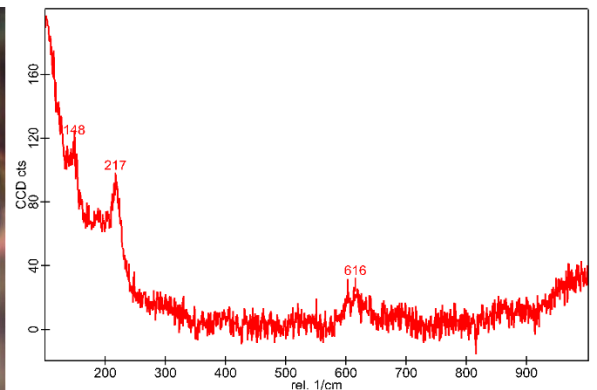
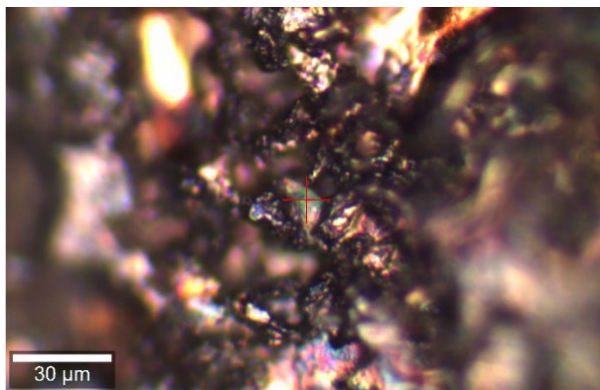


Figure 7-181. Area 9. Left: Optical image showing the area were the Raman spectrum was measured (red cross). Right: Measured Raman spectrum.